

# **Advancement of the Southeast Conservation Adaptation Strategy (SECAS) for Project- Scale Planning: Chandeleur Islands (Breton National Wildlife Refuge) Restoration**

**AUTHORS: MIKE MINER, P. SOUPY DALYANDER, DIANA DI  
LEONARDO, EVA WINDHOFFER, IOANNIS GEORGIU, NOEL  
DUDECK, TIM CARRUTHERS, AND ERIN KISKADDON**

Produced for and funded by: U.S. Fish and Wildlife Service

October 15, 2021

# Executive Summary

This study had two primary goals: 1) to develop and evaluate metrics for characterizing the restoration and conservation value of barrier islands that could inform the application of the Southeast Conservation Adaptation Strategy (SECAS) Southeast Conservation Blueprint; and 2) to characterize the geomorphic evolution and ecosystem value of the Chandeleur Islands with and without restoration action. The first phase of this study included evaluating the ecosystem value and long-term geomorphic evolution of the Chandeleur Islands (Figure I). Based on that analysis, a holistic island restoration concept for maximizing system resiliency was developed (Figure II). In the second phase, two “end member” restoration designs for enhancing the resiliency of the Chandeleur Islands were evaluated using a numerical modeling framework to identify sediment transport pathways and evaluate the performance of restoration alternatives (Section 3.0). One design represented a “traditional” dune and berm restoration that is widely used in the Gulf of Mexico, and the other represented a more novel approach of sediment placement in the backbarrier without the construction of a dune. A new set of metrics to characterize ecosystem value based on model results was developed and used to contrast the two restoration alternatives to a future without action (FWOA) scenario.

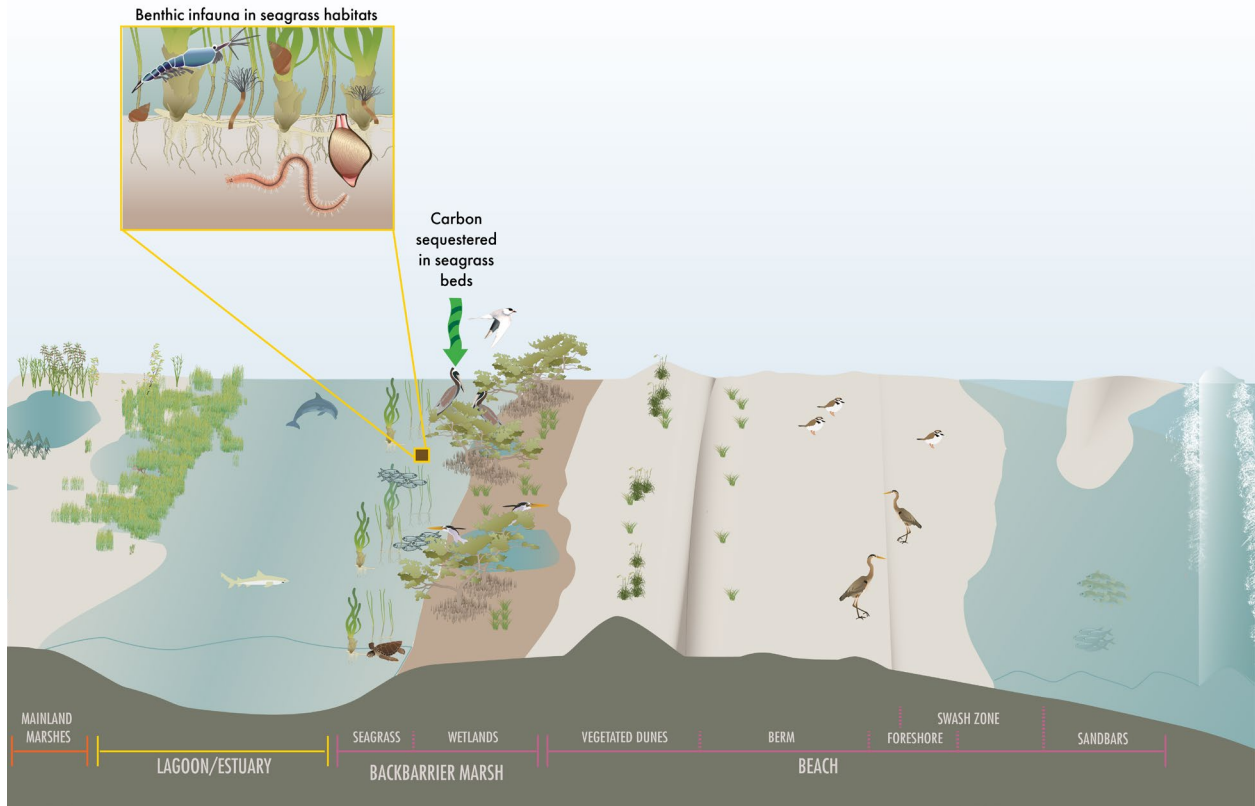


**Figure I. Ecogeomorphic conceptual model for the Chandeleur Islands.**

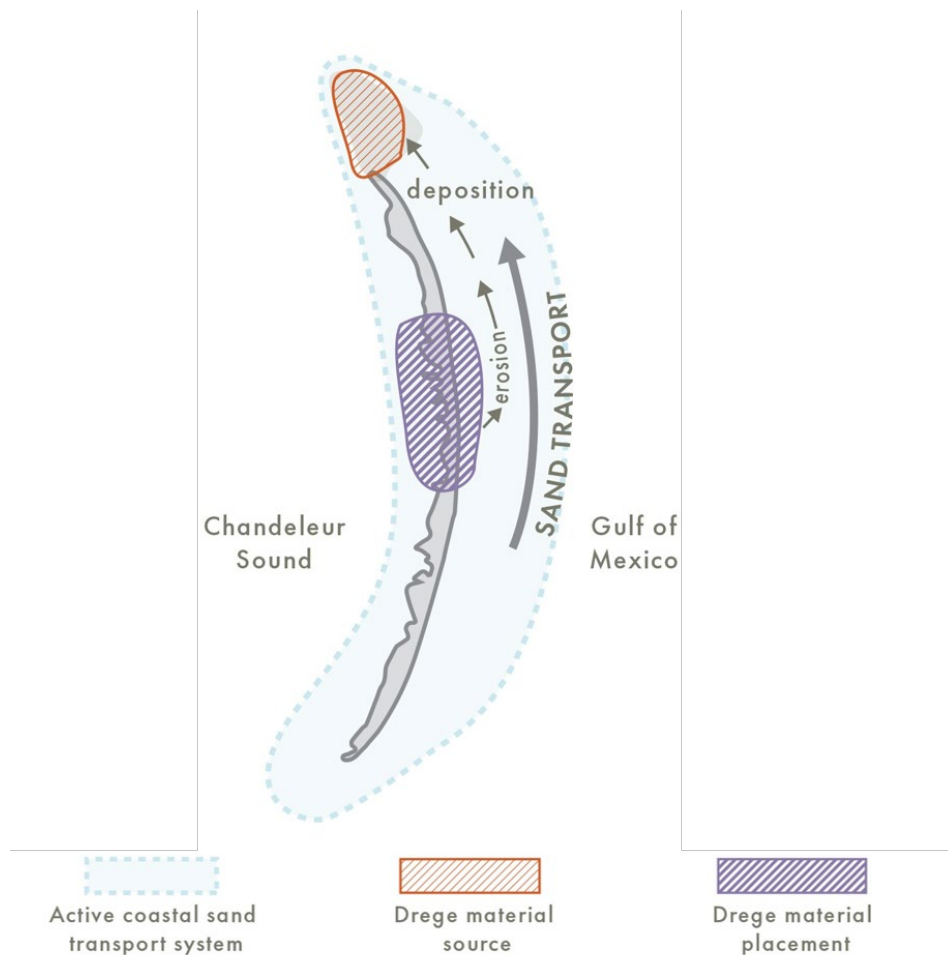


**Figure II. Conceptual model for sediment management-based restoration of the Chandeleur Islands.**

An analysis of the Chandeleur Islands geomorphic evolution and a modeling effort were combined to develop several novel findings that are relevant to restoration and management. First, a large volume of sand has accumulated in a thick platform at the northern flank of the island arc. This sand reservoir provides a unique opportunity as a resource for nourishing the Chandeleur Islands. South of this area but north of Redfish Point (Figure III), much of the island also sits on a thick platform of sand. As the shoreface erodes, this sand naturally nourishes the island. Backbarrier marshes along the island, which tend to be more resilient during storms than the island’s sandy beaches and dunes, provide a platform for island rollover and a sand source once eroded. Because these sites also serve as nucleation sites for post-storm sand deposition, they facilitate island recovery, and thus help preserve beach/dune habitat and the island integrity that is critical for establishment of seagrass meadows. Once the Gulf shoreline erodes into the backbarrier marsh, however, a threshold is crossed that results in the islands eroding faster and ultimately becoming subaqueous (island submergence). The northern Chandeleur Islands have not reached this stage. In their currently degraded state, however, historical patterns of longshore transport to the north during storms have been replaced with overwash and landward sand transport and deposition. If restoration is conducted via construction of a backbarrier marsh without a prominent dune, the lower elevation facilitates continued storm-driven overwash and sand deposition on the backbarrier platform,

which is expected to enhance island resilience and thus support seagrass in the longer term by maintaining the island form that shelters meadows in the lee. In a dune restoration scenario, the higher elevation of the restored form inhibits overwash and inundation. This leads to more seaward sand transport and deposition offshore of the island, where sand may potentially be lost from the active coastal sediment transport system and decrease island resiliency in the longer term.

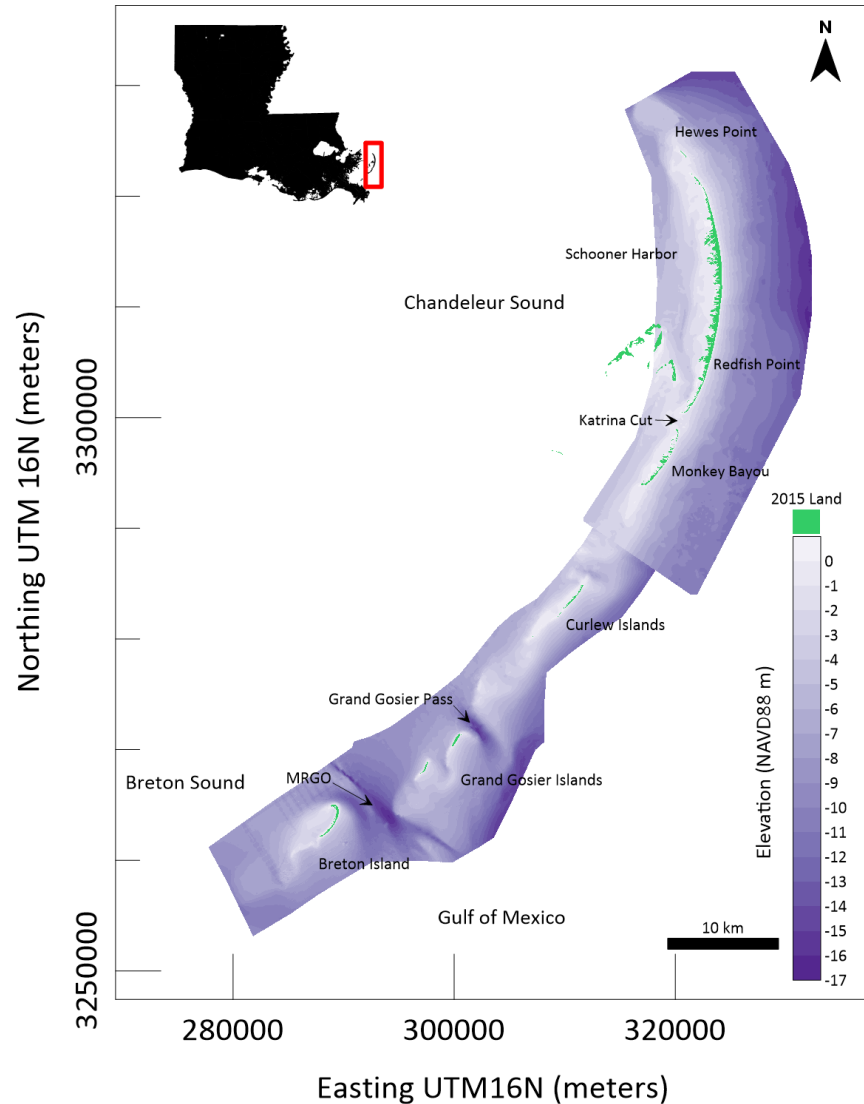


**Figure III. Chandeleur Islands study area with bathymetry collected in 2006-2015 (Kindinger et al., 2013; Mickey et al., 2017; Miner et al., 2009e; Stalk et al., 2017). The island area polygon is from the Louisiana Barrier Island Comprehensive Monitoring Program (Byrnes et al., 2018). Geographic locations discussed throughout the text are noted on this map.**

Based on these findings, the benefit of restoration can be maximized by placement of sand in a centralized sand source where it can be distributed by natural island processes and ultimately enhance the island's ability to naturally build backbarrier marsh, dunes, and a continuous sandy shoreline. In addition, placement of sediment in naturally high energy locations along the island—where erosion of placed sand will occur most rapidly—is expected to have limited benefit outside of areas where placement is needed

to restore the integrity of the island (e.g., closure of inlets or rebuilding of subaqueous shoals into a subaerial island). Sand placed in the backbarrier as vegetated, shore-perpendicular platforms can serve as long-term sand reserves as the island migrates and erodes into them, potentially as part of a hybrid design that includes dune restoration to create habitat for species reliant on these high elevations. An approach that increases island resiliency through greater retention of sediment in the system during storms is likely to benefit habitat such as seagrass in the lee that relies on the integrity of the island to attenuate wave energy in the longer term. These findings are expanded in Section 4.0, which may be of particular interest to managers focused on preserving and/or restoring the Chandeleur Islands.

In addition to the Chandeleur Islands results, the modeling effort and application of a new set of barrier island metrics (Section 3.2) were used to identify a set of key considerations relevant to the application of the Southeast Blueprint to barrier islands. First, barrier islands are highly dynamic and can change rapidly during even a single storm event. Because the Southeast Blueprint is developed based on data taken at single snapshots in time, the calculated conservation value for a barrier island may not accurately capture its current condition. Evaluation of metrics at multiple points in time and using those to determine an island's conservation/restoration value would be more useful than calculating metrics at a single point in time. Secondly, the diversity of habitat types found on barrier islands over relatively small spatial scales (several meters in the cross-shore) suggests that grid scales on larger spatial scales (30 meters in the Southeast Blueprint) may not fully capture ecosystem value for these systems. A more robust approach may be to evaluate habitat at smaller scales and then use those results to assign a conservation/ecosystem value to each barrier island. Lastly, the long-term trajectory and resiliency of barrier islands should be used in interpreting the information provided by the Southeast Blueprint, such as considering if the conservation value would be enhanced dramatically with island restoration. These findings are expanded in Section 5.0, which may be of particular interest to resource managers considering how to evaluate the conservation and restoration value of barrier islands beyond the Chandeleur Islands.

# Table of Contents

Executive Summary .....	i
Table of Contents .....	v
List of Figures .....	vi
List of Tables .....	viii
List of Acronyms .....	ix
Glossary .....	x
1.0 Introduction.....	1
2.0 Chandeleur Islands: Context for Restoration.....	7
2.1. Chandeleur Islands Setting .....	8
2.2. Ecological Benefit.....	8
2.3. Chandeleur Islands: Geomorphology and Long-Term Evolution.....	15
2.3.1 Deltaic Abandonment and Early Island Evolution .....	15
2.3.2 Historical Evolution and Modern Barrier Island Morphology.....	20
2.3.3 Restoration Concept.....	37
3.0 Evaluation of Event-Driven Sediment Transport Trends under Natural and Restored Island Configurations.....	39
3.1. Numerical Model Development and Restoration Design .....	40
3.1.1 Assessment of Existing Model Output and Data Sources.....	40
3.1.2 Model Configuration.....	42
3.1.3 Restoration Alternatives .....	42
3.1.4 Hydrodynamic Scenarios.....	50
3.2. Ecosystem Characterization for Model Analysis.....	51
3.2.1 Calculation of Metrics .....	51
3.2.2 Interpretation of Metrics .....	59
3.3. Chandeleur Islands Ecosystem Value with and without Restoration .....	61
3.3.1 Future Without Action (FWOA).....	61
3.3.2 Restoration Alternatives .....	69
3.3.3 Multiple Storms and an Extreme Storm Case.....	75
4.0 Implications for the Chandeleur Islands .....	79
4.1. Restoration and the Long-Term Evolution of the Chandeleur Islands .....	79
4.2. Suggested Next Steps in Chandeleur islands Restoration Evaluation .....	81
5.0 Use of the SECAS Southeast Blueprint in Conservation Planning for Barrier Islands .....	81
References.....	83

# List of Figures

Figure 1. Southeast Conservation Adaptation Strategy (SECAS) Southeast Blueprint.....	1
Figure 2. Chandeleur Islands study area with bathymetry collected in 2006-2015 .....	3
Figure 3. Conceptual diagram of a barrier island and associated habitats. Also shown is a cross-shore profile of barrier island habitats. ....	5
Figure 4. Ecogeomorphic conceptual model for the Chandeleur Islands. ....	14
Figure 5. Map of the Holocene Mississippi River delta plain that shows the multiple, spatially offset depocenters for each delta complex. ....	16
Figure 6. Three-stage model conceived by Penland et al. (1988) for the formation and evolution of transgressive Mississippi River delta barrier islands. ....	17
Figure 7. Conceptual model for development of the Chandeleur Islands backbarrier marshes through lateral spit accretion and progradation of recurved spits into the backbarrier .....	18
Figure 8. Conceptual model in profile view of the northern Chandeleur Islands stratigraphy. ....	19
Figure 9. Geologic cross-section trending along the northern Chandeleur island arc from the Hewes Point spit platform in the north to Monkey Bayou in the south .....	20
Figure 10. Map of BICM1 seafloor change analysis results for the Chandeleur Islands showing zones of sediment erosion and accretion for the time period 1870-2007. ....	21
Figure 11. Conceptual model for the transgressive submergence of the Chandeleur Islands following the lateral expansion (island development) phase depicted in Figure 7. ....	24
Figure 12. Chirp sonar subbottom profiles from 2007 with the exact same transect reoccupied in 2014 crossing the Mississippi River Gulf Outlet (MRGO) navigation channel. ....	26
Figure 13. Oblique aerial photograph from 2008 at Monkey Bayou along the Chandeleur Islands.....	28
Figure 14. Conceptual model for a laterally migrating inlet and the attendant inlet fill and spit platform. ....	29
Figure 15. Shoreline change maps (from the 1880s and 1950s overlain on 2019 aerial imagery) for the northern Chandeleur Islands demonstrating the variability in shoreline retreat rates governed by subsurface sand supply. ....	31
Figure 16. Chandeleur Islands area change from 1855 to 2006 from Fearnley et. al (2009b).....	32
Figure 17. Island area change for the southern Chandeleur islands annotated with tropical cyclone events from Fearnley et al. (2009b). ....	33
Figure 18. Simplified regional bathymetry map near the Chandeleur Islands (left panel), and locations where longshore sediment transport calculations were performed by Georgiou and Schindler. ....	34
Figure 19. Oblique aerial photo of the northern Chandeleur Islands (left) showing the closure of hurricane-cut inlets two years after Hurricane Katrina. ....	36
Figure 20. Conceptual model for sediment management-based restoration of the Chandeleur Islands. ....	38
Figure 21. Conceptual design for Chandeleur Island restoration from Lavoie et al. (2009).....	39
Figure 22. The model grid of the Chandeleur Islands with the restoration area shown.....	44
Figure 23. The dune end member restoration template.....	45
Figure 24. The dune template applied to topo-bathy profiles. ....	46
Figure 25. The restored topo-bathy after application of the dune end member templates.....	47
Figure 26. The marsh end member restoration template.....	48
Figure 27. The marsh restorations applied to the original topo-bathy profile.....	49
Figure 28. The restored bathymetry for the marsh end member templates.....	50
Figure 29. (A) Post-storm DEM for a low-intensity storm with incident on-shore waves. (B) To calculate the post-storm subaerial volume, areas with elevation less than -0.17 m mean low water (MLW) (0 m NAVD88) are masked out (black shading) and the total subaerial volume is integrated over the remaining cells. ....	54
Figure 30. Calculation methodology for V <sub>sea</sub> , the net volume of sediment deposition seaward of the pre-storm shoreline, and V <sub>land</sub> , the net volume of sediment deposition landward of the pre-storm shoreline.....	55

Figure 31. Calculation methodology for VHewes, the net volume of sediment transported to Hewes Point. .....	56
Figure 32. Example histograms of the distribution of shallow and subaerial elevation by area (Adist).....	57
Figure 33. Calculation methodology for potential seagrass area (Asg). .....	58
Figure 34. Distribution of seagrass at the Chandeleurs during 2010 (Kenworthy et al., 2017). .....	59
Figure 35. Pre-storm (A) and post-storm (B) DEM for a weak storm with shore-normal waves (Table 3), along with the elevation change (C) during the storm. ....	62
Figure 36. Elevation change resulting from a weak (A), intermediate (B), and strong (C) storm. Storm characteristics are provided in Table 3. ....	63
Figure 37. Elevation change along the northern half of the island chain and at Hewes Point resulting from a strong storm with shore-normal waves (A), waves coming from the SE (B), and waves coming from the NE (C). .....	63
Figure 38. (A) Pre-storm DEM and the pre- and post-storm cross-shore elevation for the transect shown in white. Results are shown for a weak (B) and strong (C) storm with SE waves. ....	65
Figure 39. (A) Pre-storm DEM and the pre- and post-storm elevation change for the region shown in white. Results are shown for a weak (B) and strong (C) storm with shore normal waves. ....	65
Figure 40. (A) Pre-storm DEM and the pre- and post-storm elevation change for the region shown in white. Results are shown for a weak (B) and strong (C) storm with SE waves. ....	66
Figure 41. Pattern of currents (A) for the northernmost portion of the Chandeleur Islands (B) during the peak of a strong storm (Table 3) with waves coming from the SE. ....	67
Figure 42. Distribution of shallow and subaqueous elevation by area (Adist) for three scenarios including future without action (FWOA), placement of sediment on the dune and berm, and placement of sediment in the backbarrier marsh. ....	68
Figure 43. Change in distribution of shallow and subaqueous elevation by area pre- and post-storm for a weak (A, B), intermediate (C, D), and strong (E, F) storm. ....	69
Figure 44. Pre-storm elevation for the FWOA (A), dune/berm sediment placement (B), and marsh sediment placement (C), along with the change in elevation during a strong storm event with waves from the SE (D-F for FWOA, dune/berm sediment placement, and marsh sediment placement, respectively). 71	
Figure 45. Change in distribution of shallow and subaqueous elevation by area (Adist) for three alternatives including future without action (FWOA), placement of sediment on the dune and berm, and placement of sediment in the backbarrier marsh. ....	73
Figure 46. Difference between the post-storm DEM for the dune/berm restoration and the FWOA scenarios. ....	74
Figure 47. Post-storm elevation (A) and elevation change (B) for an extreme storm impacting the FWOA case. Also shown are a pre- and post-storm profile (C) and the elevation change during the storm (D) for the profile shown in pink in (B). ....	77
Figure 48. Post-storm elevation (A) and elevation change (B) for an extreme storm impacting the marsh restoration case. Also shown are a pre- and post-storm profile (C) and the elevation change during the storm (D) for the profile shown in pink in (B). ....	77
Figure 49. Post-storm elevation (A) and elevation change (B) for an extreme storm impacting the dune restoration case. Also shown are a pre- and post-storm profile (C) and the elevation change during the storm (D) for the profile shown in pink in (B). ....	78
Figure 50. Difference between the dune and marsh restoration templates before (A) and after an extreme storm (B) and a strong storm after an extreme storm (C). Positive (green) values indicate the dune template is higher in elevation, negative (brown) values indicate the marsh template is higher in elevation. .....	78

## List of Tables

Table 1. Species and habitat associated with the Chandeleur Islands.....	10
Table 2. Sediment erosion/accretion change volumes for the geomorphic zones delineated as polygons in Figure 10. ....	22
Table 3. Characteristics of representative storms modeled for the Chandeleur Islands.....	51
Table 4. Indicators for subaerial and shallow water habitats associated with barrier island systems.....	51
Table 5. Metrics of characterizing the Chandeleur Island response to storms for this study.....	53
Table 6. Table summarizing habitat and resiliency metrics for the Chandeleur Islands for varying storm conditions (Table 3) for the FWOA scenario.....	64
Table 7. Summary of habitat and resiliency metrics for the Chandeleur Islands for varying storm conditions (Table 3) for the dune and marsh restoration alternatives. ....	72
Table 8. Table summarizing habitat and resiliency metrics for the Chandeleur Islands for varying storm conditions (Table 3) for the dune restoration alternative. ....	75
Table 9. Set of model runs used to evaluate the impacts of multiple and/or extreme storms on the Chandeleurs Islands under the FWOA and restoration cases. ....	76
Table 10. Volume of post-storm subaerial volume (Vaer) and the net landward sediment volume deposition (Vland). ....	76

## List of Acronyms

Acronym	Term
ADCIRC	ADvanced CIRCulation storm surge model
BICM	Barrier Island Comprehensive Monitoring Program
CERC	Coastal Engineering Research Council
CoP	Community of Practice
CPRA	Coastal Protection and Restoration Authority of Louisiana
DEM	Digital elevation model
DOI	Department of the Interior
E&D	Engineering & Design
EDGR	Empirical Dune GRowth
FWOA	Future without action
GOMA	Gulf of Mexico Alliance
GoMMAPPS	Gulf of Mexico Marine Assessment Program for Protected Species
JONSWAP	Joint North Sea Wave Project
LMACS	Louisiana, Mississippi, and Alabama Coastal System
MRGO	Mississippi River Gulf Outlet
MLW	Mean low water
NWR	National Wildlife Refuge
RSLR	Relative Sea-Level Rise
SECAS	Southeast Conservation Adaptation Strategy
STWAVE	STeady-state spectral WAVE
TWL	Total water level
UNO-PIES	University of New Orleans Pontchartrain Institute for Environmental Sciences
USACE	U.S. Army Corps of Engineers
USFWS	U.S. Fish and Wildlife Service
USGS	U.S. Geological Survey

# Glossary

<b>Term</b>	<b>Definition</b>
<b>Aeolian processes</b>	Erosion, transportation, and deposition of sediment by the wind.
<b>Avulsion</b>	Rapid abandonment of a river channel in favor of a new channel. Results in delta-switching.
<b>Arcuate</b>	Arc-shaped
<b>Backbarrier</b>	Describes an area on the landward side of the barrier island, usually used to indicate landward of the dunes. May describe subaerial portions of the island (backbarrier marsh) or simply the area landward of the dune out to the subtidal portions of the lagoon (sound) that backs the barrier.
<b>Baffling</b>	In relation to water flow, this indicates a reduction in wave energy and current velocity
<b>Berm</b>	A nearly horizontal section of the beach landward of the foreshore and seaward of the dune.
<b>Bifurcation</b>	A division or split that converts one entity into two.
<b>Bioturbation</b>	Reworking of soils and sediments by animals or plants.
<b>Bioirrigation</b>	Process by which animals bring oxygen-rich water down from the sediment-water interface into sediment burrows
<b>Breach</b>	Breaks in the island caused by storm-driven inundation that may close naturally or widen to form inlets.
<b>Cross-shore</b>	Orientation across the width of the island.
<b>Delta</b>	A landform created by deposition of sediment that is carried by a river as the flow leaves its mouth and enters slower-moving or stagnant water.
<b>Downdrift</b>	In the down-current direction of net longshore transport.
<b>Ebb tidal delta</b>	A sand shoal formed at the seaward mouth of tidal inlets as a result of interaction between tidal currents and waves.
<b>Ecogeomorphic</b>	Also, eco-geomorphic. Having to do with the interactions between organisms and the development and evolution of landforms.
<b>Emergent</b>	Subaerial
<b>Fetch</b>	The length of water over which a given wind blows without obstruction.
<b>Fluvial processes</b>	Processes associated with rivers and streams and the deposits and landforms created by them.
<b>Gravity waves</b>	On the interface of ocean and air, these are surface waves generated by wind.
<b>Headland</b>	Seaward protruding landform
<b>Holocene</b>	The current geological epoch which began approximately 12,000 years before present day.
<b>Infragravity waves</b>	Ocean surface waves consisting of both wind and sea swell with frequencies generally lower than waves generated by wind forcing alone.
<b>Intertidal</b>	Zone between the low tide line and the high tide line that is intermittently wet and dry in association with tidal fluctuations.
<b>Isobath</b>	An imaginary line or a line on a map or chart that connects all points having the same depth below the water surface.
<b>Landward migration</b>	In reference to barrier islands, this is process by which subaerial volume is lost from the original island footprint and gained on the lee side of the original footprint.
<b>Lee side</b>	Facing away from the wind, waves, or currents, usually sheltered from prevailing winds by dunes or vegetation.

<b>Term</b>	<b>Definition</b>
<b>Littoral system</b>	The zone of active sand transport by wave-generated currents that typically extends from the high-water shoreline seaward to a location that coincides with a depth where wave influence on the seabed is minimal
<b>Loafing</b>	Descriptor of bird behavior not connected with feeding or breeding activities. The term includes preening and resting.
<b>Longshore</b>	In parallel with the length of the shoreline (alongshore may also be used)
<b>Nodal Zone</b>	Areas of divergent longshore sediment transport caused by wave refraction patterns
<b>Nucleation</b>	Initial process that occurs in the formation of landforms from which they grow by addition of new sediment, vegetative productivity, etc.
<b>Overwash fans</b>	Deposits of sand behind low-lying areas of barrier island that result from storm overtopping and landward sand transport.
<b>Preening</b>	Maintenance behavior found in birds involving use of the beak to position and clean feathers.
<b>Progradation</b>	The growth of a landform over time (often used to describe seaward growth).
<b>Shoal</b>	A submerged ridge, bank, or bar that consists of, or is covered by, sand or other unconsolidated material.
<b>Shore normal</b>	Perpendicular to the shoreline.
<b>Shoreface</b>	Nearshore zone that extends from the shoreline out to a depth where wave influence on sand transport is minimal. Often referred to as a profile that is oriented perpendicular to the shoreline.
<b>Shoreface retreat</b>	Erosion of shoreface so that the shore-perpendicular profile extending to a depth defined by storm wave base migrates in a landward direction (usually coincides with shoreline retreat).
<b>Shoreline</b>	A line which designates the boundary between land and water (may be defined with a descriptor indicates water level such as the Mean High Water Shoreline).
<b>Spit</b>	A sandy ridge attached to land at one end and terminating in open water at the other
<b>Subaerial</b>	Exposed to the atmosphere; within or above the intertidal zone.
<b>Subaqueous</b>	Submerged; not exposed to the atmosphere.
<b>Surf zone</b>	Nearshore zone characterized by breaking waves (also known as the breaker zone).
<b>Threshold Crossing</b>	Geomorphic term describing an abrupt change in a landform that was formerly in equilibrium. After a threshold crossing the landform is in disequilibrium due to the governing parameters that define that landform (e.g., climate, sand supply, storm frequency) being altered. Some new equilibrium condition will ultimately be reached under the new governing parameters.
<b>Tidal Inlet</b>	A shore-perpendicular channel along a barrier shoreline that connects the larger body of water (e.g., Gulf of Mexico) with bays, lagoons, marsh, and tidal creeks and is kept open by tidal currents flushing sand transported to the tidal inlet by waves.
<b>Tidal prism</b>	The volume of water in an estuary or inlet between mean high tide and mean low tide.
<b>Transgression</b>	Landward migration of the shoreline, a landform, coastal system, wetland, etc in response to sea-level rise.
<b>Transgressive submergence</b>	Conversion from emergent transgressive barrier islands to submerged shoals that continue to migrate landward.
<b>Welding</b>	(Bar welding) process of sand bar landward migration due to the influence of waves and attaching to the beach resulting in progradation (moving out in a seaward direction) of the shoreline.

## Acknowledgements

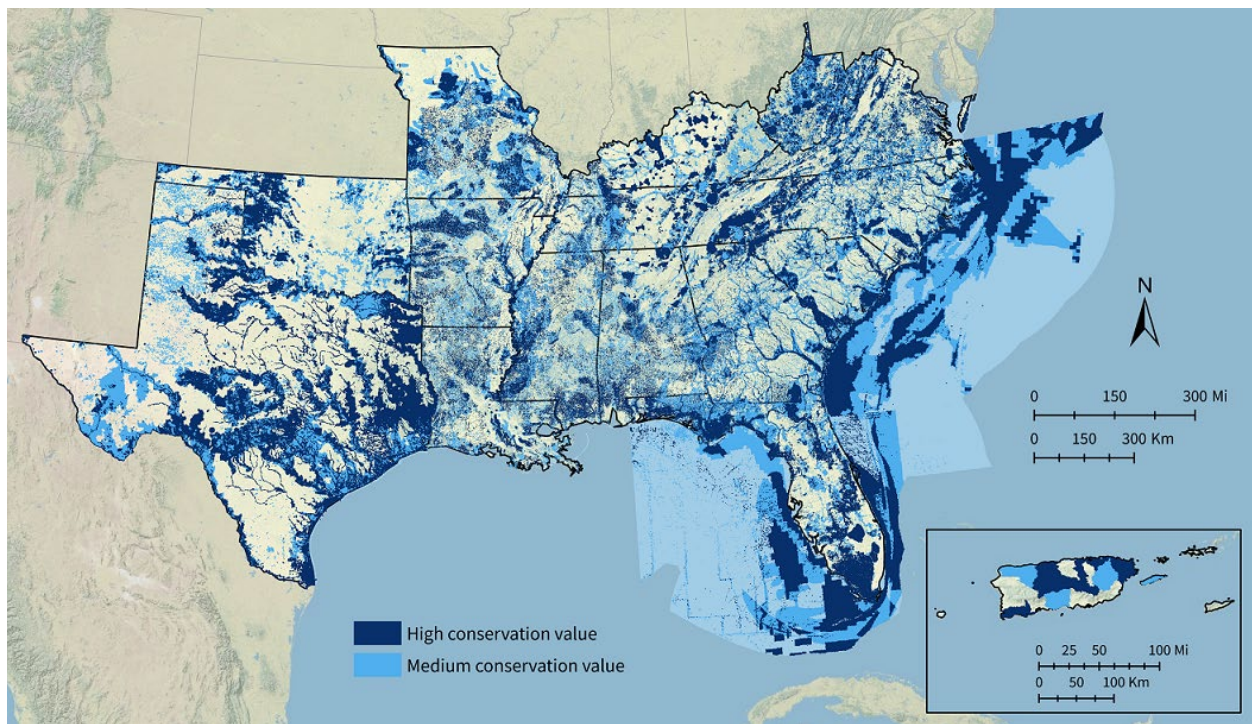
Funding for this report was provided via Cooperative Agreement F20AC00082 from the U.S. Fish and Wildlife Service.

Support in adapting and extending the Chandeleur Islands model for this study was provided by Ranglely C. Mickey (U.S. Geological Survey).

The following individuals participated in discussions, provided additional information, and/or provided review: Todd E. Hopkins, Mallory Martin, Yvonne Allen, Barret Fortier, Jon Hemming, David Jones-Farrand, Rua Mordecai, Blair E. Tirpak, and John Tirpak (U.S. Fish and Wildlife Service)

# 1.0 Introduction

The Southeast Conservation Adaptation Strategy (SECAS) is a regional initiative that lays out a shared vision for ecosystem conservation in the Southeastern United States and Caribbean that can be advanced by public and private entities at the federal, state, and local level. The goal of SECAS is a 10 percent or greater improvement in the health, function, and connectivity of southeastern ecosystems by 2060, with progress tracked using regional metrics that are reported on an annual basis. To support SECAS, a regional Southeast Conservation Blueprint (the Southeast Blueprint; <https://secassoutheast.org/blueprint>; Figure 1) has been developed that identifies high priority spatial areas for conservation and restoration. The Southeast Blueprint is a living, spatial plan designed to help guide responsible ecosystem stewardship by identifying areas that are of “high” and “medium” conservation value, supporting ecosystem managers working to identify where and how to focus limited conservation resources. Partnering agencies also use the Southeast Blueprint to support locally focused conservation and restoration projects (<https://secassoutheast.org/story-map>). For example, the Southeast Blueprint was used as part of a successful proposal to bring nearly \$3 million in funds from the Department of Interior’s Wildland Fire Resilient Landscapes program for use in prescribed burns to benefit the longleaf pine ecosystem. In Florida, the Southeast Blueprint was used as part of articulating the value of the St. Marks National Wildlife Refuge and surrounding area as a habitat for frosted flatwoods salamander, leading to a successful Cooperative Recovery Initiative and acquisition of funds to preserve this region.

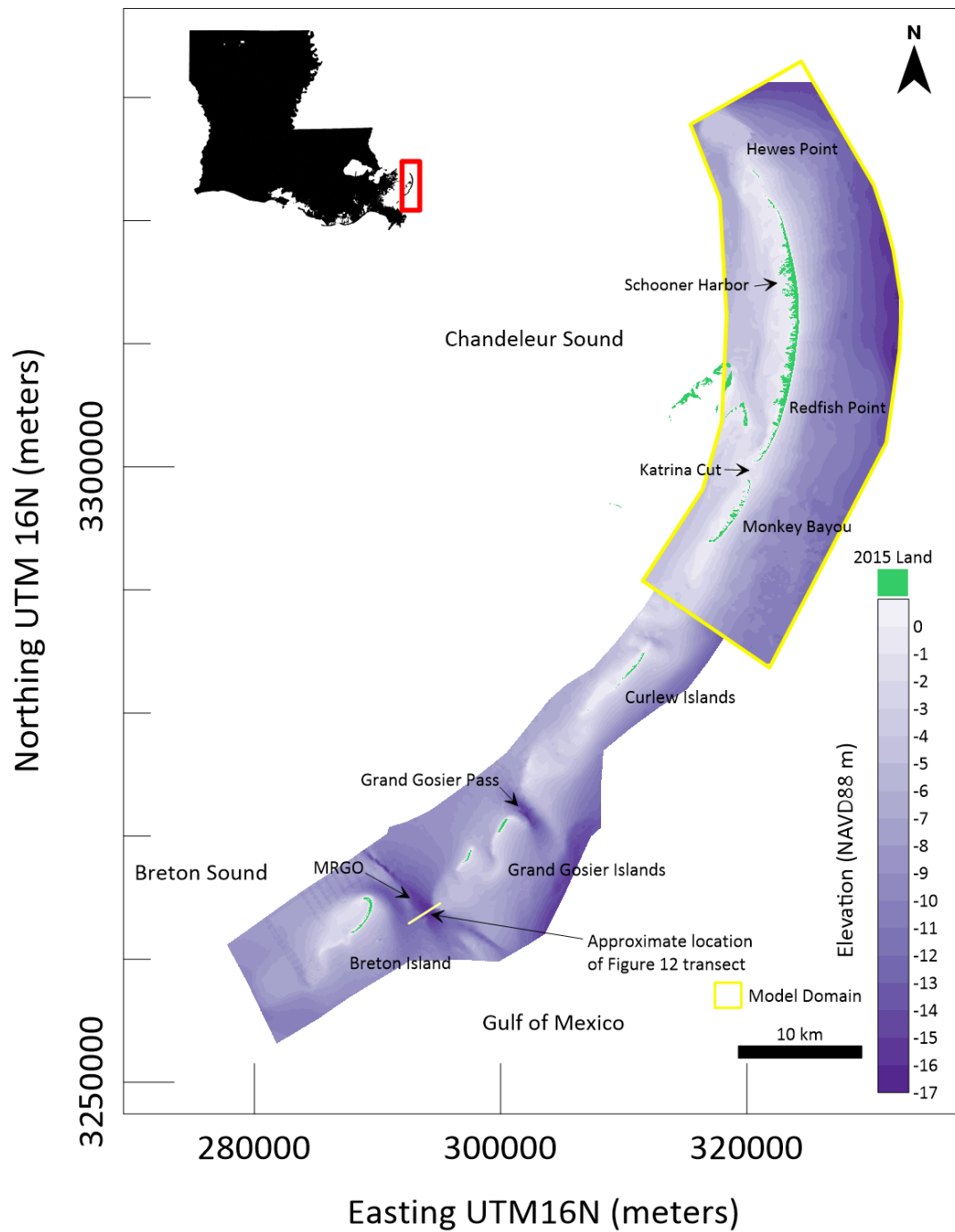


The Southeast Blueprint “stiches together smaller subregional plans into one consistent map, incorporating the best available information about key species, ecosystems, and future threats” (Southeast Conservation Adaptation Strategy, 2021). Each subregional plan is created by applying a metric-based

evaluation process for quantifying relative conservation value based on a combination of federal and local priorities. In this process, factors that contribute to the quality of an ecosystem, such as ecosystem resilience and the presence of threatened and endangered species, are evaluated and combined so that those spatial areas identified as having greater relative conservation value can be delineated. The Southeast Blueprint then combines the separate subregional plans, each of which was built from varying individual data layers with somewhat different creation methodologies and conservation evaluation priorities. As a result, there is some spatial variability in the valuation of conservation prioritization across the landscape (see Cameron et al., (2020) for further information on the Southeast Blueprint origination and methodology). Nevertheless, the Southeast Blueprint provides a way to quickly assess the relative conservation value across the region and its component ecosystems.

Included within the Southeast Blueprint are barrier islands. These coastal landforms consist of relatively long, thin islands (generally hundreds of meters in length and meters to tens of meters in width) that stretch along mainland coasts throughout the world (Stutz & Pilkey, 2001). Throughout the Gulf of Mexico, barrier islands are threatened by land loss associated with relative sea-level rise (RSLR), subsidence, decreased sediment supply, coastal development, and storms (List et al., 1997; McBride et al., 1992; McBride & Byrnes, 1995; Miner et al., 2009b; Morton, 2008; Otvos & Carter, 2013; Penland & Boyd, 1981). To preserve the ecological benefits provided by barrier islands, barrier island systems are often the focus of conservation and restoration efforts supported by local, state (e.g., the Louisiana Coastal Protection and Restoration Authority [CPRA]), and federal programs (e.g., the National Fish and Wildlife Foundation, Gulf Environmental Benefit Fund). As such, it is important to be able to accurately evaluate their conservation value through mechanisms such as the Southeast Blueprint.

There are indications, however, that the methodologies used to quantify barrier island conservation value in the Gulf of Mexico could be enhanced to more fully characterize the habitat and ecosystem services these systems are providing. For example, the Chandeleur Islands, a barrier island chain located off the coast of Louisiana in the Gulf of Mexico (Figure 2), is not identified as having “high” or “medium” conservation value within the Southeast Blueprint. However, these islands are part of the U.S. Fish and Wildlife Service (USFWS) Breton National Wildlife Refuge (NWR; <https://www.fws.gov/refuge/Breton/>) and provide key habitat for species such as the Brown Pelican (Selman et al., 2016) and nesting sea turtles (Ogren, 1989). In addition, the Chandeleur Islands provide regional benefits including attenuation of wave energy (Grzegorzewski et al., 2009) that may otherwise erode mainland marshes and Cat Island in the Mississippi-Alabama barrier island chain (Miselis et al., 2014). Similarly, this attenuation of wave energy protects seagrass beds in Chandeleur Sound and elsewhere (Darnell et al., 2017; Pham et al., 2014) and regulates salinity levels in Chandeleur and Mississippi Sounds (Schindler, 2010), with subsequent implications for the health of oyster reefs (Eleuterius, 1977).



**3.0) and this portion of the island chain is often referred to as the northern Chandeleur Islands. South of the yellow polygon are the southern Chandeleur Islands. MRGO = Mississippi River Gulf Outlet (decommissioned).**

There are several reasons why the conservation value of barrier islands may be underestimated within the Southeast Blueprint. First, with the exception of the subregional Florida Marine Blueprint, the Southeast Blueprint and the subregional Blueprints it builds upon were originally developed for terrestrial and freshwater aquatic habitats and therefore the metrics used in calculating conservation value do not capture some of the important regional ecosystem benefits these islands provide.

Second, the Southeast Blueprint evaluation capability might be somewhat limited for barrier islands due to the small spatial scale of narrow barrier island habitats. Undisturbed barrier islands in the Gulf of Mexico are typically low-lying landforms (maximum elevation of a few meters) with a narrow width (i.e., “cross-shore profile”; meters to approximately a kilometer in width) that are elongated in the alongshore direction (kms to tens of kms in length; Figure 3; Morton, 2008; Otvos & Carter, 2013). Across that narrow width, there is considerable variability in barrier island habitat. Intertidal habitat (wet or dry depending on the tidal level) is found in a thin strip along the Gulf of Mexico shoreline, transitioning to a sparsely vegetated beach or berm. Moving in a landward direction cross-shore, the elevation increases and the habitat transitions into dunes—typically the highest elevations on the island—that are associated with various types of vegetation. Behind the dunes there may be vegetated or unvegetated barrier meadows or flats, which extend to a backbarrier shoreline that may include a marsh or unvegetated intertidal region (Enwright et al., 2018b, 2019). In the alongshore direction, barrier islands may be punctuated by geomorphic features including: overwash fans (relic deposits of sand behind low-lying areas of dune that result from storm overtopping of the barrier island which provide foraging habitat for shorebirds); tidal inlets (channels that convey water and sediment between the Gulf of Mexico and sound and are associated with shallow subaqueous sandy tidal deltas and associated shallow water habitat); and breaches (breaks in the island caused by storm-driven inundation that may close naturally or widen to form inlets) (Enwright et al., 2018a; Schupp et al., 2013). Barrier islands can also be associated with oyster reefs or seagrass in the protected, low-energy shallow areas in the lee of the islands (Carter et al., 2009; Park et al., 2014; Pham et al., 2014). Each of these unique barrier island habitats and geomorphic features provides valuable habitat to a variety of species. However, an entire barrier island may occupy a single cell in the cross-shore of the 30-m spatial resolution of the Southeast Blueprint, with limited (if any) resolution of individual habitat types.

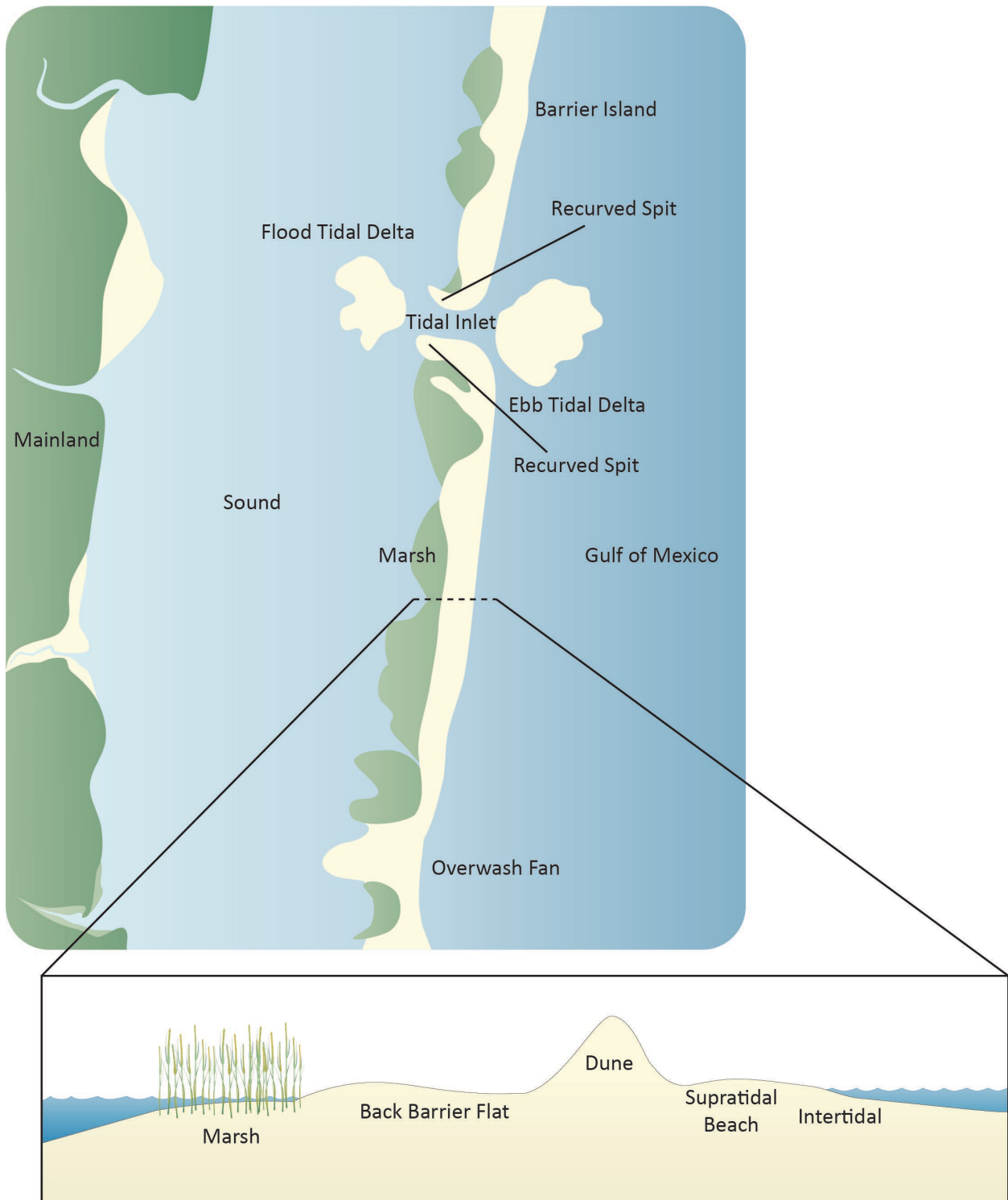


**Figure 3. Conceptual diagram of a barrier island and associated habitats. Also shown is a cross-shore profile of barrier island habitats. Diagram created by modifying symbology available courtesy of the Integration and Application Network, University of Maryland Center for Environmental Science ([ian.umces.edu/symbols/](http://ian.umces.edu/symbols/)).**

Third, the highly dynamic nature of barrier island systems complicates the assessment of conservation value within the Southeast Blueprint, which is based on static data layers that provide single “snapshots in time.” Storms drastically alter barrier islands in the time span of hours to days (Otvos & Carter, 2013; Stone, 2006; Stone et al., 2004), while wave-driven patterns in longshore transport and the cumulative effect of multiple storms can lead to an entire island migrating out of its original footprint on timescales of months to years (Cipriani & Stone, 2001; Georgiou & Schindler, 2009b; Rosati & Stone, 2009; Stone & Stapor Jr, 1996). Even when habitat is temporarily lost, such as when a storm overwashes or breaches an island and destroys the dune vegetation, there may be recovery on time scales of months to years (Houser et al., 2015). Because of the dynamic nature of barrier island systems, a barrier island at any given point in time may have a different habitat distribution than the same barrier island months, weeks, or even days later, and the conservation value calculated using single snapshot in time may not accurately reflect the overall ecosystem condition of the barrier island.

In addition to the challenges of assessing the conservation value of barrier islands, the active management of barrier island ecosystems has some unique considerations. Throughout the Gulf of Mexico and around the world, barrier islands are threatened by land loss associated with RSLR, subsidence, decreased sediment supply, coastal development, and storms (List et al., 1997; McBride et al., 1992; McBride & Byrnes, 1995; Miner et al., 2009b; Morton, 2008; Otvos & Carter, 2013; Penland & Boyd, 1981). These forces can result in rapid disintegration and submergence of barrier islands on the time scale of years to decades. Along the Chandeleur Islands, for example, Fearnley et al. (2009), Miner et al. (2009e), and Sallenger Jr. et al. (2009) show that the system has entered a regime where it is on a rapid trajectory toward completely being converted to ephemeral islands and submerged shoals. However, the timing of this threshold crossing could be years to decades depending on tropical cyclone frequency and magnitude. Therefore “conservation” (i.e., managing a region so the associated habitats and species are sustained and not negatively impacted by human interaction) for many barrier islands is insufficient to preserve these landforms and their associated habitats for any significant length of time. Instead, active restoration of the underlying landform itself to mitigate for sediment deficits is often required. Barrier island restoration typically involves strategic sediment placement within a barrier island system to prolong the length of time that it will remain subaerial. For example, the barrier islands within the Assateague Island National Seashore have been managed through actions including sediment placement and modification of the dune and beach in order to preserve natural processes and landforms that support species such as Piping Plover (Carruthers et al., 2011; Schupp et al., 2013). For this reason, natural resource managers require information on the short- and long-term “restoration value” of barrier islands, including if and how restoration can be conducted to maximize that value, rather than approaching from the system from a purely “conservation value” (habitat and species management) perspective.

The objective of the SECAS effort is to align with active management and restoration planning for these barrier islands through investigation of barrier island restoration options and calculate the potential future ecosystem value of these options. The results are then used to provide recommendations for characterization of barrier islands within the Southeast Blueprint. The study is designed to follow the general process of restoration strategy conceptualization and planning for barrier island management. For this case study, a component of that plan development includes ecosystem value characterization which can additionally provide recommendations for improving the Southeast Blueprint. The focus area of the study is the Chandeleur Islands within the Breton NWR, a barrier island chain located along the coast of

Louisiana and Mississippi in the northern Gulf of Mexico (Figure 2). Study of these barrier islands is timely since the site will soon be part of an Engineering and Design (E&D) effort to evaluate potential restoration alternatives. Therefore, this study can inform that process by highlighting the benefits and tradeoffs of different restoration strategies over different time scales to focus alternative refinement on those with both short- and long-term benefit, in addition to advancing continued refinement and application of the Southeast Blueprint to barrier islands.

The first phase of this study (Section 2.0) covers the initial process a management team might undertake to identify the need for restoration of a barrier island and develop an initial concept of the restoration approach to retain natural barrier island processes. These steps then support assessment of potential future ecosystem value of the restored system. First, the ecosystem value provided by the Chandeleur Islands is characterized through the development of a conceptual model based on literature review. This defines the potential benefits of restoring this system from an ecosystem perspective and identifies what ecosystem functions would provide the most informative restoration goals. A literature synthesis and analysis of the formation and long-term geomorphic evolution of the Chandeleur Islands is conducted and used to identify key processes and trends that are relevant to island restoration. From this, a holistic island restoration concept for maximizing system resiliency given the available sediment resources (i.e., to extend the length of time that the island itself is emergent and capable of providing ecosystem value) is developed and presented.

Restoration planning typically encompasses refining a restoration concept into specific restoration alternatives and then using numerical modeling to predict the geomorphic evolution of the barrier island with and without restoration implementation. In the second phase of this study (Section 3.0), two “end member” restoration designs for enhancing Chandeleur Islands resiliency are evaluated using a numerical modeling framework that is similar to approaches used in evaluating the performance of restoration alternatives in management applications (e.g. Long et al., 2020). Existing frameworks and metrics from the literature for characterizing barrier islands and their ecosystem services are used to develop a new set of metrics for characterizing ecosystem value that are derived from numerical model output. These metrics are applied to the Chandeleur Islands model predictions to contrast the two restoration scenarios and a future without action (FWOA). The implications of these results in the context of the long-term evolution of the Chandeleur Islands is discussed, including considerations for restoration design and evaluation (Section 4.0). Lastly, a set of lessons learned for application of the Southeast Blueprint to barrier islands is presented (Section 5.0).

## **2.0 Chandeleur Islands: Context for Restoration**

The Chandeleur Islands are on a rapid trajectory toward a major regime shift as a result of a significant sand deficit that was greatly exacerbated by the impacts of Hurricane Katrina in 2005 (Fearnley et al., 2009b; Lavoie, 2009 and chapters therein; Moore et al., 2014; U.S. Fish and Wildlife Service, 2008). The islands experience a net loss of barrier island sand to deep water downdrift sinks that has resulted in an 85 percent reduction of total island area over the past 170 years (Fearnley et al., 2009b). Increased hurricane intensity and frequency in the northern Gulf of Mexico between 1998 and 2005 accelerated this land loss trend, forcing the Chandeleur Islands into a mode of rapid dissection and transgressive submergence (conversion from emergent barrier islands to submerged shoals; Fearnley et al., 2009b; Sallenger Jr. et al., 2009). Based on extrapolated historical land loss and shoreface retreat rates, the islands will be

completely converted to a system of ephemeral islands and submerged shoals within the next few decades (Fearnley et al., 2009b; Miner et al., 2009d; Sallenger Jr. et al., 2009). This geomorphic trajectory of island loss has resulted in reduced ecosystem service value and function related to estuarine stability, island emergent vegetation, bird nesting, seagrass area, and associated marine fauna (e.g., Darnell et al., 2017; U.S. Fish and Wildlife Service, 2013). Given these trends, and concerns by resource managers that a collapse of the system is imminent post-Hurricane Katrina, there have been extensive investigations and monitoring efforts conducted to better understand system dynamics and quantify trends to inform island management and potential restoration strategies (e.g., Enwright et al., 2020; Kindinger et al., 2013, p. 20; Lavoie, 2009; U.S. Fish and Wildlife Service, 2013). This section provides an overview of the ecosystem context for island restoration including background on the geomorphic evolution of the Chandeleur Islands that defines habitat extent and dynamics for biological natural resources. This ecogeomorphic context is applied to inform a restoration strategy that reintroduces sediment to the depleted system at strategic locations employing natural geomorphic processes to provide for enhanced ecosystem function, value, and resiliency.

## 2.1. CHANDELEUR ISLANDS SETTING

The Chandeleur Islands are composed of an 80 km (50 mi) long arc-shaped barrier island chain. They are separated from the Louisiana mainland wetlands by the ~25–40 km (15–25 mi) wide Breton and Chandeleur Sound where depths average 3–5 m (10–16 ft). The Chandeleur Islands are the oldest barrier island system in the Mississippi River delta plain that is still emergent (Ship Shoal and Tiger/Trinity Shoal east of the modern Mississippi River represent submerged reworked remnants of older deltaic barrier island systems; Penland et al., 1988). The island chain is composed of the northern island arc that extends from Hewes Point in the north to Monkey Bayou in the south; a series of ephemeral barrier islands (Curlew and Grand Gosier) south of Monkey Bayou; and Breton Island, the southernmost island in the chain (Figure 2). These islands are extremely dynamic, but in their present state they are characterized by a relatively sand-rich northern section (north of Redfish Point) where islands are backed by established backbarrier marsh and a sand-starved southern section that extends south to Breton Island where backbarrier marshes are rare and ephemeral. Backing much of the northern portion of the island chain are extensive marine seagrass meadows containing *Thalassia testudinum*. This is the only occurrence of *T. testudinum* across ~1,000 km of the northern Gulf of Mexico between west Florida and the central Texas coast (Darnell et al., 2017).

## 2.2. ECOLOGICAL BENEFIT

Because of their overall length, position, and orientation the Chandeleur Islands comprise a significant barrier that plays a crucial role in: 1) attenuating storm impacts for mainland Louisiana and Mississippi; 2) regulating conditions (including salinity gradients, circulation patterns, larval transport, nutrient retention and distribution, and magnitude of wave and tidal energy) for the 4,650 mi<sup>2</sup> Breton Sound/eastern Mississippi Sound/Pontchartrain Basin estuary (Georgiou et al., 2009; Reyes et al., 2005; Schindler, 2010); 3) supporting a \$2.7 billion fisheries industry (Fearnley et al., 2009b); and 4) providing unique habitat for threatened, endangered, and other species including sea turtles, Piping Plovers, Brown Pelicans, and red knot (Lavoie, 2009; Poirrier & Handley, 2007; U.S. Fish and Wildlife Service, 2008, 2013; USFWS, 2021).

In recognition of the importance of the Chandeleurs to fish and wildlife resources, the island chain was designated as the Breton NWR by President Theodore Roosevelt in 1904 and was only the second NWR

to be established nationwide. The islands have also been designated a Globally Important Bird Area by the American Bird Conservancy and The Nature Conservancy (Cecil et al., 2009). The Chandeleur Islands provide extensive ecological benefits through a range of habitats including beaches, dunes, backbarrier marsh, black mangroves (*Avicennia germinans*), and shallow submerged flats for a variety of birds including nesting Brown Pelicans (historically the largest colony in the Gulf; U.S. Fish and Wildlife Service, 2008), Snowy Plovers, Wilson's Plovers, Reddish Egrets, American Oystercatchers, Black Skimmers, and a variety of other terns, including the largest Sandwich Tern and Royal Tern nesting colonies in North America (U.S. Fish and Wildlife Service, 2008; Table 1). The Chandeleurs are also the only known breeding location of the Chandeleur Gull, a species that has emerged as a hybrid cross between Herring and Kelp Gulls that uniquely co-occur there (Remsen et al., 2019; U.S. Fish and Wildlife Service, 2008). The Chandeleurs also serve as important habitat for wintering waterfowl, notably one of the larger concentrations of Redheads (a species of waterfowl), a species for which >80% of the global population winters in the Gulf. Shorebirds (e.g., Sandpipers, Dunlin, Sanderling, etc.) are also abundant on the islands and the site has been identified as a critically important wintering site by the Western Hemisphere Shorebird Reserve Network (Johnson et al., 2013; U.S. Fish and Wildlife Service, 2013; Zdravkovic, 2013). The Chandeleurs contain Endangered Species Act-designated critical habitat for the federally threatened Piping Plover (USFWS, 2001) and based on recent surveys they may also provide wintering grounds for the largest population of federally threatened Red Knots in the Gulf of Mexico (John Tirpak USFWS, 2020 personal communication).

The Chandeleurs also provide habitat for many other federal threatened and endangered species or other conservation priority designation, including loggerhead, green, and Kemp's ridley sea turtles, the West Indian manatee, and lemon sharks (see Table 1 for more details and references).

**Table 1. Species and habitat associated with the Chandeleur Islands. Species in red have designated conservation concern (Louisiana Department of Wildlife and Fisheries, 2021). Row shading is for visual purposes only and is used to delineate different animal classes. References noted in table designated by numerical superscript: <sup>1</sup>USFWS (2013), <sup>2</sup>Handley et al. (2007), <sup>3</sup>USFWS (2021), <sup>4</sup>Kenworthy et al (2017), <sup>5</sup>Michot and Chadwick (1994), <sup>6</sup>(Deepwater Horizon Natural Resource Damage Assessment Trustees, 2016), <sup>7</sup>Ogren (1989), <sup>8</sup>Zdravkovic (2013), <sup>9</sup>Catlin et al. (2011), <sup>10</sup> USFWS (2008), <sup>11</sup>Peterson & Waggy (2004), <sup>12</sup>Ellinwood (2008), <sup>13</sup>McKenzie (2013), <sup>14</sup>Darnell et al. (2017), <sup>15</sup>Remsen et al. (2019), <sup>16</sup>Handley et al. (2018), <sup>17</sup>GOMA (2021), <sup>18</sup>BOEM (2021), <sup>19</sup>Fertl et al. (2005), <sup>20</sup>Boudreau & Jorgensen (2001), <sup>21</sup>Middelburg (2019), and <sup>22</sup>Meysman et al (2006), <sup>23</sup>Fodrie & Heck, 2011), <sup>24</sup>(Mullin, 1988).**

Category/Guild	Species	Habitat Association	Value/Special Considerations	Restoration Plans
Waterfowl	Redhead <sup>5</sup> , Scaup, Gadwall, Bufflehead, Mergansers, Blue-winged Teal	Seagrass beds <sup>5,6</sup> and shallow open water Use: Wintering habitat – loafing and foraging	Mississippi Delta is one of the most important waterfowl wintering habitats in North America <sup>1</sup>  Southern terminus of the Mississippi Flyway <sup>1</sup>	North American Waterfowl Management Plan  Louisiana Comprehensive Wildlife Conservation Strategy (Wildlife Action Plan)
Shorebirds	<b>Wilson’s Plover, American Oystercatcher</b> , Willet	Maritime and coastal marsh habitats (sandy beach, dune, wrack) <sup>1</sup> Use: Breeding, foraging, loafing	<b>Wilson’s Plover</b> – (G4, S2B, S1N) – Chandeleur Island supports one of the highest breeding densities on the Gulf Coast <sup>8</sup>	U.S. Shorebird Conservation Plan  Louisiana Comprehensive Wildlife Conservation Strategy (Wildlife Action Plan)
	<b>Piping Plover, Snowy Plover</b> , Black-bellied Plover, Dowitchers, Sanderling, Dunlin, <b>Red Knot</b> , Least Sandpiper, Western Sandpiper, Whimbrel, Long-billed Curlew, Godwits	Maritime and coastal marsh habitats (sandy beach, dune, tidal sand flats, mudflats) <sup>1,9</sup> Use: Foraging, loafing	<b>Piping Plover</b> (Federally Threatened) - Chandeleur Island designated as critical habitat in 2001 <sup>1</sup> <b>Red Knot</b> (Federally Threatened) – Chandeleur Island regularly support large numbers of Red Knots during migration <sup>3</sup>	
Pelicans	Brown Pelican	Breed on high dunes and black mangroves, forage in open water - Breeding, foraging, loafing	Delisted but still hold G4, S3 ranking. Historically the largest nesting colony in the Gulf <sup>10</sup>	Louisiana Comprehensive Wildlife Conservation Strategy (Wildlife Action Plan)  Annual Brown Pelican monitoring and banding <sup>11</sup>

Category/Guild	Species	Habitat Association	Value/Special Considerations	Restoration Plans
Secretive Marsh Birds <sup>1</sup>	Clapper Rail, Purple Gallinule, Pied-billed Grebes	Emergent marsh - Breeding, foraging, loafing	n/a	
Colonial wading Birds	Reddish Egret, Snowy Egret, Great Blue Heron, Tricolored Heron	High dune/woody veg including black mangrove – nesting/roosting	Reddish Egret (G4, S1) – Bird of conservation concern in Louisiana	Louisiana Comprehensive Wildlife Conservation Strategy (Wildlife Action Plan)
Gulls and Terns	Laughing gull, Chandeaur Gull <sup>15</sup> , Royal Tern, Caspian Tern, Sandwich Tern, Black Skimmer, Sooty Tern, Common Tern, Least Tern, Forster’s Tern, Gull-billed Tern	Sandy beach habitat – Breeding, loafing	Caspian Tern (G5, S1 S2B, S3N) Least Tern (G4T3Q, S1B) Gull-billed Tern (G5, S2)  Gulls and Terns make up the largest group of nesting birds on Breton NWR <sup>1</sup>	Louisiana Comprehensive Wildlife Conservation Strategy (Wildlife Action Plan)
Sea Turtles	Loggerhead Sea Turtle, leatherback, Kemp’s ridley, green	Seagrass beds for foraging and shelter <sup>2, 6</sup>	Primary sea turtle nesting outside of Florida once occurred on Chandeaur Island but nesting activity has declined over time <sup>7</sup>	Monitoring by Gulf of Mexico Marine Assessment Program for Protected Species (GoMMAPPS) <sup>C</sup>
Marine Mammals	West Indian manatee <sup>19</sup> , common bottlenose dolphins <sup>24</sup>	Seagrass beds for foraging, shallow sound for resting and foraging	West Indian manatee - ESA listed Threatened; Marine Mammal Protection Act - Very limited reports of occurrence at Chandeaur Islands	
Fish	Perch, anchovy, croaker, mullet, goby, grouper, pinfish, silver jenny, silverside, catfish, herring, stingray, menhaden, shad, seatrout, flounder, mullet, lemon shark	Seagrass beds: perch, anchovy, silverside, croaker, seatrout, mullet, goby, grouper <sup>11, 23</sup> , (in demersal seagrass: pinfish, silver jenny, in intertidal seagrass: catfish, croaker, herring) <sup>12</sup> Muddy/sandy bottoms: Stingray, anchovy, silverside, menhaden, shad, seatrout, croaker, flounder, mullet <sup>11</sup> Surf Zone: anchovy, menhaden, mullet, stingray <sup>11</sup>	Lemon shark (Near Threatened) – Chandeaur Islands are a nursery ground for immature sharks – the only area in northern Gulf of Mexico where they have been recorded <sup>13</sup>	

Category/Guild	Species	Habitat Association	Value/Special Considerations	Restoration Plans
Invertebrates	Arthropods (e.g., blue crab, hermit crab, grass shrimp, brown shrimp, white shrimp), mollusks (e.g., marsh periwinkle, olive nerite), and annelids	Seagrass beds: blue crab, hermit crab, shrimp, quahog <sup>11</sup> Muddy/sandy bottoms: mantis shrimp, white shrimp, brown shrimp, grass shrimp, ghost shrimp, blue crab, horseshoe crab, hermit crab <sup>11</sup> Salt marsh: fiddler crabs, shrimp, ribbed mussel, marsh periwinkle, olive nerite <sup>11</sup> Surf Zone: blue crab, mole crab, coquina clam, ghost shrimp <sup>11</sup>	- Contribution of substantial secondary productivity to local marine food webs supporting critical fisheries <sup>20, 21</sup> - Critical roles in nutrient cycling, organic matter burial, and remineralization through bioturbation and bioirrigation activities <sup>22</sup>	USFWS Delta and Breton NWRs Wildlife Inventory Plan <sup>1</sup>
Seagrass	<i>Thalassia testudinum</i> , <i>Ruppia maritima</i> , <i>Halodule wrightii</i> , <i>Syringodium filiforme</i> , <i>Halophila engelmannii</i>	Waters with high salinity, low nutrients, low turbidity	- Chandeleur Islands support the only marine seagrass beds in Louisiana <sup>14</sup> - Serve as the base of nearshore food webs <sup>6</sup> - Provide habitat and shelter for fish, inverts, sea turtles, birds <sup>5, 2, 6</sup> - Provide direct and indirect ecological connectivity between intertidal nearshore habitats and deeper subtidal habitats <sup>6</sup> - Remove nutrients from the water column <sup>6</sup> - Trap sediments and improve water clarity Stabilize sea bottom <sup>6</sup> - Ecosystem indicators of surrounding nutrient conditions <sup>14</sup>	Gulf of Mexico Alliance (GOMA) Seagrass Community of Practice (CoP) <sup>17</sup>  Gulf-wide Seagrass Monitoring and Needs Assessment Workshop Report <sup>16</sup>

The seagrass beds found along the islands are of particular importance as they provide shelter (structured habitat) and food (primary productivity) for hundreds of species including migratory waterfowl, sea turtles, marine mammals, fish, and invertebrates. Seagrasses also serve a role in improving water quality and in connecting nearshore and subtidal habitats (Deepwater Horizon Natural Resource Damage Assessment Trustees, 2016; Heck et al., 2008). The Chandeleur Islands attenuate wave energy from the open Gulf of Mexico (Georgiou & Schindler, 2009a), creating habitat suitable for seagrasses on the shallow flats on the lee side of the islands. These seagrass meadows provide an important nursery ground for many commercially and recreationally important fishes and are potentially important in dispersion and recruitment of nekton in a westerly direction along the northern Gulf of Mexico (Ellinwood, 2008; Fodrie et al., 2020). For these seagrass meadows to persist, they require wave attenuation and reduction in water current within the backbarrier lagoon (Darnell et al., 2017).

Beyond the wave attenuation and current reduction benefits the barrier islands provide locally to the seagrass beds, the Chandeleurs also modulate estuarine salinities in the region. Without the island chain in place, the high salinity waters of the Gulf of Mexico would penetrate further into Chandeleur Sound and be transported into Mississippi Sound and elsewhere (Reyes et al., 2005; Schindler, 2010). These shifts in salinity would significantly alter the estuarine character of the entire system and would likely cause large-scale shifts in the abundance and distribution of many species (Park et al., 2014). In addition, increased salinity could accelerate land loss in the Biloxi Marsh, Lake Pontchartrain, and the Pearl River Delta (Alymov et al., 2017, 2017; CPRA, 2017).

Based on the background information synthesized above, a conceptual model was developed illustrating the ecological benefits of the Chandeleur Islands (Figure 4).

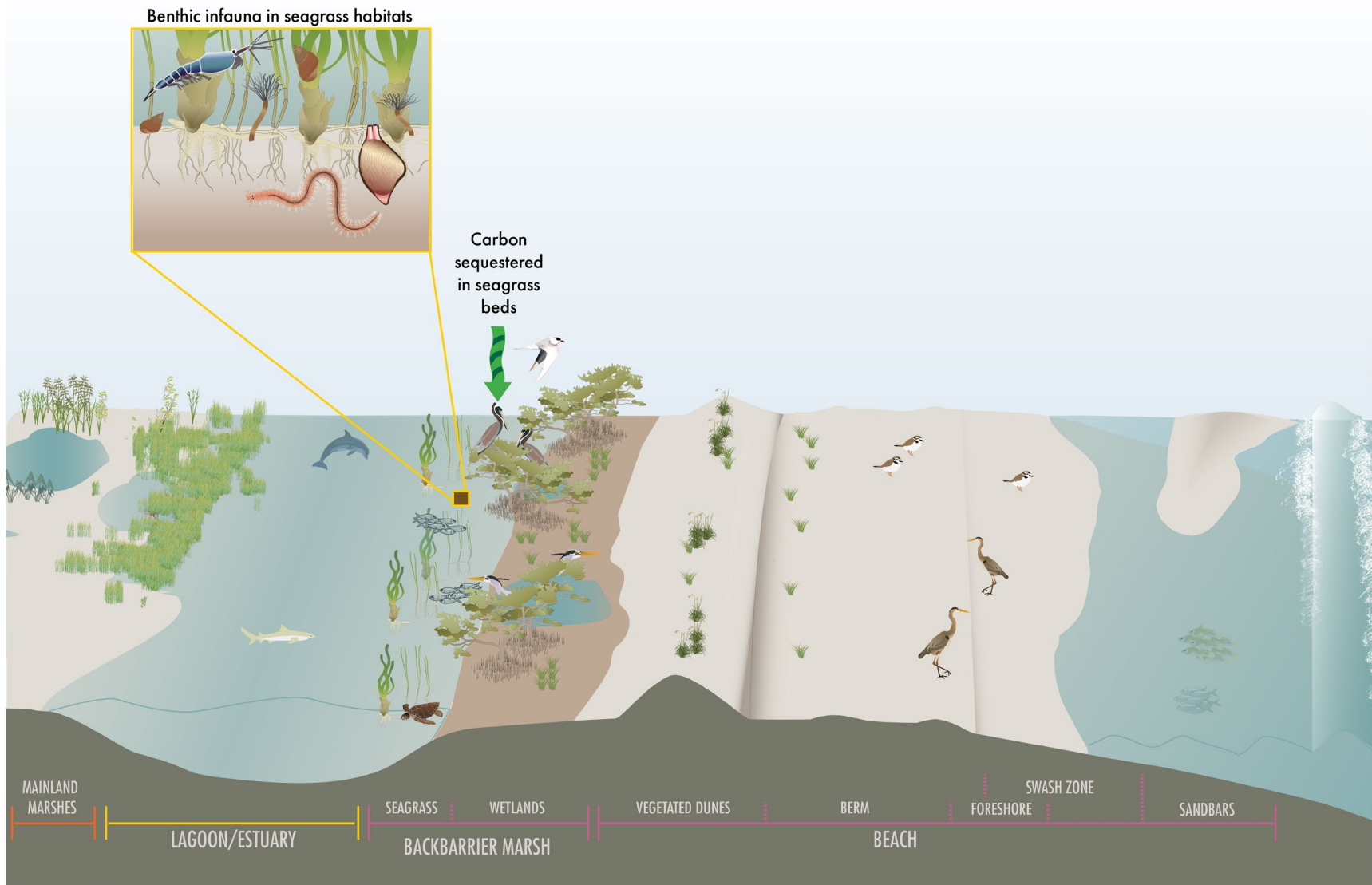


**Figure 4. Ecogeomorphic conceptual model for the Chandeleur Islands.**

## Chandeleur Islands: Geomorphology and Long-term Evolution

### Key Findings and Implications for Restoration

- Large volumes of sand have accumulated over time in a thick subaqueous spit platform at the northern flank of the island arc (Hewes Point). This downdrift sand reservoir lies outside of the littoral system and provides a unique opportunity as a resource for nourishing the updrift barrier system (i.e., the central arc).
- North of Redfish Point, much of the remaining sections of island today are built over thick spit platform sands. When the islands originally formed and built laterally to north, successive recurved spits extended into the backbarrier to become the foundation for the backbarrier marshes observed over the historical record. As the shoreline and shoreface erode, these relict spit platform sands are liberated in the surf zone and naturally nourish the island north of Redfish Point.
- The backbarrier marshes that extend into the sound are critical for the long-term resiliency of the islands. They provide a platform for island rollover and a sand source once eroded, and after major storms they also serve as nucleation sites for bar welding and spit development. This process of island stabilization supports a longshore sediment transport system that distributes sediment along the island, providing beach and dune habitat and preserving island integrity to protect the backbarrier and enable establishment of seagrass meadows.
- Once the Gulf shoreline erodes into the backbarrier marsh shoreline (i.e., it consumes the marsh platform entirely), a threshold is crossed that results in the islands eroding faster, becoming ephemeral and ultimately turning into submerged subaqueous shoals.

### 2.3. CHANDELEUR ISLANDS: GEOMORPHOLOGY AND LONG-TERM EVOLUTION

#### 2.3.1 Deltaic Abandonment and Early Island Evolution

The Mississippi River delta plain was produced by deposition of multiple, spatially and temporally offset delta complexes fed by distributary channel systems that developed as the river's main trunk stream channel bifurcated (divided into smaller channels) and expanded into open water (Fisk, 1944; Roberts, 1997; Russell, 1936). Chronological alterations in the location of an active delta complex were the result of delta switching (i.e., avulsion, the process by which a new channel becomes occupied thereby capturing the majority of the flow, while the former channel is slowly abandoned and forms a bayou). With each avulsion event, a new distributary network and attendant delta complex was formed. In total, the Holocene delta plain consists of six delta complexes: Maringouin (active from 7,500 – 5,000 yrs BP), Teche (5,500 – 3,800 yrs BP), St. Bernard (4,000 – 1,800 yrs BP), Lafourche (2,500 – 400 yrs BP), Balize (1,000 yrs BP – present), and Atchafalaya (400 yrs BP – present) (Chamberlain et al., 2018; Coleman, 1988; Frazier, 1967; Kolb & van Lopik, 1958; Penland et al., 1988; Roberts, 1997; Tornqvist et al., 1996; Figure 5). Subsequent to abandonment by the river, previously active delta lobes become erosional headlands, and subsidence and marine reworking results in the landward migration of the shoreline. The headland sediment is reworked laterally by waves and storm impacts to form barrier islands that

eventually undergo submergence and reworking to form inner-shelf shoals (Kwon, 1969; Penland et al., 1988).

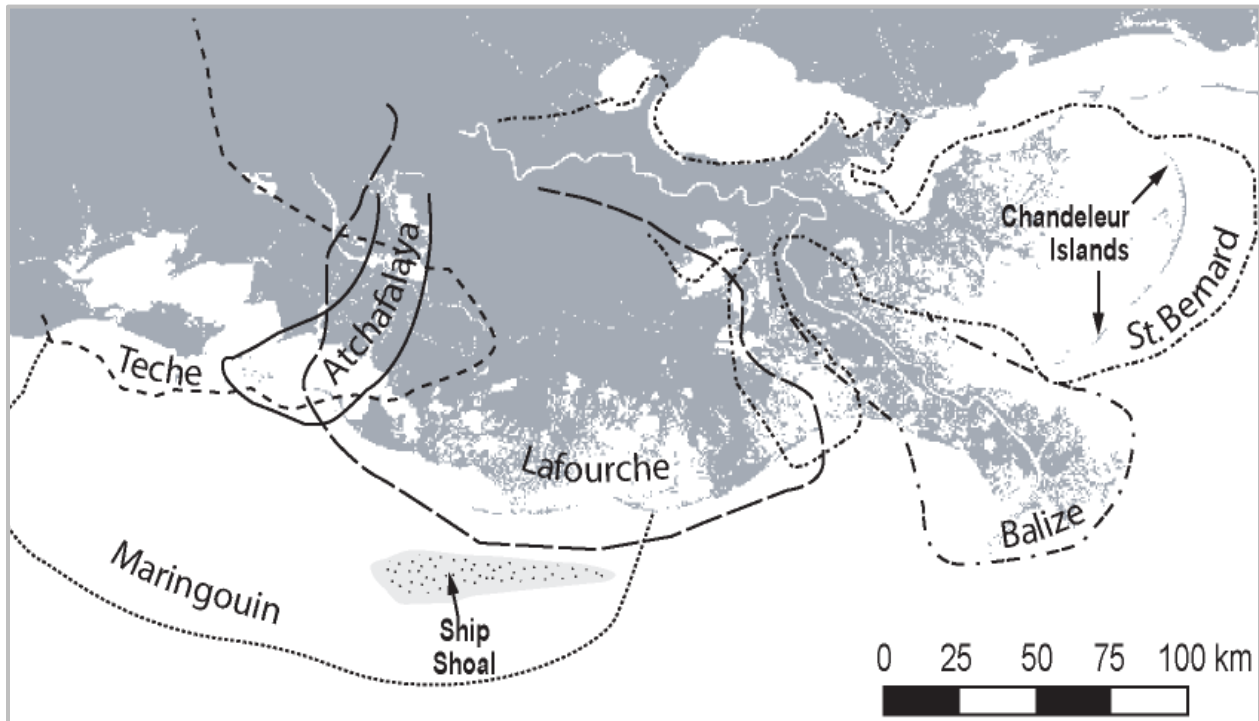


**Figure 5. Map of the Holocene Mississippi River delta plain that shows the multiple, spatially offset depocenters for each delta complex. Depocenter shifts result from upstream fluvial avulsions, the infilling of accommodation space within interdistributary basins, and ultimately deltaic progradation. Mid Holocene deposition started with the Maringouin-Teche complexes (7,500–3,800 yrs BP), followed by St. Bernard (4,000–2,000 yrs BP), Lafourche (2,500–400 yrs BP), and modern deposition at the Balize (1,000 yrs BP–present) and the Atchafalaya (400 yrs BP– present). Names, location, and chronology for delta complexes are derived from Frazier (1967), Penland et al. (1988), Törnqvist et al. (1996), Roberts (1997), and Kulp et al. (2005, p. 2005).**

Penland et al. (1988) conceived a conceptual model that depicts the geomorphic evolution of deltaic headland abandonment leading to development of barrier islands that ultimately become submerged to form an inner-shelf shoal (Figure 6). The model is presented in three distinct stages, each representing the landscape transition in response to dominant driving forces transitioning from river-dominated with high sediment supply to marine-dominated and sediment starved. During Stage 1, the abandoned deltaic headland is reworked to form an erosional headland with flanking barrier islands. Submergence and interior wetland erosion due to subsidence and decreased fluvial sediment supply leads to mainland detachment and formation of a Stage 2 transgressive barrier island arc. In Stage 3, continued subsidence results in transgressive submergence of the island arc to form an inner-shelf barrier shoal (Penland et al., 1988). It is important to note that throughout this evolution, sand is continually reworked and transported laterally away from the original centralized delta sand deposits and out to the flanks of the barrier system. Ultimately, this process exhausts the sand supplies needed to maintain barrier island exposure and forces transgressive submergence: conversion of the barrier islands to submerged shoals (Stage 3).

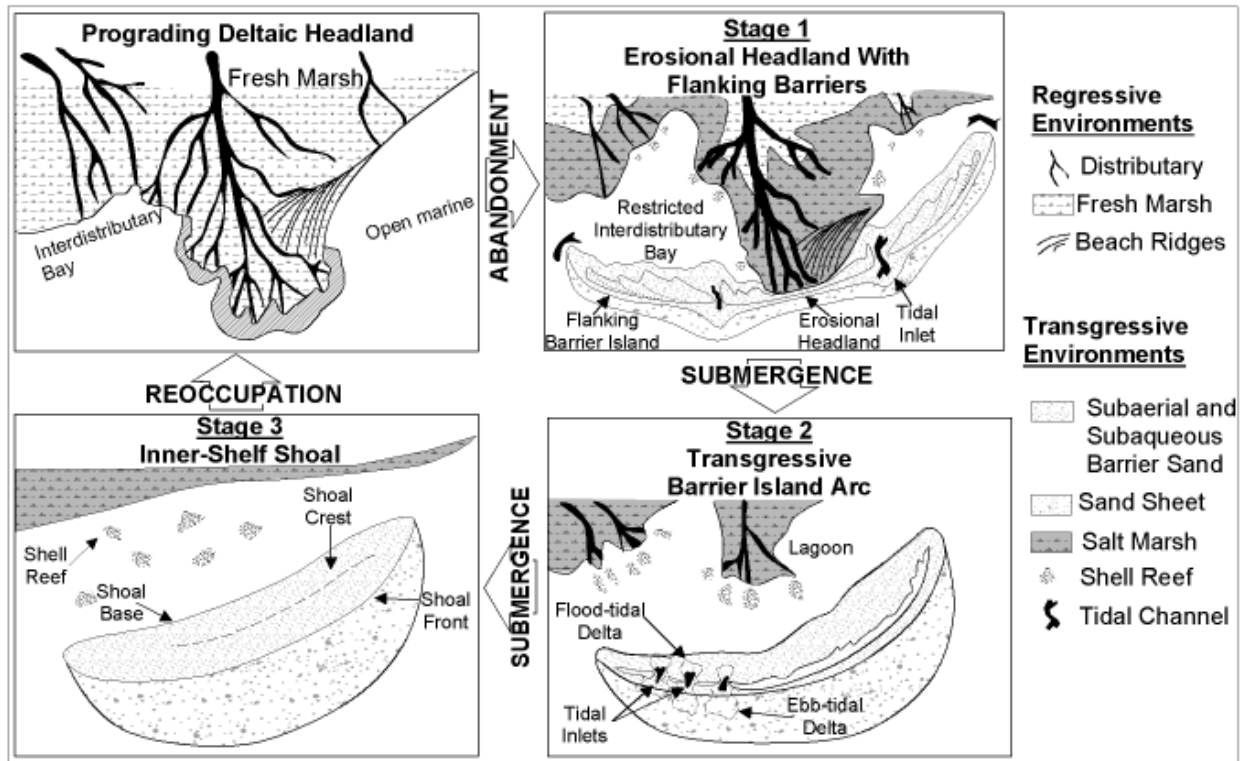


**Figure 6. Three-stage model conceived by Penland et al. (1988) for the formation and evolution of transgressive Mississippi River delta barrier islands. Deltaic abandonment results in the formation of a Stage 1 erosional headland with flanking barriers separated by tidal inlets. RSLR and marsh erosion results in mainland detachment and the formation of a Stage 2 transgressive barrier island arc. In Stages 1 and 2, lateral transport dominates and sand is shed from the central portion of the system to the flanks. Continued RSLR and loss of sediment to deep water sinks results in transgressive submergence and the formation of a transgressive inner-shelf shoal. From Kulp et al. (2005) modified from Penland et al. (1988). The Chandeleur Islands are presently in late Stage 2.**

The Chandeleur Islands represent a Stage 2 barrier island arc in the Penland et al. (1988) conceptual model, the product of abandonment and reworking of the St. Bernard delta complex (Frazier, 1967; Penland et al., 1988). The most recent distributary active in the region is associated with Bayou La Loutre that was abandoned by fluvial processes approximately 1,800 yrs BP (Frazier, 1967; Rogers et al., 2009). Shoreline development and barrier geometry are controlled by orientation of the abandoned deltaic headland relative to the dominant wave approach. Wave-induced lateral transport is the most significant factor in the development of a Louisiana barrier coastline (Penland & Boyd, 1981) and produces sand-rich flanking barrier islands as recurved spits develop and prograde (build out) away from the original deltaic sediment source (Figure 7). Because the transgressive shoreline is naturally isolated from the continuous sediment load of the Mississippi River, there is a finite and punctuated supply of sand for natural island maintenance. In earlier stages of barrier development, a significant sand source is derived from erosion of deltaic deposits by waves. Once the deltaic sediment source has been completely reworked or has subsided below effective wave base of ~7–8 m for the Chandeleur Islands (Miner et al., 2009d; Penland & Boyd, 1981), the barrier and lagoonal deposits are continually recycled at the shoreface during retreat. For a period of time, this allows the barrier system to maintain its exposure during RSLR. Much of this sand recycling during shoreface retreat is not in the form of hurricane overwash deposits that eventually

become exposed at the shoreface (although this is a component), but by recycling of relict recurved spit and large terminal spit deposits at the shoreface (Figure 8). Figure 9 is a stratigraphic cross section demonstrating the relationship between these sandy lateral accretion deposits that underlie the northern half of the Chandeleur Islands from Redfish Point, north to Hewes Point and the mud-rich deltaic deposits that underlie the southern half of the islands in the vicinity of Monkey Bayou that coincides with the former location of Bayou La Loutre.

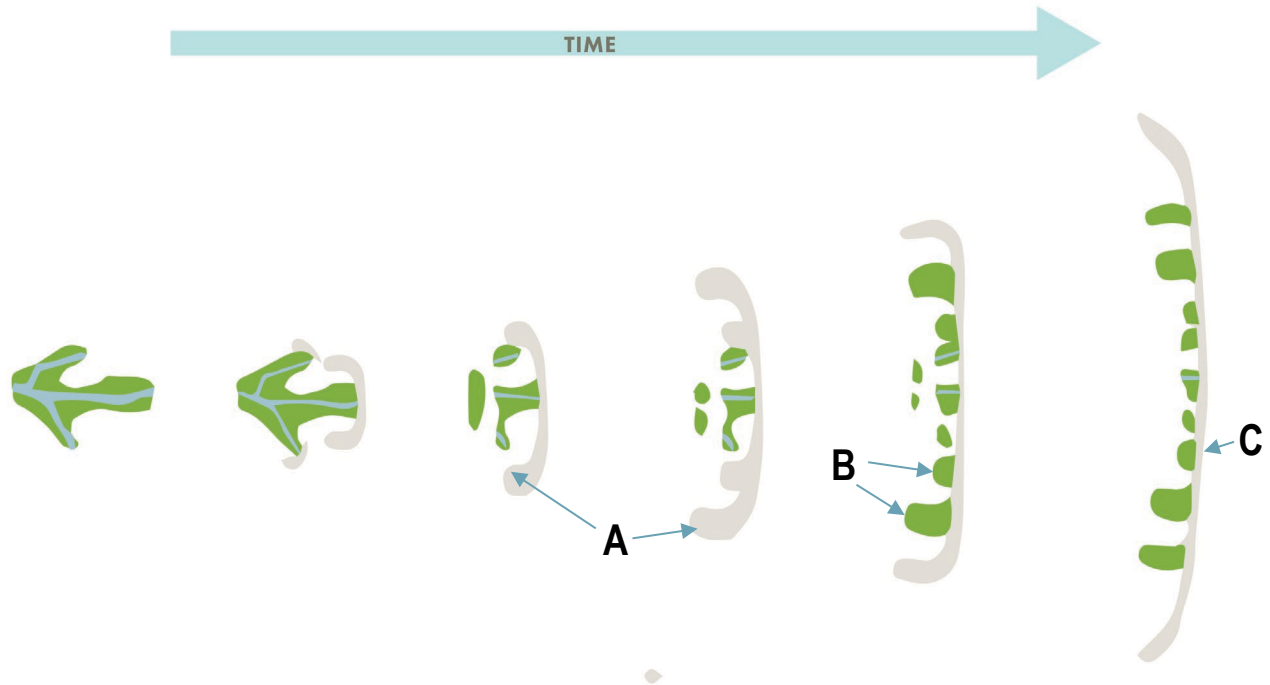


**Figure 7. Conceptual model for development of the Chandeleur Islands backbarrier marshes through lateral spit accretion and progradation of recurved spits into the backbarrier (A). As the island continues to grow laterally, the relict recurved spit deposits serve as platforms for emergent marsh colonization in the protected backbarrier environment (B). As the Gulf shoreline erodes and the beach/dune system migrate landward, these relict spit deposits outcrop on the Gulf shoreface (C) and serve to reintroduce sand to the active littoral system for further spit building downdrift.**

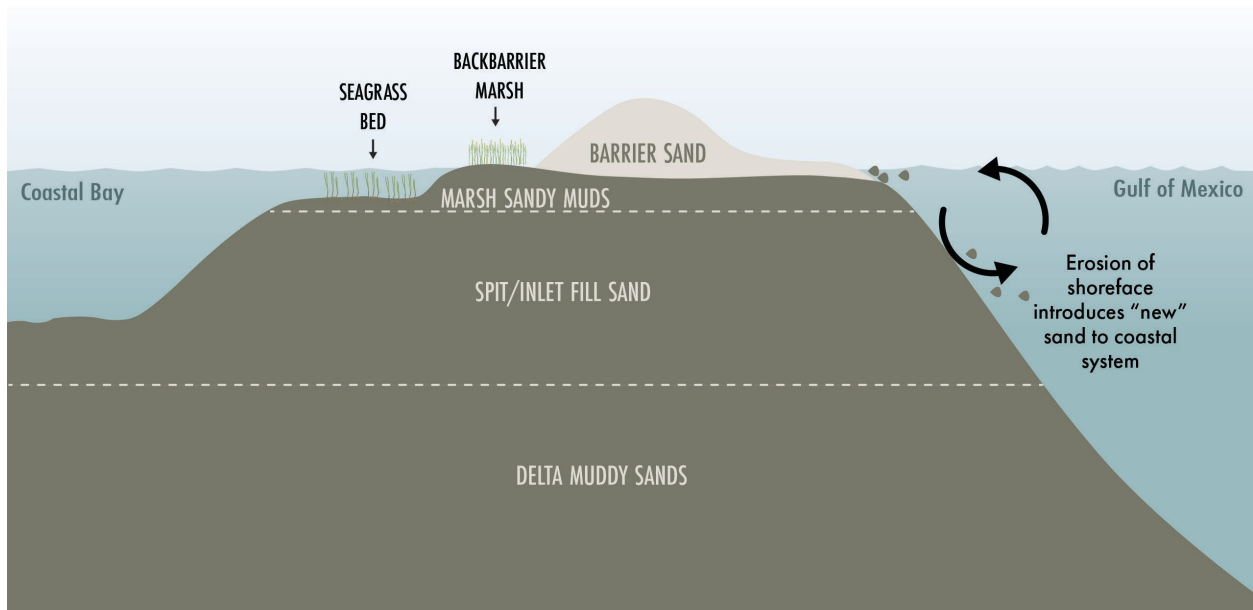


**Figure 8. Conceptual model in profile view of the northern Chandeleur Islands stratigraphy. This section of the island chain overlies thick spit/inlet fill deposits that were laid down as the island migrated laterally to the north during early phases of island evolution. In its present state, erosion by waves at the shoreface erodes this spit/inlet fill sand. That sand is injected into the active coastal system and transported onshore. In this way, the erosion and retreat of the shoreface serves to reintroduce this sand to form beaches and dunes and this process (and the sandy substrate) is responsible for the relative resiliency of this sector of coast that extends from Redfish Point north to just above Schooner Harbor (see Figure 2 for locations).**

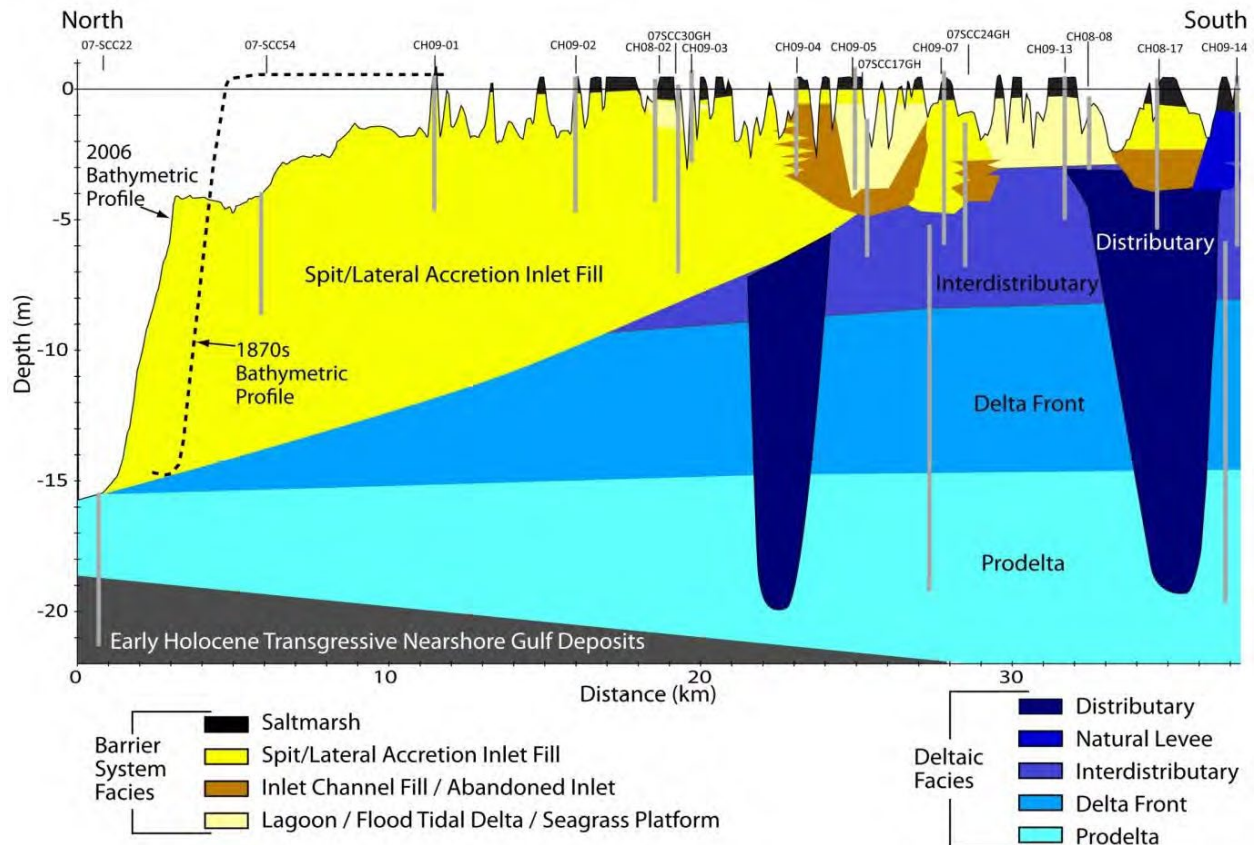


**Figure 9. Geologic cross-section trending along the northern Chandeleur island arc from the Hewes Point spit platform in the north to Monkey Bayou in the south (see map in Figure 2 for locations). Bathymetric profiles from Miner et al. (2009d). Subsurface data from University of New Orleans Pontchartrain Institute for Environmental Sciences (UNO-PIES) and U.S. Geological Survey (USGS) vibracores (unpublished and Flocks et al., 2009), high-resolution shallow seismic profiles (Twichell et al. [2011] and USACE [1958]). Note that the salt marsh north of Redfish Point (location of core CH-09-07 on cross-section) is underlain by sandy spit and sandy lateral accretion inlet fill deposits that thicken to the north whereas salt marsh south of this location is underlain by muddy relict deltaic and lagoonal deposits. This cross-section demonstrates in alongshore view the importance of lateral sand transport in the development and ultimately, the demise of Louisiana transgressive barrier islands. Also note that the dashed line representing the 1870s position of the Hewes Point spit relative to the 2006 bathymetric profile. Approximately 170 million cubic yards ( $130 \times 10^6 \text{ m}^3$ ) of sand has accumulated north of Hewes Point since 1870s.**

### 2.3.2 Historical Evolution and Modern Barrier Island Morphology

The historical evolution is documented in seafloor change analysis conducted by Miner et al. (2009e, 2012). Detailed accounts of the historical shoreline change and seafloor changes along the Chandeleur Islands can be found in Martinez et al. (2009); Fearnley et al., (2009a, 2009b); and Miner et al. (2009b, 2012). What follows is a summary of those reports with a focus on long-term sediment dynamics and shoreface evolution that provide an important background and basis for island management designs herein.

Gulf shoreline retreat rates average  $\sim 15 \text{ m/yr}$  ( $\sim 50 \text{ ft/yr}$ ) for 1855–2008 (Martinez et al., 2009). These historical retreat rates are not associated with efficient conservation of sand in a landward direction,

landward translation of the barrier island footprint, or formation of new backbarrier marsh. Instead, lateral transport to the flanks of the island arc (north of Hewes Point) was the dominant trend driving island evolution during the historical record (1855–2005). The results from the BICM historical seafloor change analysis (Miner et al., 2012) are presented in Figure 10.

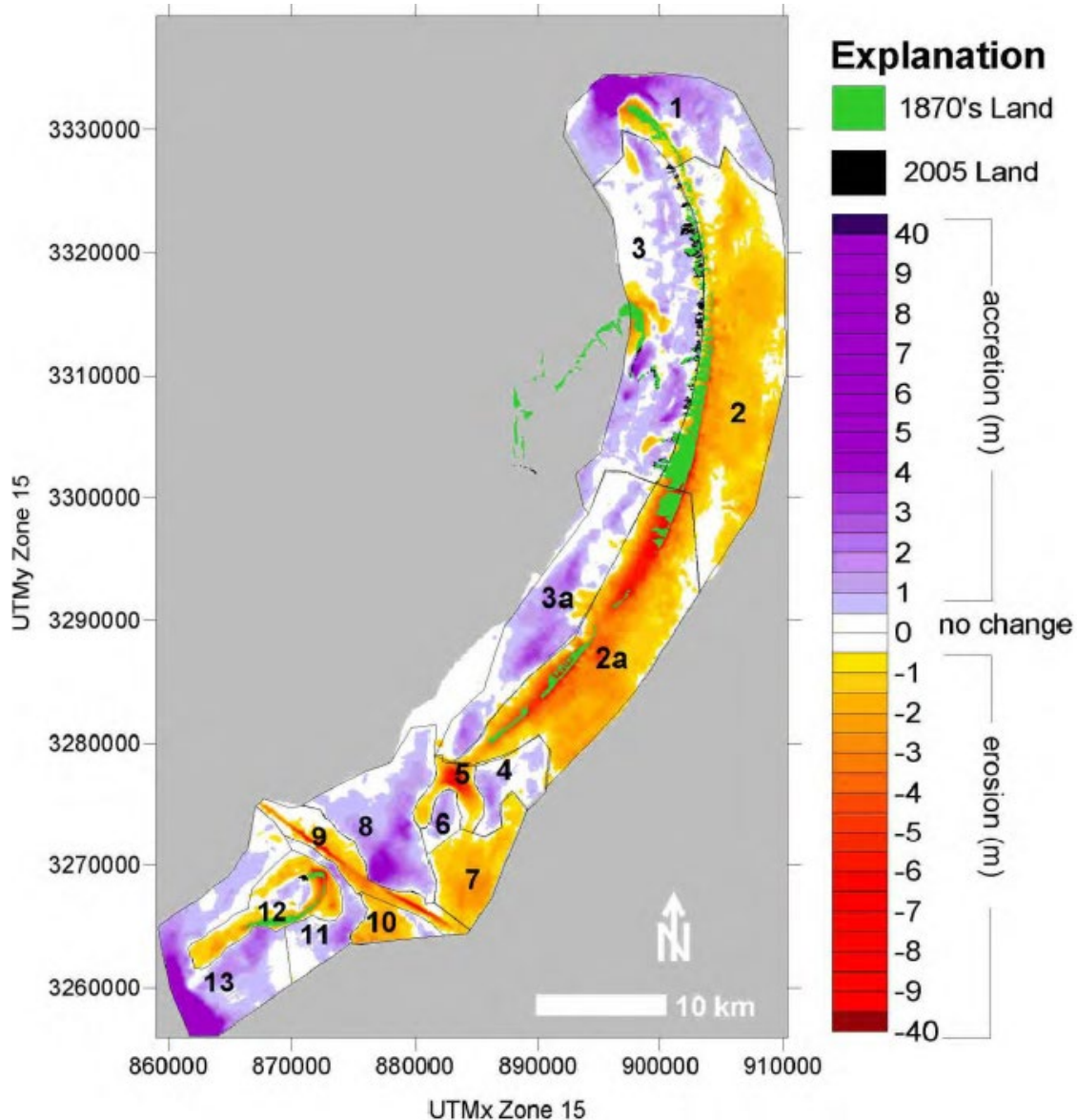


**Figure 10. Map of BICM1 seafloor change analysis results for the Chandeleur Islands showing zones of sediment erosion and accretion for the time period 1870-2007. Numbered polygons delineate zones for which sediment volumetric change data are presented in Table 2. Note the widespread erosion along the shoreface fronting the island chain and depositional sinks at the flanks in the north and south. These results demonstrate that during the 125 years covered by the BICM1 analysis, approximately  $300 \times 10^6 \text{ m}^3$  (392 million cubic yards) of sand accumulated in deepwater sinks at the flanks of the barrier island arc; twice as much of the volume deposited in the backbarrier. This net loss of sediment to flanking sinks has resulted in island area reduction from  $44.5 \text{ km}^2$  [ $17.2 \text{ mi}^2$ ] in 1855 to  $4.6 \text{ km}^2$  [ $1.8 \text{ mi}^2$ ] in 2005 (Fearnley et al., 2009b; Miner et al., 2009d). Island area shoreline polygons from 1855/69 and 2005 are from Martinez et al. (2009). Bathymetry**

and shoreline change analysis from Miner et al. (2009d). Figure reproduced from Miner et al. (2009c).

**Table 2. Sediment erosion/accretion change volumes for the geomorphic zones delineated as polygons in Figure 10. Dz min = largest magnitude of vertical erosion within each polygon; Dz max = greatest magnitude of vertical accretion within each polygon. Data from Miner et al. (2012). Reproduced from Miner et al. (2009d).**

Zone	Accretion ( $\times 10^6 \text{ m}^3$ )	Erosion ( $\times 10^6 \text{ m}^3$ )	Net Vol ( $\times 10^6 \text{ m}^3$ )	Area ( $\times 10^6 \text{ m}^2$ )	Net vol Error +/- ( $\times 10^6 \text{ m}^3$ )	Dz min	Dz max
1. Hewes Point/ North Inlet	147.03	-18.26	128.77	91.67	25.67	-4.28	10.82
2. Northern Chandeleur Shoreface	4.68	-289.98	-285.29	212.19	59.41	-8.06	1.5
3. Northern Chandeleur Backbarrier	110.61	-26.50	84.11	166.76	46.69	-3.68	5.88
2a. Southern Chandeleur Shoreface	1.49	-406.63	-405.14	163.52	45.78	-8.89	1.70
3a. Southern Chandeleur Backbarrier	80.19	-4.72	75.47	84.92	23.78	-2.32	3.30
4. Updrift Curlew Pass Ebb Delta	14.30	-1.62	12.68	24.78	6.94	-1.20	2.85
5. Curlew Pass Inlet Scour	0.66	-34.27	-33.61	18.93	5.30	-7.20	1.40
6. Downdrift Curlew Pass Ebb Delta	7.74	-0.35	7.39	9.33	2.61	-0.64	2.82
7. Grand Gosier Shoreface	0.29	-56.29	-55.99	40.61	11.37	-3.43	0.81
8. Updrift MRGO	91.20	-0.16	91.04	70.41	19.71	-1.00	4.67
9. MRGO	0.10	-52.18	-52.08	25.34	7.10	-8.54	1.91
10. Downdrift MRGO shoreface	1.72	-21.35	-19.62	15.88	4.45	-3.43	1.85
11. Breton Pass Ebb delta and inlet fill	20.17	-0.13	20.04	20.69	5.79	-1.18	3.23
12. Breton Island Nearshore/Backbarrier	3.45	-51.03	-47.58	39.49	11.06	-7.95	1.33
13. Downdrift Breton Island	176.46	-0.10	176.35	74.98	2.10	-0.59	12.18
<b>TOTAL</b>	<b>660.09</b>	<b>-963.57</b>	<b>-303.47</b>	<b>1,059.49</b>	<b>296.66</b>		

Results from the previous studies capture a transition from relatively sediment-rich barriers (1855–1922) that build new land in the backbarrier by overwash, flood tidal delta, and recurved spit formation to sediment-starved barriers that no longer build new backbarrier land and begin to thin in place (1922–2005). Once the thinning has reached the point where no backbarrier marsh exists, the barriers cross the transgressive submergence threshold becoming mobile sand bodies that migrate landward through a cycle encompassed by storm destruction followed by emergence landward of their former positions during calm weather (Figure 11).

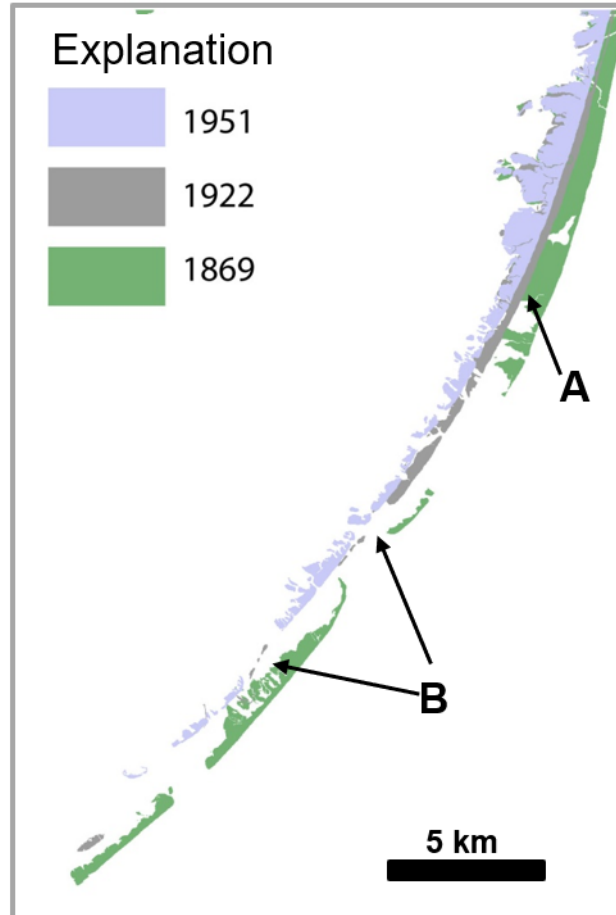


**Figure 11. Map showing island positions of the southern Chandealeur Islands from Monkey Bayou down to Errol Island in the south. Note that in the northernmost portion of the map (A), in the vicinity of Monkey Bayou, Gulf shoreline retreat is not accompanied by island “rollover” with new land forming in the backbarrier. However, more southern portions for the island chain (B) experience rollover that is manifested by almost complete destruction of the islands during major storms (note 1922 islands) and then reemergence in a more landward position during periods of reduced tropical cyclone activity. This landform response now encompasses all of the southern Chandealeurs up to Redfish Point. Data from U.S. Coast and Geodetic Survey.**

The threshold crossing of a barrier island becoming a submerged shoal is characterized by: 1) sand lost to flanks decreases barrier sand supply restricting new backbarrier marsh development, 2) continued loss to flanks forces barrier thinning and segmentation with fragmented marsh islands serving as spit nucleation sites, and 3) Gulf shoreline and backbarrier shoreline meet resulting in sandy ephemeral barrier islands/shoals that are destroyed by storms but reemerge during calm weather landward of their pre-storm location (Figure 11; Fearnley et al., 2009b; Miner et al., 2009d; Nelson, 2017). It is not until this final stage of disintegration that cross-shore sand distribution becomes an efficient enough process to translate the barrier sand body landward during shoreface retreat (Figure 11; Miner et al., 2009d).

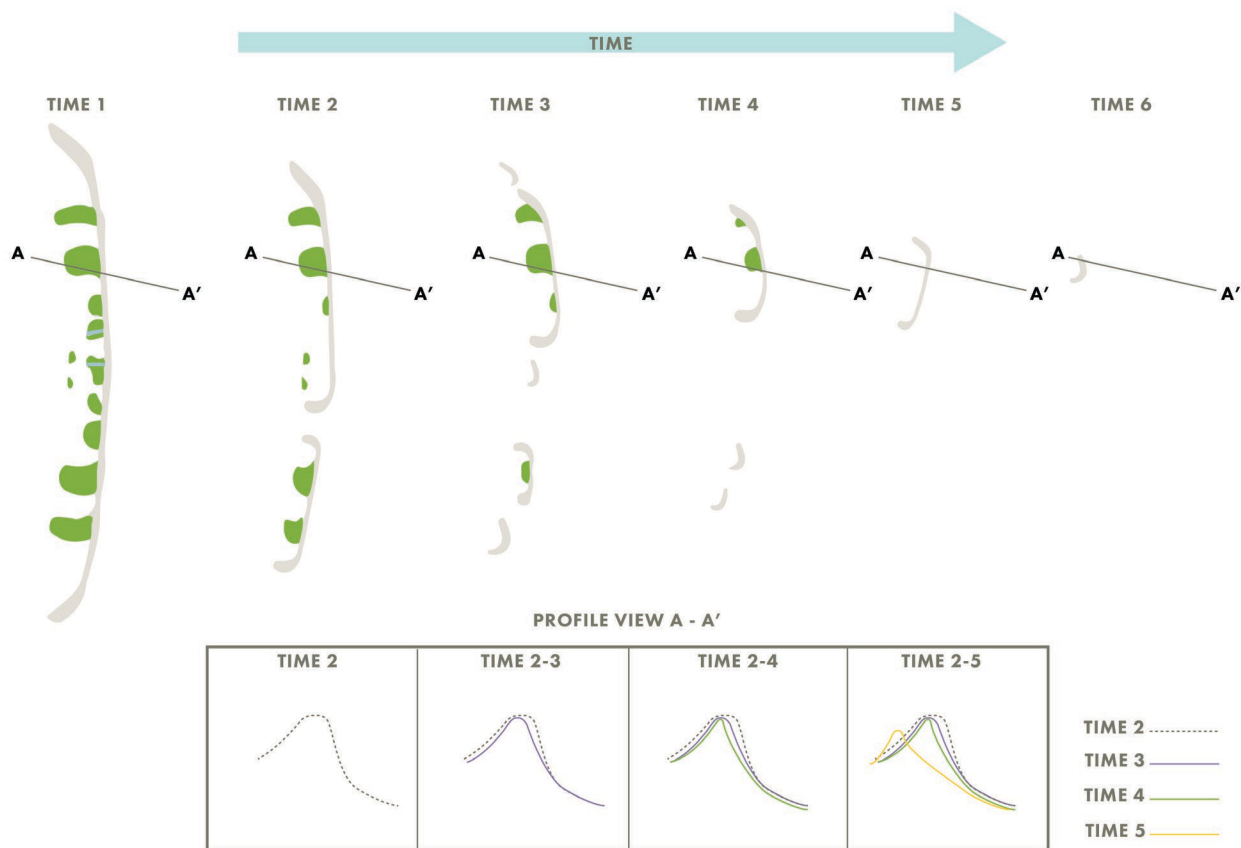


**Figure 11. Conceptual model for the transgressive submergence of the Chandeleur Islands following the lateral expansion (island development) phase depicted in Figure 7. This multistage process is driven by decreased sand supply, relative sea-level rise, and tropical cyclone impacts. The lateral accretion of sand away from the original deltaic sand source (Figure 7) is responsible for building the barrier island system, however sand supply is limited and ultimately the source becomes exhausted. This results in sand-starved central portions of the island chain. Continued Gulf shoreline erosion in a regime of limited sand results in island thinning and segmentation. The relict sandy recurve spit deposits that are overlain by backbarrier marsh continue to provide a localized sand source to the coastal system as they are eroded at the Gulf shoreline. These backbarrier marshes help to stabilize the island and prevent submergence because they serve as nucleation sites for sand to weld to as beaches redevelop after storms. Once the Gulf shoreline has eroded to where the bay shoreline (e.g., backbarrier marshes have been totally eroded), that sector of island enters a new regime dominated by rapid landward migration and ultimately submergence. Modified from Miner et al. (2009d).**

### 2.3.2.1 Role of Tidal Inlets

A tidal inlet is a shore-perpendicular channel along a barrier shoreline that connects the Gulf with bays, lagoons, marsh, and tidal creeks (Brown, 1928; Escoffier, 1940; FitzGerald & Miner, 2021). Tidal currents keep the inlet channel open by flushing of sediment that is transported alongshore by waves (Brown, 1928; Escoffier, 1940). There are five tidal inlets responsible for the majority of tidal exchange between the Gulf of Mexico and the Chandeleur and Breton Sounds and numerous ephemeral hurricane-cut inlets along the northern island arc.

The major tidal inlets in the Chandeleur Islands system are the channels that flank the terminal spits (e.g., Hewes Point) of the barrier arc and include the inlet north of Hewes Point and an inlet that is south of Breton Island. Based on current measurements and numerical modeling, these two channels that flank the island chain are responsible for the majority of tidal flow into and out of Chandeleur and Breton Sounds and the Pontchartrain Basin (Hart & Murray, 1978). North Inlet extends from the backbarrier and curves around Hewes Point where maximum channel depths are >16 m (50 ft). Lateral spit accretion toward the north at Hewes Point has forced a northerly (alongshore) migration of this inlet.

The inlet at the southern extent of the Chandeleur Islands located south of Breton Island has migrated south and undergone considerable infilling, some of which can be attributed to progradation (building out) of the modern Baptiste Collette subdelta of the Mississippi River from the south. Observations during bathymetric surveying and subsequent aerial reconnaissance flights confirm strong tidal currents flowing through this broad channel.

The Mississippi River Gulf Outlet (MRGO), a navigation channel that was deauthorized in 2008, intersects the Chandeleur Islands just north of Breton Island and was cut (12 m [36 ft] deep) through the existing tidal inlet of Breton Island Pass. Although the natural inlet configuration was downdrift-offset (the inlet channel was oriented to the south in an alongshore direction), the MRGO trends perpendicular to the shoreline. The MRGO construction did not result in the abandonment of the natural channel in favor of the engineered one, and both channels remained open. The MRGO required frequent maintenance dredging to remove sand before being decommissioned in 2008. Strong tidal currents flow through MRGO because it is a major conduit for tidal exchange for much of the Lake Pontchartrain Basin. Results from recent surveys show that portions of the MRGO bar channel have infilled (Flocks et al., 2015; Figure 12), allowing for more efficient sediment bypassing to Breton Island. The shoaling of MRGO has also likely facilitated more of the Chandeleur and Breton Sounds tidal prism being conveyed through other inlets including Grand Gosier Pass and Katrina Cut to the north.

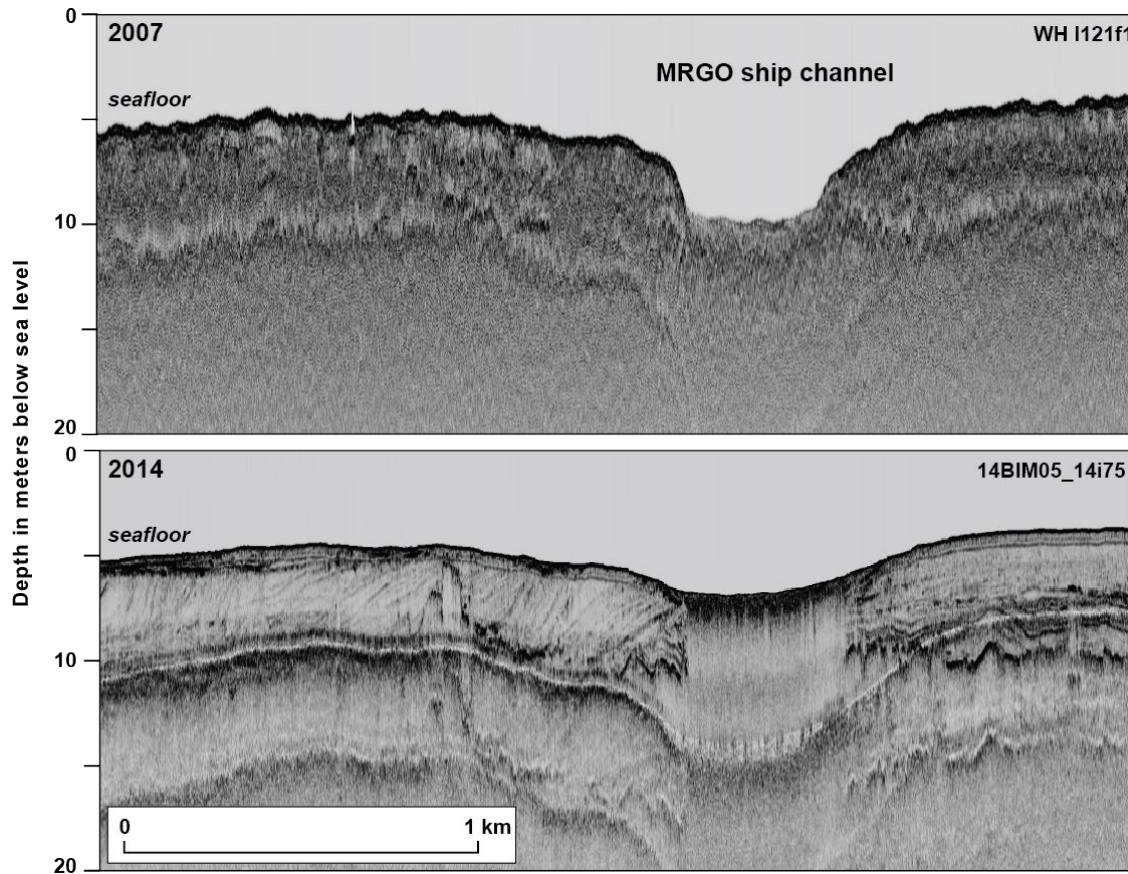


**Figure 12.** Chirp sonar subbottom profiles from 2007 with the exact same transect reoccupied in 2014 crossing the Mississippi River Gulf Outlet (MRGO) navigation channel. MRGO was decommissioned in 2008. Note the infilling in the 2014 profile versus the 2007. From Flocks et al. (2015).

Grand Gosier Pass is a natural tidal inlet located between Curlew and Grand Gosier Shoals that trends perpendicular to Curlew and Grand Gosier Shoals. This inlet was not recorded in bathymetry maps from surveys conducted the 1870s, but by 2007 had scoured to a depth of >9 m (30 ft). The date of inlet formation is not known, but the inlet is denoted on navigational charts dating to the 1950s (McBride et al., 1992). An ebb tidal delta has developed here as indicated by a seaward excursion of the 3 m contour offshore of Curlew Shoal since the 1870s.

‘Katrina Cut’ is located along the southern portion of the northern island arc between Redfish Point and Monkey Bayou. As the name implies this is the site of a breach that occurred during Hurricane Katrina in 2005 that has continued to evolve into a stable tidal inlet with developed flood and ebb tidal deltas. Maximum depth measured in 2015 was 5 m (16 ft).

Numerous ephemeral hurricane-cut inlets along the barrier chain have historically been active for several years after a storm impact and then filled in to form a continuous barrier shoreline along the northern arc during extended periods of calm weather (Kahn, 1986). Hurricane Katrina caused more than 60 hurricane cut tidal inlets to develop (Sallenger Jr. et al., 2009), some of which have not fully healed (closed).

### 2.3.2.2 Backbarrier Platform and Seagrass Beds

As previously discussed, the northern island arc (north of Monkey Bayou) is backed by a broad (maximum width ~ 2.4 km [1.5 mi]), sandy platform that averages ~0.9 to 1.8 m (3 to 6 ft) in depth (Miner et al., 2009d) and contains extensive marine seagrass meadows (Bethel & Martinez, 2008; Poirrier & Handley, 2007). The backbarrier platform is intersected by channels that were scoured during storms. Storm-generated flood tidal deltas have formed landward of deeper hurricane-cut inlets. Besides the vertebrate and invertebrate habitat provided by these seagrasses as discussed in Section 2.2, these seagrass meadows provide important physical benefits to the stability of the Chandeleur Islands by baffling water flow, attenuating wave energy and reducing current velocity, and increasing cohesion of sediment grains within the seagrass below ground biomass (Chen et al., 2007; Georgiou & Schindler, 2009a; Koch et al., 2006). This process results in backbarrier sediment trapping (vertical accretion) and protection of backbarrier marsh shorelines from wave attack in Chandeleur Sound. The latter is important at the Chandeleurs because of the large fetch distance across Chandeleur Sound, especially during the passage of winter cold fronts (Georgiou & Schindler, 2009a). These seagrass beds are highly resistant to hurricanes and recover rapidly after storms when destroyed; however, the occurrence and distribution of seagrass at the Chandeleur Islands is directly related to the presence of a fronting barrier island (Bethel & Martinez, 2008; Darnell et al., 2017; Poirrier & Handley, 2007). The island dissection and rapid land loss since Hurricane Katrina has resulted in decreased suitable conditions for the seagrass colonization (Bethel & Martinez, 2008; Darnell et al., 2017).

### 2.3.2.3 Spits

A spit is a sandy ridge attached to land at one end and terminating in open water at the other (Evans, 1942). Spits are built by lateral accretion of sand due to wave-induced transport. Spits accrete laterally over the subaqueous spit platform, which progrades ahead of the subaerial spit. Seasonal variations in wave approach and the refraction of waves bending around the spit end often form a hook-shaped recurved spit that extends into the backbarrier (Figure 13). Lateral accretion of a terminal spit (at the end of a barrier island) usually results in development of a thick sand body because the leading edge of the prograding spit fills a relatively deep inlet channel (Figure 14; Hoyt & Henry Jr., 1967). Hewes Point is the terminal spit system at the northern end of the Chandeleur Islands and has historically prograded north (Figure 7), due to northerly direct longshore transport, into the marginal deltaic basin that flanks the St. Bernard delta complex (Miner et al., 2009d; Twichell et al., 2011). The scale of this terminal spit accretionary process is important because it demonstrates how an abandoned deltaic headland is reworked by marine processes to form Stage 1 flanking barriers, and eventually a Stage 2 barrier island arc (Figure 6; Penland et al., 1988). Lateral spit accretion remains an important process throughout Stage 2, as shown by the lateral accretion of Hewes Point in a northerly direction (Penland et al., 1988); this concept is important to informing the restoration strategy discussed later.



**Figure 13. Oblique aerial photograph from 2008 at Monkey Bayou along the Chandeleur Islands. View is to the west with the Gulf of Mexico in the foreground and Chandeleur Sound in the background. Note the sandy recurved spits that extend into the backbarrier**

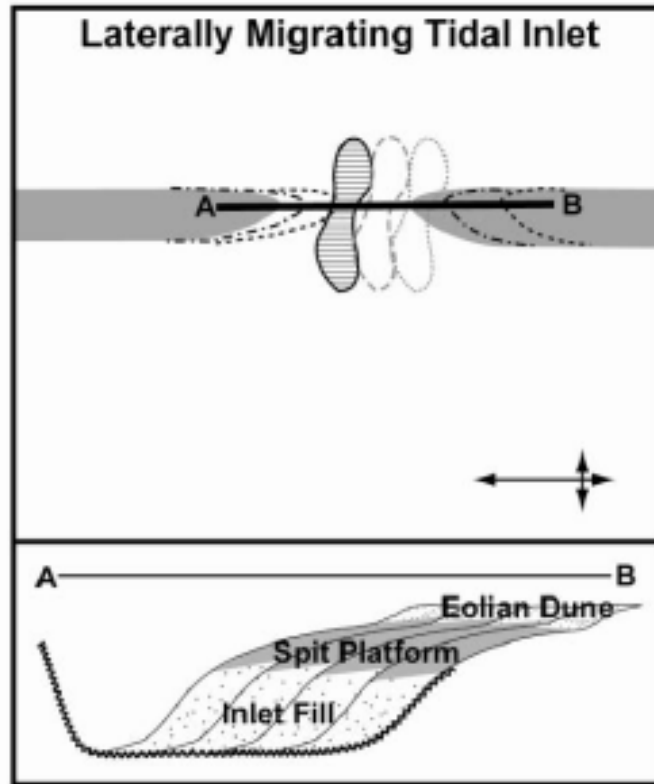


**Figure 14. Conceptual model for a laterally migrating inlet and the attendant inlet fill and spit platform. This is the process responsible for development of the northern Chandeleur Islands north of Monkey Bayou as sand reworked from the abandoned delta deposits was reworked by waves and transported laterally to the north, ultimately building Hewes Point and the large sand deposit north of Hewes Point. This also resulted in thick sands underlying the northern part of the arc that get reintroduced to the active coastal system as the shoreface erodes. From Miner et al. (2007) modified from Hoyt and Henry (1967).**

#### 2.3.2.4 Ephemeral Barrier Islands and Barrier Shoals

The ephemeral barrier islands and barrier shoals that occur along the Chandeleur Islands are present in the southern portion south of Monkey Bayou and include Curlew and Grand Gosier Islands. These are ephemeral barrier islands that are destroyed during storms and reemerge during extended periods of minimal tropical cyclone activity (Fearnley et al., 2009b; Miner et al., 2009d; Nelson, 2017; Otvos, 1981; Penland & Boyd, 1985). The same factors leading to submergence and inhibiting reemergence have also forced other historically more stable portions of the Chandeleur Islands into ephemeral island/shoal mode. It is predicted that this coastal behavior will eventually be characteristic of the entire island arc as it is

converted to an inner shelf shoal through transgressive submergence (Miner et al., 2009d; Penland & Boyd, 1985).

#### 2.3.2.5 *The Role of Tropical Cyclones*

It has been suggested that the long-term evolution of the Chandeleur Islands and their fate are governed by tropical cyclone impacts, which result in a long-term net land loss driven by insufficient post-storm recovery leading to the islands' conversion to an inner shelf shoal through transgressive submergence (Fearnley et al., 2009b; Kahn & Roberts, 1982, 1982; Miner et al., 2009d; Penland et al., 1988; Suter et al., 1988). McBride et al. (1992) proposed that the Chandeleur Islands would remain supratidal until the year 2360 on the basis of projected shoreline change and linear regression analysis of island area changes between 1855 and 1989. However, these predictions did not account for the increase in northern Gulf of Mexico storm frequency and intensity that ensued in the decade following their analysis (Fearnley et al., 2009b).

A period of increased storminess (i.e., relative high frequency of strong storm events) associated with the impacts of Hurricanes Georges (1998), Ivan (2004), and Katrina (2005) was unprecedented for the Chandeleur Islands during the historic record (Fearnley et al., 2009b). This sequence of more frequent, strong storm events culminated with Hurricane Katrina completely inundating the islands, removing >90% of the sand, exposing backbarrier marsh along the Gulf shoreline to wave attack (Miner et al., 2009d; Sallenger Jr. et al., 2009) and reducing total island area by ~50 percent (Fearnley et al., 2009b; Sallenger Jr. et al., 2009). Based on aerial reconnaissance surveys conducted by USFWS Refuge Managers, the active 2020 hurricane season also had significant impacts to the islands, but high-resolution data were not available at the time of this publication.

Fearnley et al. (2009a, 2009b) investigated the role of storm frequency, intensity, and track on island evolution for the time-period spanning from 1855 to 2005, with the goal of forecasting the transition from islands to shoals based on historical island area changes. For the northern island arc, the average rate of island shoreline retreat was ~12 m/yr (40 ft/yr) between 1922 and 2004 with retreat rates increasing to >48 m/yr (160 ft/yr) after storm impacts. Hurricanes Ivan and Katrina along the northern Chandeleur Islands were extreme erosional events and the average amount of linear shoreline erosion for the two storms combined (-200 m/yr [660 ft/yr]) was unprecedented throughout the rest of the analysis time period (1855 to 2004). A linear regression analysis of island area change demonstrates a land loss rate of 0.16 km<sup>2</sup>/yr (40 acres/yr) between 1922 and 1996 and a land loss rate of 1.01 km<sup>2</sup>/yr (250 acres/yr) between 1996 and 2005 (Fearnley et al 2009a; Figure 16). By projecting trends calculated from the linear regression analysis of island area change through time, Fearnley et al. (2009a, 2009b) projected that the northern Chandeleur Islands' will cross the transgressive submergence threshold and conversion to ephemeral barrier island/shoals between 2013 and 2037 (Fearnley et al., 2009a, 2009b; Figure 16). The earlier date was based on a projected high storm frequency consistent with that of the preceding decade (1996–2005), whereas the later date represents a projected low storm recurrence interval similar to that for the period from 1922 to 1996. In areas of the northern arc south of Redfish Point this threshold has been met. Based on aerial image analysis, in the spring of 2019 the Gulf shoreline retreat at Monkey Bayou had consumed all of the backbarrier marsh at that location (Figure 15).

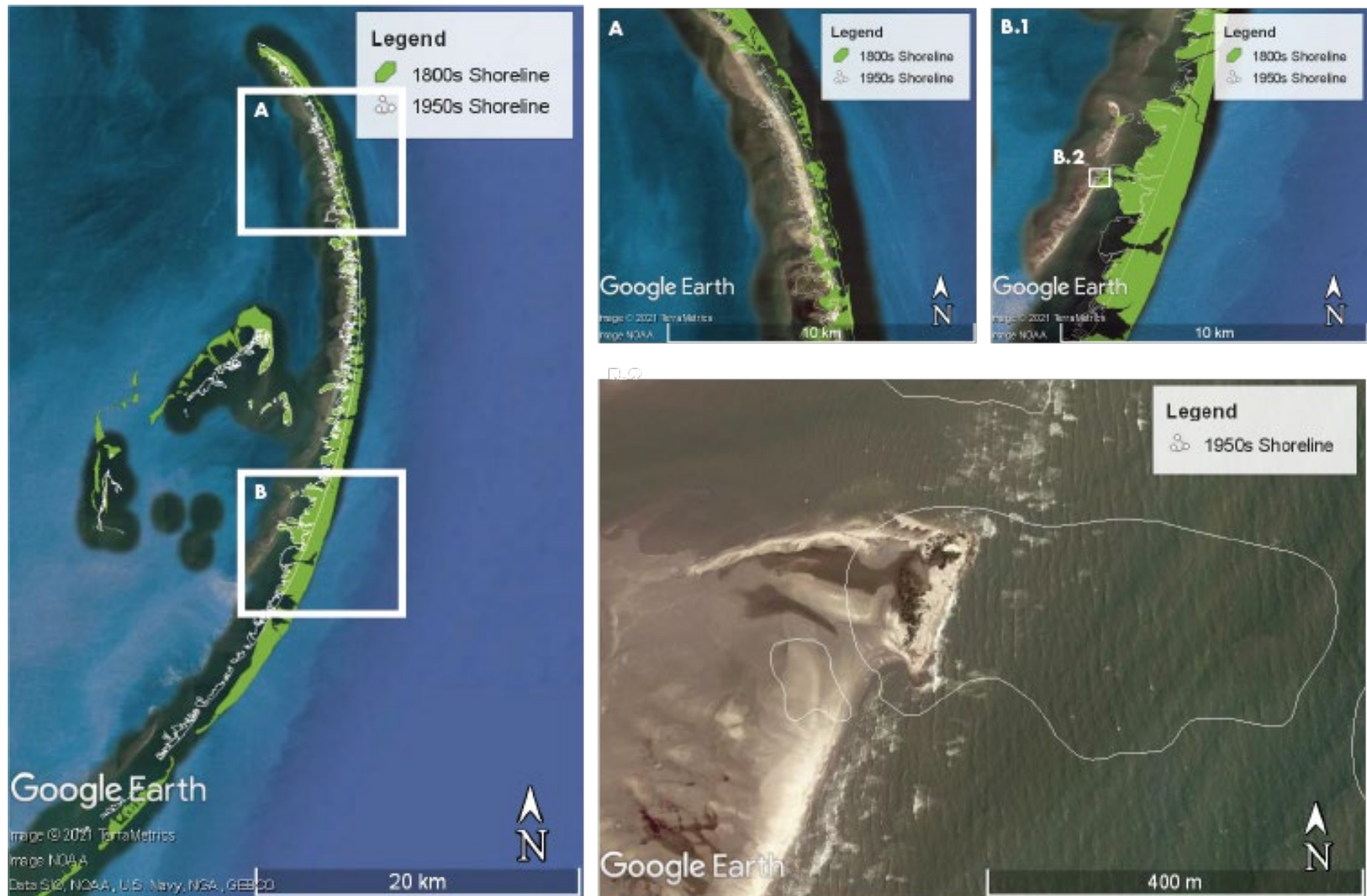


**Figure 15. Shoreline change maps (from the 1880s and 1950s overlain on 2019 aerial imagery) for the northern Chandeaur Islands demonstrating the variability in shoreline retreat rates governed by subsurface sand supply. Northern portions of the island chain have lower rates of shoreline retreat (A) and overlie thick sand deposits that are eroded and injected into the active coastal system. Southern portions of the northern island chain (B.1) are rapidly retreating and overlie relatively sand-poor muddy deltaic deposits. This section of the island arc at Monkey Bayou (B.2) was the location of the most recent deltaic deposition and primary sand source for island development. This sand source has now been depleted. Note in B.2 the 1950s shoreline versus the 2019 aerial image. The last remaining backbarrier marsh at Monkey Bayou is located seaward of the 2019 Gulf shoreline indicating that at this location the criteria for the transgressive submergence threshold crossing has been met (when the eroding Gulf shoreline meets the historical backbarrier marsh shoreline). Shoreline data from the Louisiana Barrier Island Comprehensive Monitoring Program (BICM; Miner et al., 2009e).**

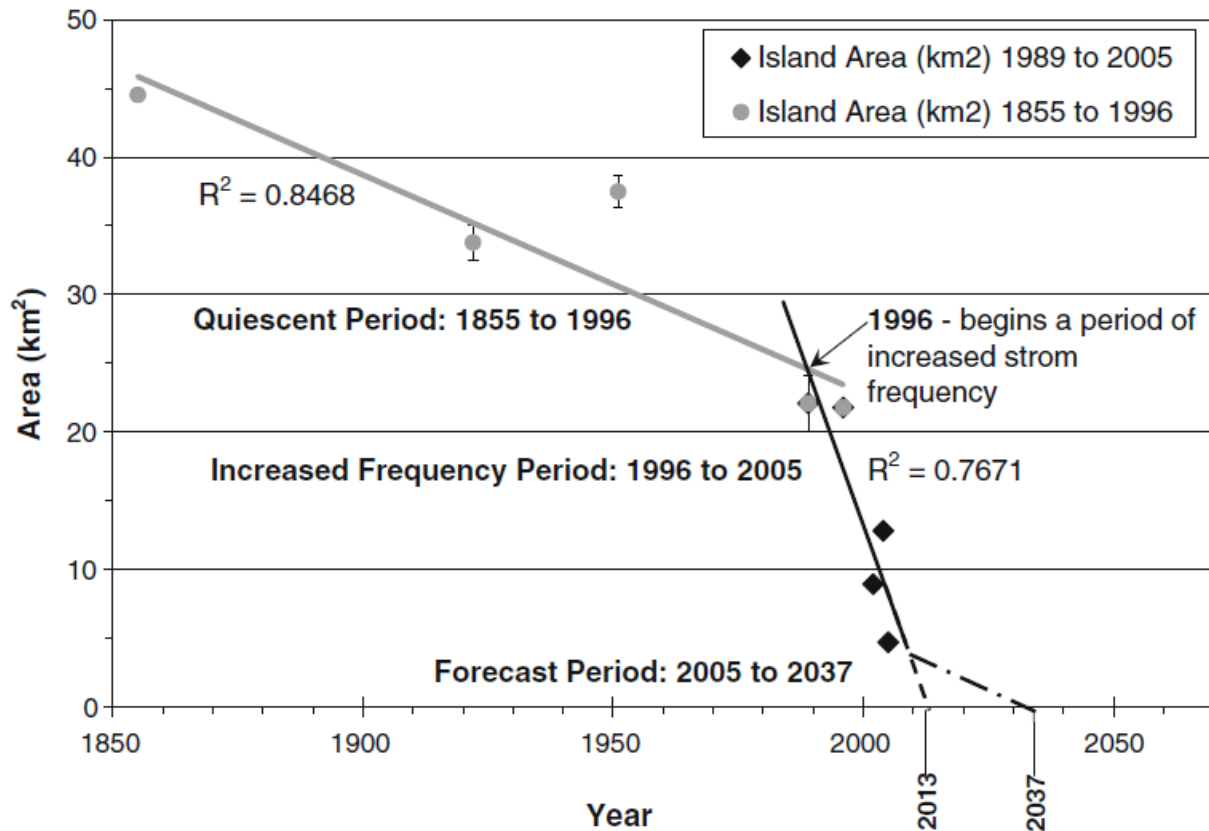


**Figure 16. Chandealeur Islands area change from 1855 to 2006 from Fearnley et. al (2009b). Note the drastic increase in island area loss rates associated with the increased storm frequency period between 1996 and 2005. The dashed projection of the 1989 to 2005 trend (increased storm frequency) predicted transgressive submergence could have occurred as early as 2013 if storm frequency observed 1996-2005 remained high into the future. The dash-dot-dash line represents the trajectory of the islands in their 2006 state under low frequency storm conditions such as existed during the 1855 to 1996 time period, indicating a transgressive submergence date of 2037.**

The southern Chandealeur Islands encompass a different storm impact response and mode of recovery than the northern Chandealeur Islands. Like the northern barrier arc, the southern Chandealeur Islands are characterized by shoreface retreat; however, major storm impacts result in almost complete island destruction and conversion to inner shelf shoals (Breton Island is an exception to this trend). During extended periods of lower tropical cyclone activity following major storm impacts, new islands reemerge along this sector (Fearnley et al., 2009b; Miner et al., 2009d). During long term periods (>100 yrs) the rate of shoreline retreat along the southern islands was approximately 15 m/yr (50 ft/yr) for the time period from 1869 to 1996 and island area decreased from 50 km<sup>2</sup> (19 mi<sup>2</sup>) to 1.8 km<sup>2</sup> (0.7 mi<sup>2</sup>) between the years 1869 to 2005 (Fearnley et al., 2009a, 2009b).

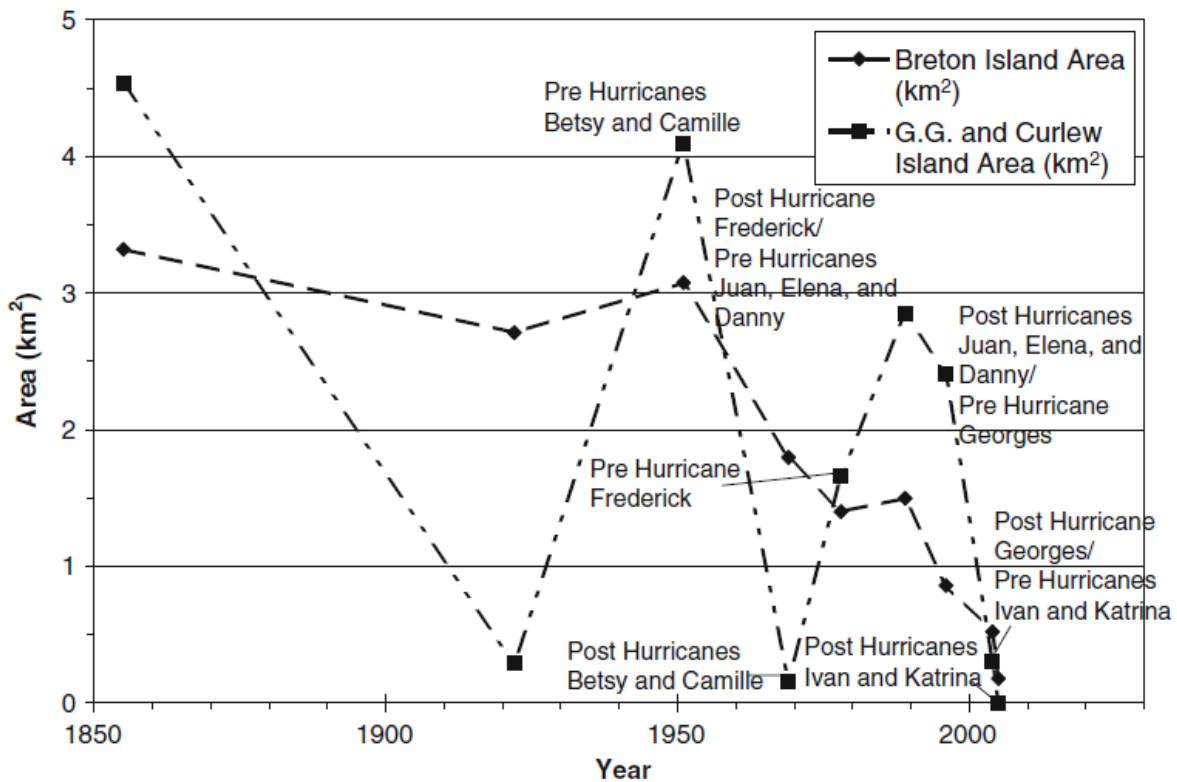


**Figure 17. Island area change for the southern Chandeleur islands annotated with tropical cyclone events from Fearnley et al. (2009b). Note the dynamic nature of Curlew and Grand Gosier Islands through time. These islands are almost completely destroyed during storms and reemerge landward of their former locations during extensive periods of calm weather. This coastal behavior is predicted to encompass the entire island chain once backbarrier marshes have eroded.**

### 2.3.2.6 Sediment Dynamics

With regard to longshore sediment transport, the arcuate barrier island trend is characterized by a bidirectional system, with sediment moving from the central arc to the flanks (Figure 18; Georgiou & Schindler, 2009b). Seasonal variations in wind dominance, related to the approach angles of winter cold front passages and summer tropical systems, cause an imbalance in transport gradients through time, forcing higher rates of transport potential in a northward direction (Georgiou & Schindler, 2009b). Significant wave heights along the northern portion of the barrier have a peak of 0.46 m (1.5 ft) based on a 25-year hourly average with significant wave heights in excess of 1 m (3.3 ft) occurring ~4% of the year and > 2 m (6.6 ft) waves having a return period of less than 1% (Georgiou & Schindler, 2009b). Net longshore transport rate potential north of the nodal zone (where dominant longshore transport directions diverge) in the central island arc are directed northward with rates increasing away from the nodal zone toward the flanks reaching values >110,000 m<sup>3</sup>/yr (144,000 cubic yds/yr) (Georgiou & Schindler, 2009b). Transport rate potential south of the nodal point are generally directed to the south with potential rates reaching ~115,000 m<sup>3</sup>/yr (150,000 cubic yds/yr) (Georgiou & Schindler, 2009b).

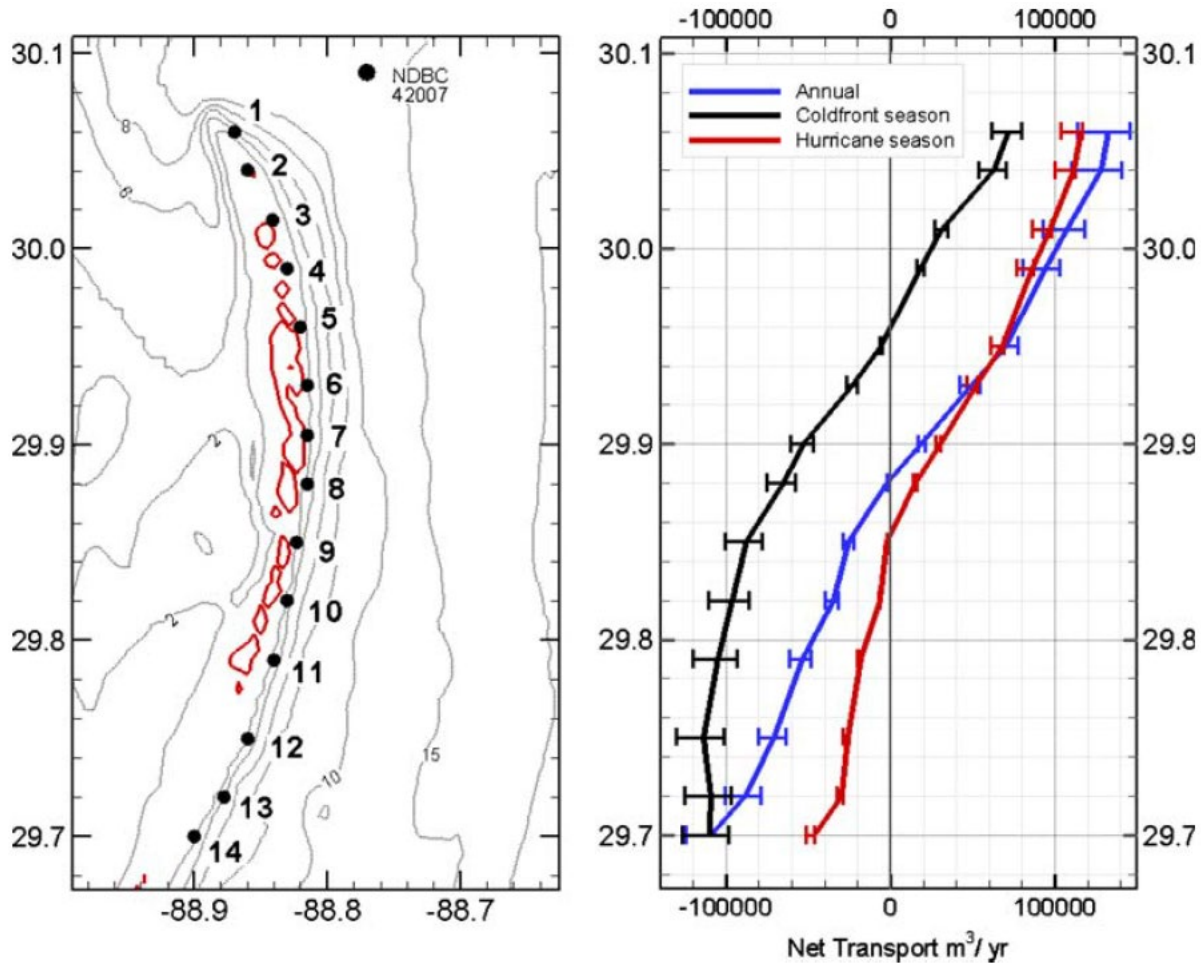


**Figure 18. Simplified regional bathymetry map near the Chandeleur Islands (left panel), and locations where longshore sediment transport calculations were performed by Georgiou and Schindler. Plot on right shows potential net longshore sediment transport in m<sup>3</sup>/year along the island arc (note the corresponding latitude tic-marks in both left and right panels) as a function of seasonal forcing: blue line long-term annual average from 1985 to 2006, black line seasonal averaging during the cold front seasons, red line seasonal averaging during the hurricane seasons for the same time period. Error bars indicate fluctuations in the potential transport rate due to uncertainty in the parametric equations used for wave forecasting. A positive net transport rate indicates northerly transport and a negative indicates southerly. Note the “nodal zone” in the central portion of the island arc where sand is either transported north or south depending on seasonal wave climate. These calculations assume a continuous island chain. Figure from Georgiou and Schindler (2009b).**

Under non-storm conditions, significant sediment transport is restricted to the upper shoreface, landward of the 3 m (16 ft) isobath (Penland & Boyd, 1981), however recent studies along Louisiana barrier islands demonstrate that storm-associated seafloor scour and transport occurs at depths >15 m (50 ft) (Allison et al., 2010; Miner et al., 2009b, 2009c). It is important to note that the predicted rates of longshore sediment transport discussed above are an order of magnitude lower than the rates of deposition at the island flanks inferred from the sediment volumetric change analysis discussed above based on bathymetric data (~1 x 10<sup>5</sup> m<sup>3</sup>/yr for versus ~1 x 10<sup>6</sup> m<sup>3</sup>/yr). Observational and numerical modeling studies suggest that storm wave-induced currents play a major role in sediment transport within the lower shoreface zone and inner

continental shelf off the Louisiana coast (Allison et al., 2010; Georgiou & Schindler, 2009b; Jaffe et al., 1997; Miner et al., 2009b; Teague et al., 2006).

#### 2.3.2.7 Hurricane Katrina Impact and Recovery

Hurricane Katrina segmented the island arc into multiple small marsh islets separated by wide hurricane-cut tidal passes. More than 90% of sand comprising the barriers was removed, exposing backbarrier marshes to Gulf wave attack (Sallenger Jr. et al., 2009). Additionally, offshore surveys conducted post-Katrina in 2006 did not identify any large sand accumulations on the shoreface south of Schooner Harbor near Hewes Point, and in fact, much of the shoreface was characterized by outcropping relict deltaic deposits with no coastal sand present (Twichell et al., 2009b, 2009a, 2011). During the following year, >50 percent of the length of the northern Chandeleur Islands shoreline continued to erode. However, during year two of recovery, marsh islands served as nucleation sites for sand accumulation along the northern arc, north of Redfish Point. Early stages of recovery along this sector were marked by sand and shell recurved spit formation at hurricane-cut tidal passes followed by onshore bar migration and welding (attaching to the shore); a process that resulted in the closure of some inlets (Figure 19). Prior to the 2008 Hurricane Season, elevation along the northern section began to increase as aeolian processes (movement of sand by wind) constructed dune fields in the wind shadow of black mangroves (*Avicennia germinans*) and roseau cane (*Phragmites australis*) thickets. Contrastingly, recovery along the southern segment of the northern arc (between Redfish Point and Monkey Bayou) was not characterized by sandy shoreline development and closing of inlets. Here, marsh islands fronted by a shell berm continue to undergo rapid shoreline retreat (>200 m/yr [650 ft/yr], locally). Over the past 15 years since Hurricane Katrina, shoreline retreat has continued, but the closure of hurricane cut inlets along the central portion of the northern arc has resulted in a more continuous sandy shoreline and efficient longshore sediment transport system.

Where marsh islands were absent prior to Hurricane Katrina's impact (south of Monkey Bayou to Grand Gosier Islands), the sandy barriers underwent transgressive submergence. These southern shoals persisted for 2 years after Hurricane Katrina's impact, but began to emerge as narrow, ephemeral barrier islands until they were once again destroyed by Hurricanes Gustav and Ike in 2008. Curlew and Gosier Islands once again became exposed in a position landward of their pre-2008 locations between 2014 and 2020 but based on LANDSAT imagery, the active 2020 hurricane season resulted in complete submergence of the Gosier Islands and partial submergence of Curlew Island.



**Figure 19. Oblique aerial photo of the northern Chandeleur Islands (left) showing the closure of hurricane-cut inlets two years after Hurricane Katrina. Vertical aerial image on the left has white arrow indicating location of the oblique aerial photograph.**

An understanding of what governs the disparity in recovery behavior between the northern (resilient and recover after storm impacts with backbarrier marshes) and southern (ephemeral islands) sections of the island arc is important for predicting future island sustainability and development of a long-term island management plan. In order to address this, the University of New Orleans Pontchartrain Institute for Environmental Sciences (UNO-PIES) and USGS conducted a subsurface investigation along the island arc. Results demonstrate that recovery is controlled by the relative abundance of local subsurface sand supply; the marsh islands along the northern sand-rich sector are underlain by thick (up to ~ 10 m [33 ft]) relict spit platform and lateral accretion inlet fill deposits, whereas the section south of Redfish Point is underlain by muddy lagoonal and deltaic deposits (Figure 9). Therefore, as the shoreline retreats landward (a process that is greatly accelerated during post-storm recovery phases; Fearnley et al., 2009b; Sallenger Jr. et al., 2009), relict sandy spit deposits underlying the backbarrier marsh in the north are liberated at the shoreface and introduced to the littoral system. As previously noted, Hurricane Katrina removed all of the visible sand in the subaerial island system and no large sand accumulations were identified offshore. Given this context, it is reasonable to assume that the majority of sand present in the existing subaerial island system was sourced over the past 15 yrs via shoreline erosion liberating sand from these relict spits

and other backbarrier deposits, introducing it into the active littoral system for development of spits, beaches, and dunes.

In the southern Chandeleurs, local sand supply is limited, inhibiting rapid recovery. This disparity in sand distribution along the island arc is a consequence of long-term lateral accretion away from the original, centralized deltaic sand source in the vicinity of Monkey Bayou. Over the past several centuries the deltaic sand source has been exhausted leaving a sand-starved zone of islands between Redfish Point and Monkey Bayou and relatively sand-rich zones north of Redfish Point. Ultimately, in the north, the sand is lost from the barrier island littoral system to a deepwater sink north of Hewes Point. South of Monkey Bayou and extending beyond Breton Island exists a similar sand-rich trend; however, with the exception of Breton Island, there are no marsh islands for sand to accumulate upon subaerially, resulting in rapidly retreating ephemeral barriers of Curlew and Grand Gosier Island Shoals and a deepwater sand sink offshore of Breton Island similar to Hewes Point. These downdrift sand reservoirs provide a unique, quasi-renewable resource for nourishing the updrift barrier system.

### **2.3.3 Restoration Concept**

The envisioned restoration approach for the Chandeleur Islands employs concepts proposed in Lavoie et al. (2009) and Miner et al. (2009a) to address the root cause of island disintegration—loss of sand from the system—by reintroducing sand at locations where natural processes can rebuild the islands over time in a way that mimics the way they naturally formed (Figure 20 and Figure 21). This involves placing sand lost from the system (presently at Hewes Point) in updrift (central portion of the arc) backbarrier feeder sites and using the natural island shoreline retreat (erosion) to liberate placed sand into the littoral system for lateral distribution. This overall sediment management approach would be coupled with vegetative plantings and focused habitat elevation restoration goals. By employing the natural geomorphic processes to rework placed sand over time, ecosystem value will also increase for some time after construction as more robust barrier island habitat is established or enhanced beyond the placement areas. This holistic ecosystem restoration concept derives from extensive studies on long term geomorphic evolution (e.g., Miner et al., 2009d; Penland et al., 1988; Rogers et al., 2009; Suter et al., 1988; Twichell et al., 2009b, 2011) and short-term changes (e.g. Bernier et al., 2019; Darnell et al., 2017; Georgiou & Schindler, 2009b, 2009a; Grzegorzewski & Georgiou, 2011; Long et al., 2020; Mickey et al., 2018; Miselis et al., 2015a; Sherwood et al., 2014), driven primarily by rapid RSLR and hurricanes, to provide the barrier island system the means to be self-sustainable for decades. To prolong island lifespan, the backbarrier sand feeders should extend substantially in a landward direction to stave off the system crossing the transgressive submergence threshold. Targeted numerical modeling is needed to assess the outcomes of this approach on multiple spatial scales (island-wide and regional) and temporal scales and under the range of forces driving island evolution including multiple storm impacts.

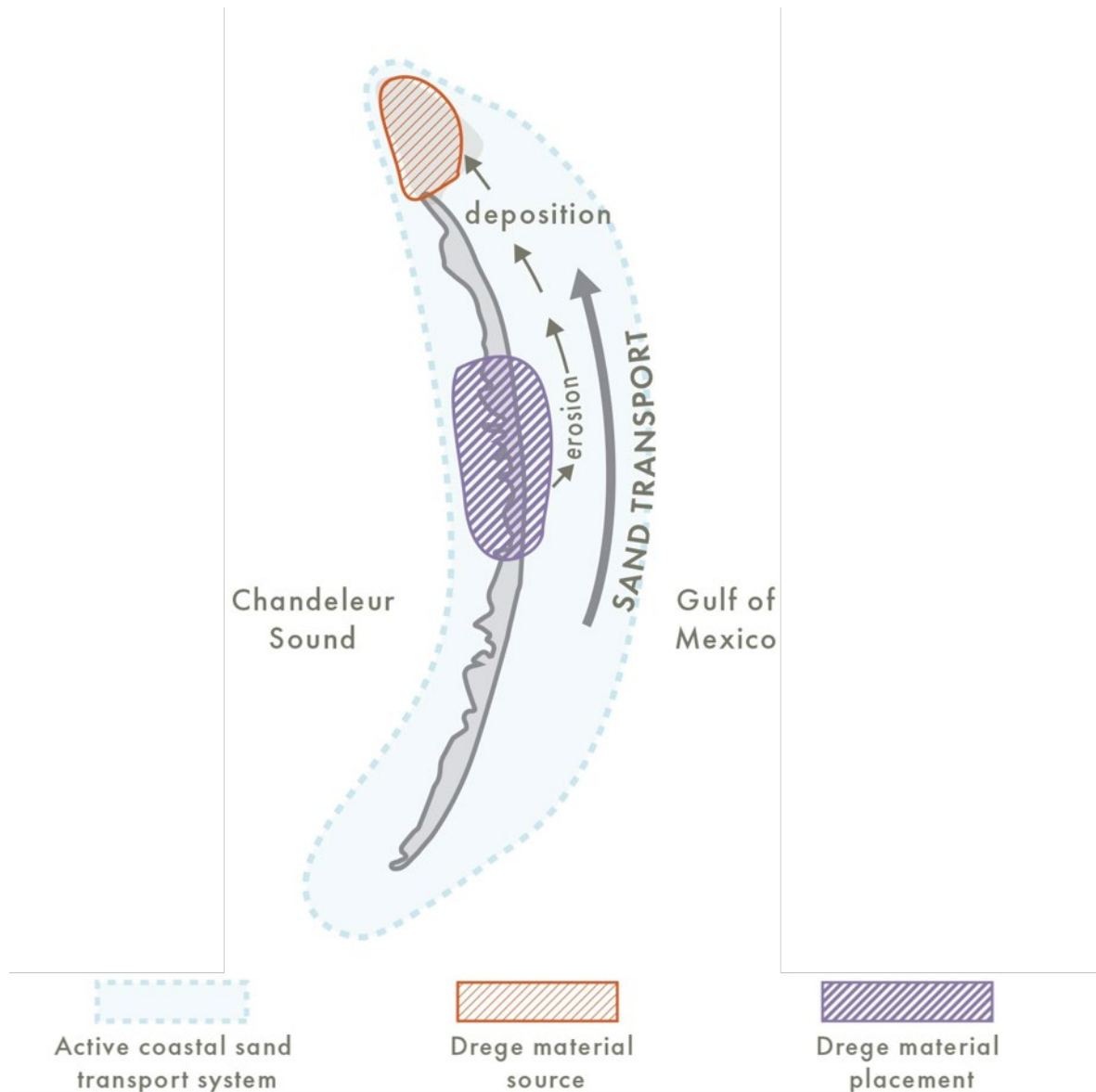


**Figure 20. Conceptual model for sediment management-based restoration of the Chandeleur Islands. Natural processes have historically transported sand to a deep water sink north of the islands, removing it from the active coastal system and exhausting the natural sand source in the central portion of the islands. Restoration would involve dredging sand from this sink in the north and reintroducing it to the central part of the island; most of which would be placed in the backbarrier and provide a long-term sand source that is gradually reintroduced to the active coastal system as the islands erode into the backbarrier marsh, mimicking the natural processes of island building.**

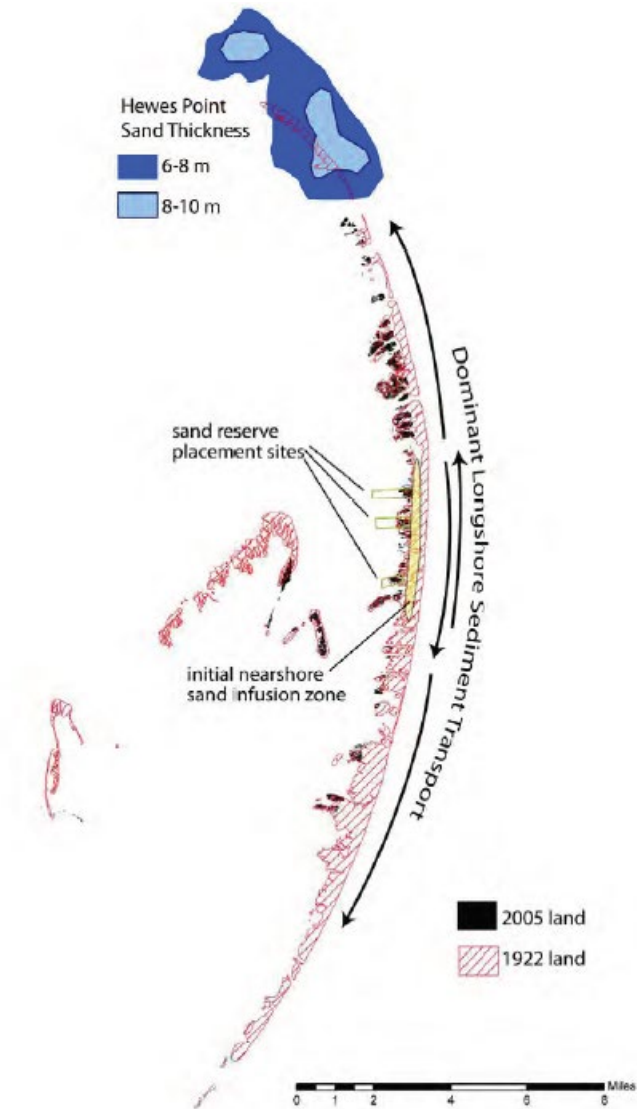


Figure 21. Conceptual design for Chandealeur Island restoration from Lavoie et al. (2009) involving backbarrier sand feeders placed in the central portion of the island arc constructed using sand from Hewes Point.

### 3.0 Evaluation of Event-Driven Sediment Transport Trends under Natural and Restored Island Configurations

This section describes a numerical modeling experiment conducted to determine sediment transport dynamics under storm conditions for the existing conditions at the Chandealeur Islands. This can be compared to the long-term evolution and sediment dynamics described above to provide a better understanding of how sediment is distributed around the island system today given that it is in a highly degraded state post Hurricane Katrina. The trends identified in the historical data with a more robust island system might not fully represent the existing sediment dynamics. In addition to modeling storm response for the existing island configuration, two restoration alternatives are applied to evaluate how

restored island profile geometry may influence sediment transport trends and how sediment placement template design may best provide ecosystem benefits in the context of storm response and resiliency.

### 3.1. NUMERICAL MODEL DEVELOPMENT AND RESTORATION DESIGN

Developing and applying a numerical model to restoration design in the Chandeleurs allows for the identification of sediment transport pathways and for the performance of different restoration scenarios to be compared.

#### 3.1.1 Assessment of Existing Model Output and Data Sources

To inform development of a numerical modeling framework for evaluating the benefits of Chandeleur Islands restoration, prior studies were reviewed. The focus of this review was on work evaluating sediment transport and geomorphic change at the Chandeleurs to identify the main drivers of these processes; advance development of a numerical model for evaluating restoration alternatives; and inform the selection of metrics for quantifying the ecological function and value of the Chandeleur Islands. An inventory of modeling efforts that focused more broadly on numerical modeling approaches for predicting water quality in the Louisiana, Mississippi, and Alabama Coastal System (LMACS), including Chandeleur Sound, is also available (Dalyander et al., 2020b).

Several numerical modeling studies have characterized sediment transport and geomorphic response of the northern Chandeleur Islands to individual storm events. Mickey et al. (2018) characterized the storm climate at the Chandeleur Islands into a set of scenarios that varied in duration and intensity. Storm intensity was characterized by the maximum total water level (TWL), a single parameter that includes the combined impact of storm surge, tides, wave set-up, and wave runup and which is frequently compared to topographic elevation benchmarks to predict the erosional impact of storms on barrier islands (Sallenger Jr., 2000; Stockdon et al., 2005, 2006). The impact of these storms on the Chandeleur Islands was characterized using the XBeach model (Roelvink et al., 2009), with the topographic conditions reflecting the island configuration shortly after a berm was constructed along the northern Chandeleurs during the *Deepwater Horizon* oil spill (Plant et al., 2014; Suir & Sasser, 2019). Mickey et al. (2018) captured storm duration as the number of hours the TWL exceeded 1.013 m, selected as the base of the Chandeleur Islands berm as an appropriate threshold for a storm to drive erosion of the subaerial beach. Their numerical experiments captured a shift in island impacts wherein shorter duration and/or less intense storms resulted in berm and dune erosion and deposition in the nearshore, i.e., the “collision regime” with offshore sand transport dominating (Sallenger Jr., 2000). Increases in storm intensity and/or duration resulted in overwash and/or inundation and a shift in sediment transport from offshore to landward at locations where the maximum TWL increased beyond the crest of the dune where breaching and/or inundation occurred. Mickey et al. (2018) also identified that low-lying areas of the island are particularly vulnerable to overwash and inundation. Sherwood et al. (2014) used a combination of observed water level gradients and XBeach modeling of the Chandeleur Islands to characterize the island response to the Category 1 Hurricane Isaac in 2012. They similarly found that the storm drove overwash and inundation (sections of island completely covered by water) of the islands initially forcing westward (landward) sediment transport. However, elevated water levels in the backbarrier during the latter half of the storm resulted in flow reversal (inshore to offshore) and deposition of sediment in the nearshore in their model results.

Numerical studies have also characterized long-term sand transport patterns at the Chandeleur Islands and their dominant drivers. Georgiou and Schindler (2009a, 2009b) characterized wave conditions in the northern Gulf, then combined wave modeling with estimates of the potential for longshore transport using the USACE Coastal Engineering Research Council (CERC) formulation (USACE, 1984) to analyze sediment transport along the northern portion of the Chandeleur Islands. They found a bidirectional longshore transport pattern with a nodal point along the arc of the island, with dominant transport to the north in the northern section and to the south in the southern portion. Seasonal variation was found with a higher rate of transport and an increase in net northern transport during tropical storms and hurricanes. Although Georgiou and Schindler's primary focus was on the southern Chandeleur Islands, Nelson (2017) similarly characterized sediment transport patterns at the northern Chandeleur Islands using the Delft3D model, noting that the location of the nodal point shifts north and south depending on the season. The combined influence of storms and asymmetric sediment transport to the north results in significant sediment deposition at the northern terminus of the arc (Hewes Point). Although quiescent conditions were found to have some potential to transport sediment to the south from this region, there was insufficient energy and sediment reworking to reintroduce sediment deposited in this area to the littoral system (Georgiou & Schindler, 2009a).

Miselis et al. (2015b) used a combination of process-based numerical wave and circulation models with observation of sediment deposition and bathymetric change to analyze the relative contribution of storm events and sediment supply to longshore transport at the Chandeleur Islands. They identified the same overall pattern in longshore transport with a nodal point in the central portion of the arc, with the occurrence of storms identified as a primary driver in interannual variability in sediment flux to the north and deposition at Hewes Point. Grzegorzewski and Georgiou (2011) used the Advanced Circulation (ADCIRC) Hydrodynamic model with waves from STWAVE-FP (STeady-state spectral WAVE) to compare and contrast hydrodynamic conditions during a cold front passage and a hurricane, then used the results to predict sediment transport due to currents and waves along the Chandeleur Islands using methods described in Soulsby (1997). They found that the longshore sediment transport to the north, in the northern portion of the island, was two orders of magnitude greater during the hurricane than the cold front passage.

These numerical studies suggest that large tropical storm events are the dominant drivers of cross-shore and longshore transport in the northern arc of the Chandeleur Islands and are responsible for the large volumes of sand that have accumulated on the spit platform north of Hewes Point (Miner et al., 2009d). These findings are consistent with observational data analysis results, which document that tropical storms are the dominant drivers of evolution of the Chandeleur Islands. In addition to driving longshore transport, storm frequency and intensity drives the cycle of island submergence, reemergence, and sediment transport that results in net island transgression (landward migration to the west) and deposition of material from the central portion of the island to the northern and southern flanks (Fearnley et al., 2009b).

Based on the analyses described above, the focus of this effort is on modeling the impacts of storm events on the Chandeleur Islands with and without restoration alternatives. It is hypothesized that storms are the dominant driver of sediment delivery to Hewes Point, and the modeling experiment will help to quantify rates of sand delivery to this depositional sink based on existing island conditions and with restoration

alternatives. The results will be analyzed using a suite of metrics, described below, to characterize the ecosystem value with and without restoration pre- and post-storm. Sediment transport pathways, directions, and volumes will also be analyzed during storms and used to evaluate the implications of restoration strategies. Modeling short-term impacts and sedimentary response provides for an overall understanding of sediment transport pathways and susceptibility to storms, but it does not provide for a long-term evaluation on restoration strategy effectiveness in prolonging island lifespan by mitigating for transgressive submergence, which should be a focus of future numerical modeling to inform Chandeleurs restoration design.

### **3.1.2 Model Configuration**

Storm impacts were modeled using XBeach (version 5809) (Roelvink et al., 2009). XBeach is a two-dimensional model that resolves gravity wave propagation, infragravity wave generation and propagation, wave-driven currents, sediment transport, and morphologic change on times scales of hours to days during storm events. XBeach has been previously used to evaluate the evolution of the Chandeleur Islands on the temporal and spatial scales of interest in this study (Mickey et al., 2017, 2018; Sherwood et al., 2014). A curvilinear model grid originally developed for Mickey et al. (2017, 2018) was used as a baseline and was adapted for the current study in the following ways: 1) extending the grid to the north and south to capture Hewes Point and the southern arc of the Chandeleurs; 2) extending the grid to the west to capture the leeward portion of the island where there are extensive seagrass beds; and 3) updating the topography and bathymetry. The model domain is delineated on the map in Figure 2. Model grid extensions to the north, south, and east retained the resolution of the original model domain. The cross-shore resolution of the model grid varies from onshore (~2.5 m over the subaerial island, shallow surf zone, and immediately leeward of the island) to offshore (~74 m at the Gulfward extent and ~30 m resolution in Mississippi Sound). The longshore resolution of the model is ~20 m.

Because the focus of this experiment is evaluating event-driven sediment transport pathways and storm-driven sand transport response to different restoration approaches, the primary requirement for the digital elevation model (DEM) is that it captures key geomorphic characteristics of the island chain rather than resolving the exact island configuration at a point in time. Topography and bathymetry in the model were therefore updated using data from the early 2010s where available (Kindinger et al., 2013; Mickey et al., 2017; Miner et al., 2009e; Stalk et al., 2017). The majority of the data, and the entirety of the subaerial data, are from Stalk et al. (2017) and were collected in 2015. A small amount of data in the lee of the island and at the southern offshore grid extent is from 2006 (Miner et al., 2009e). To create a representative bathymetry without sharp transitions between the different datasets, smoothed, representative contours were created in ArcGIS from the bathymetry and topography data. The contours were then sampled every 100 m and these points were used to create a spline surface from which the grid bathymetry was extracted. The resulting bathymetry is representative of the bathymetry and topography of the Chandeleurs but does not exactly match any point in time. All other parameters were the same as Mickey et al. (2017, 2018).

### **3.1.3 Restoration Alternatives**

Typical barrier island restoration in Louisiana involves construction of a beach berm, dune, and backbarrier marsh. The geometry of the fill template profile varies depending upon project objectives and geographic location. In some cases, the marsh fill component of the profile extends well into the

backbarrier while in others it may be nonexistent. The same goes for the dune component; in some cases it is constructed higher when project objectives involve storm surge protection as a priority. In other cases, it is built to a minimal elevation with the expectation that vegetation will establish and natural dune elevations will develop over time given wind-blown sand supplied from the beach fill is available. In order to evaluate the influence of the dune versus marsh creation on storm-driven sediment redistribution, two end member restoration alternative templates were created for this modeling investigation: a dune end member (with no backbarrier marsh restored) and a marsh end member (with no dune construction). The two restoration alternatives were separately applied to the base topo-bathy surface using schematized fill templates that represent the post construction profile (beach and upper shoreface, dune, and/or backbarrier marsh). Restoration templates for the northern Chandeleurs were applied to the model domain from (324040 m E, 3315270 m N UTM 16 N) to (319900 m E, 3297260 m N UTM 16 N) in the central part of the island chain (Figure 22). The dune end member template consists of a 2 m (6.5 ft) high dune with a 60 m (200 ft) wide fronting beach (Figure 23 and Figure 24). This template is applied continuously through the restoration area, except at Katrina Cut, where a 245 m (800 ft) wide beach is ‘constructed’ (Figure 23). The marsh end member does not have a dune. It consists of two restoration templates. The first has a lower beach (0.9 m [3 ft] high; ~120 m [~400 ft] wide) with a wide backing marsh (0.6 m [2 ft] high; 700 m [2300 ft] wide). The second template has the same beach height and width as the dune alternative but lacks the backbarrier marsh (Figure 26 and Figure 27). For the marsh alternative, the marsh fill template is applied discontinuously in the restoration area with the beach fill template filling the areas in between. The wide marsh template is applied where there is existing marsh behind the island and across Katrina Cut (Figure 28). It should be noted that both templates have a continuous beach fronting either the dune or backbarrier marsh. The templates were aligned with the approximate peak of the natural profile, while also smoothing template placement location to obtain a continuous dune and beach berm line to represent a realistic constructed profile. For each alternative the total volume of sand placed was approximately  $8.5 \times 10^6$  cubic yards ( $6.5 \times 10^6$  cubic meters).

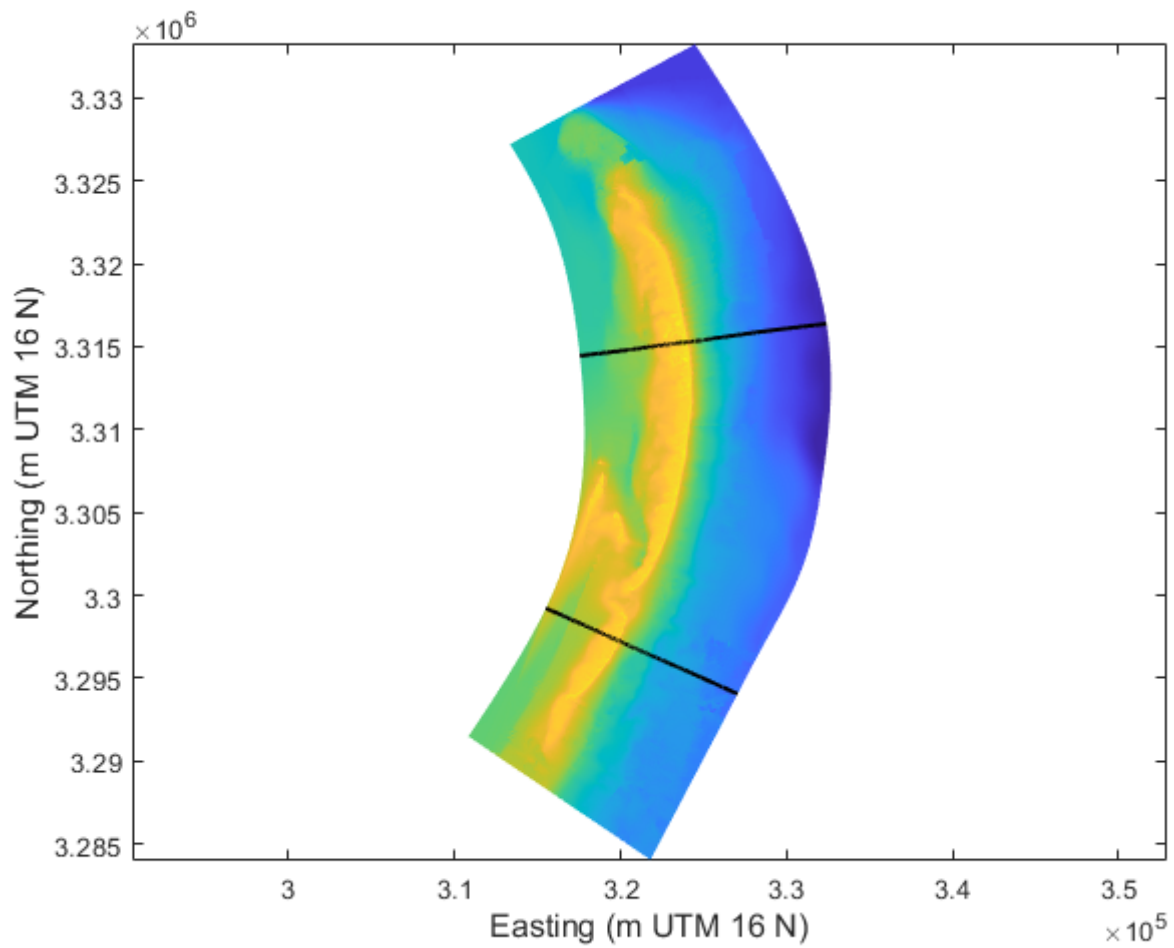


**Figure 22. The model grid of the Chandeleur Islands with the restoration area shown. Between the two black lines the restoration profiles were applied.**

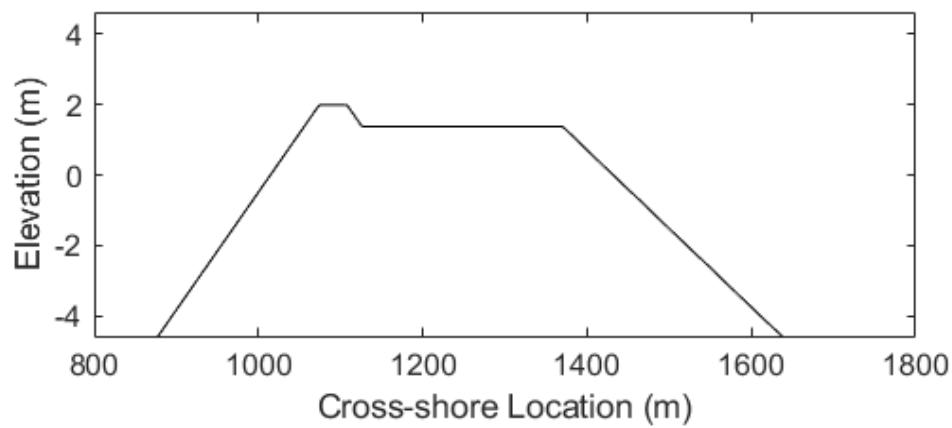
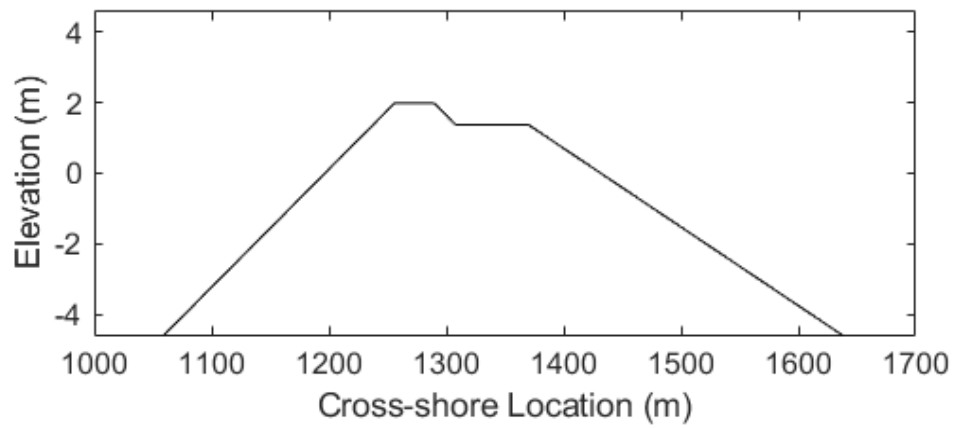


**Figure 23. The dune end member restoration template. Top: The dune and beach template applied to most of the profiles. Bottom: The dune and beach template applied in Katrina Cut.**

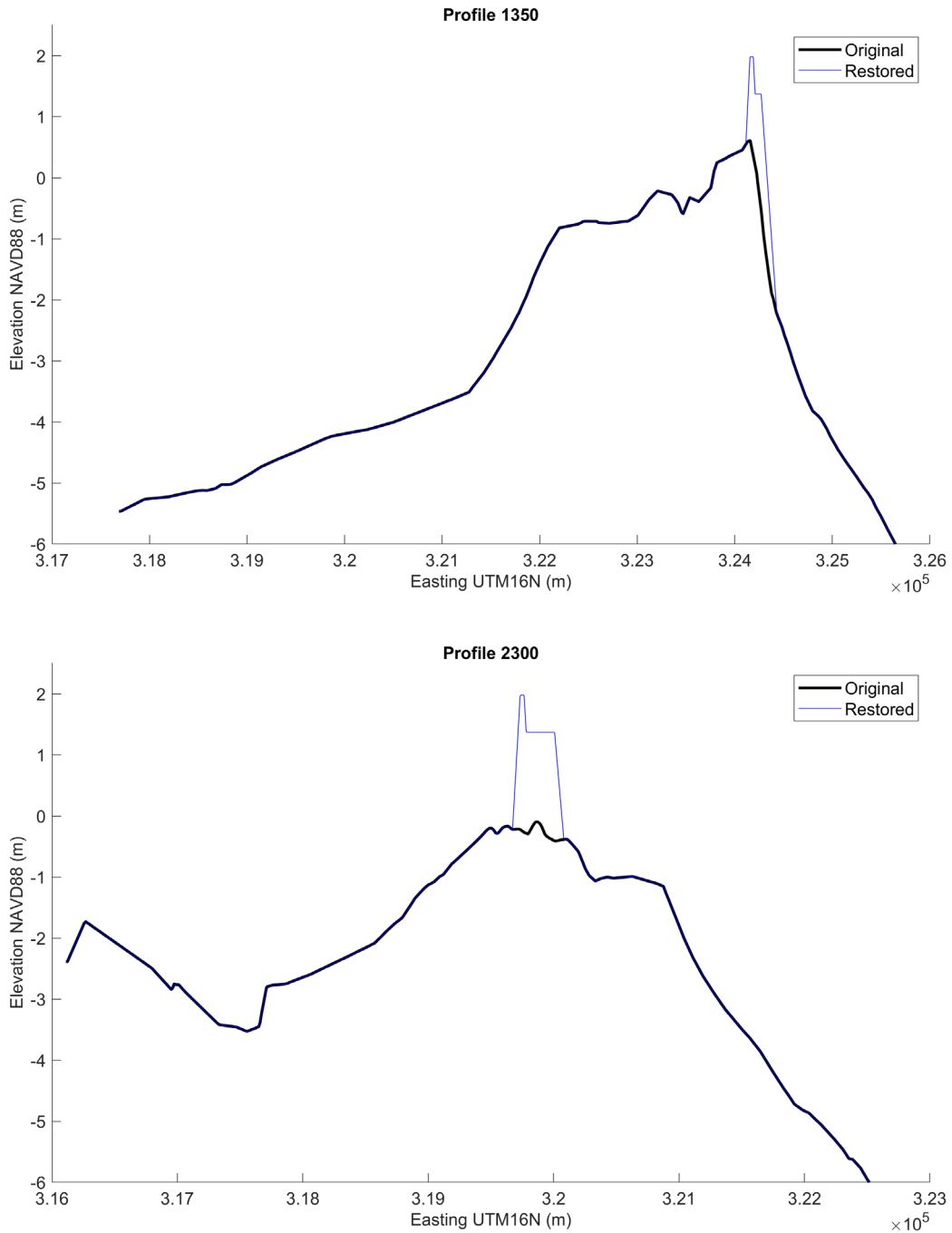


**Figure 24. The dune template applied to topo-bathy profiles. Top: The dune template applied through the restoration area, except for Katrina Cut. Bottom: The dune template applied at Katrina Cut.**

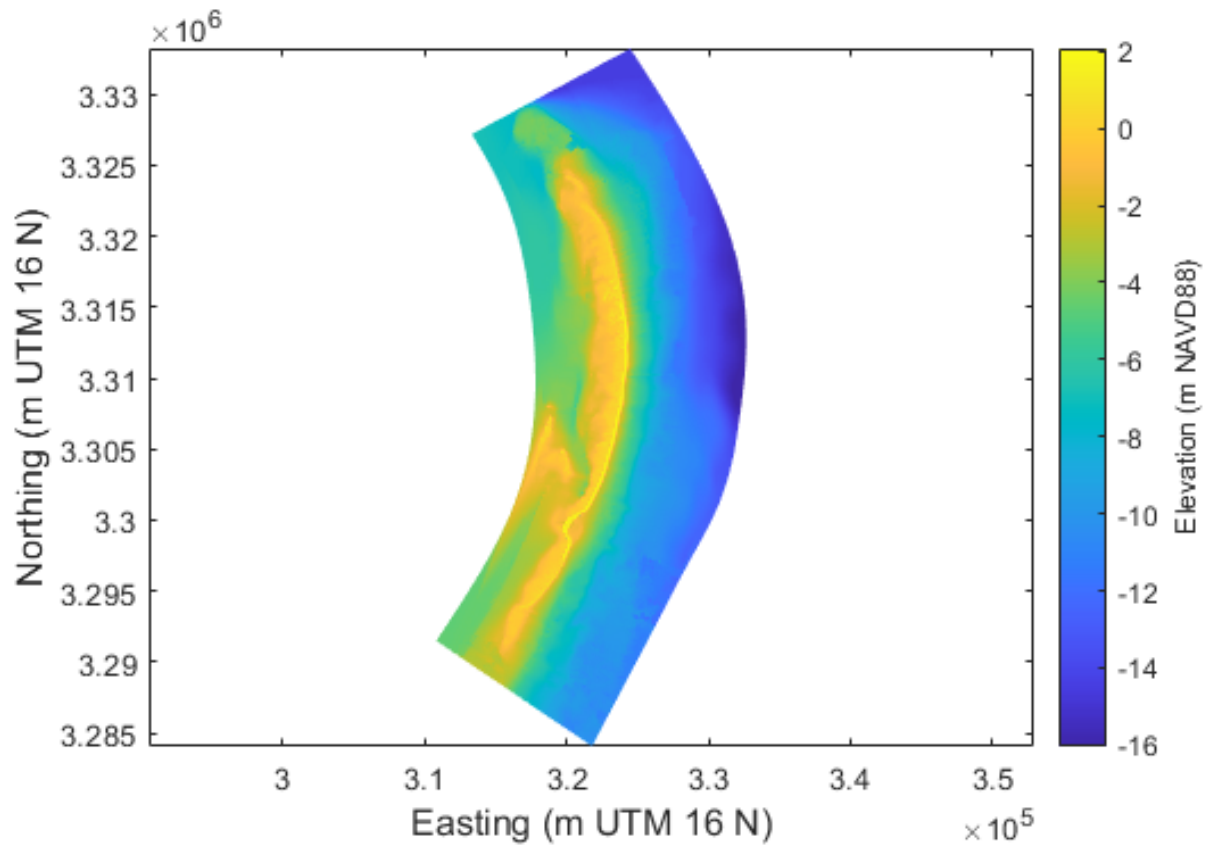


**Figure 25. The restored topo-bathy after application of the dune end member templates.**

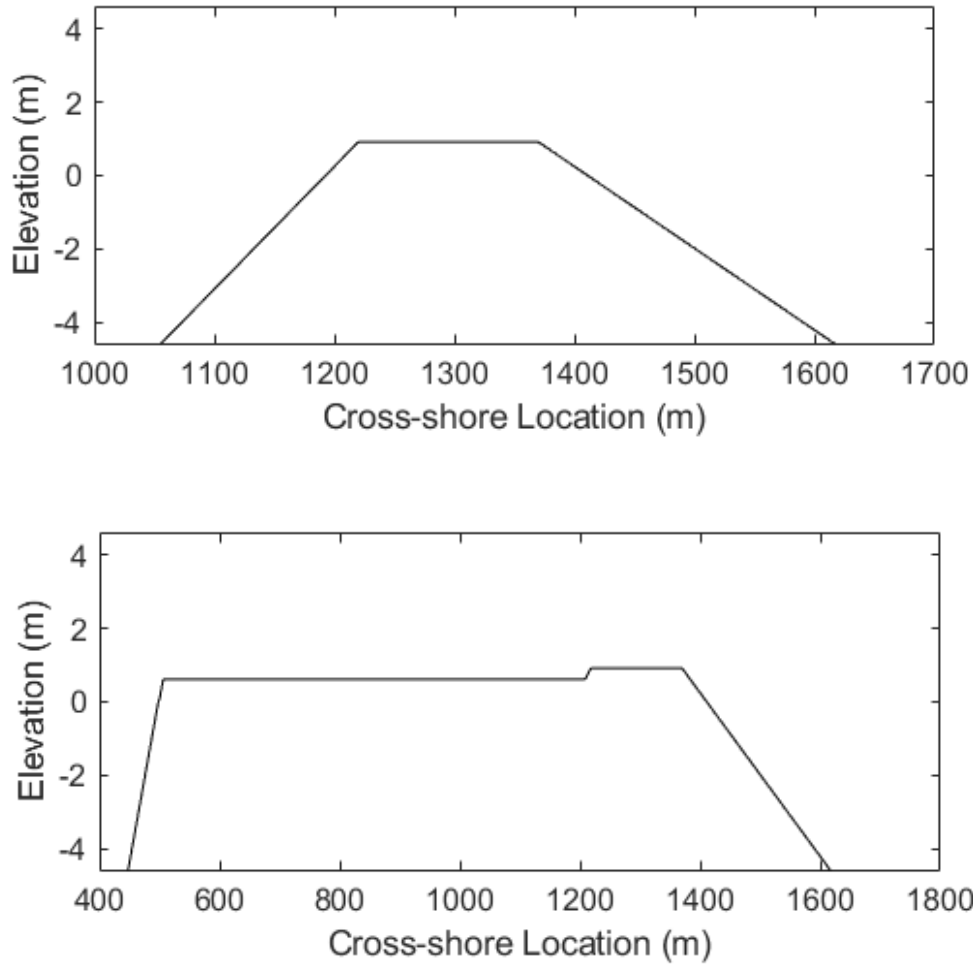


**Figure 26. The marsh end member restoration template. Top: Beach only template that is applied to most profiles. Bottom: The beach with backing marsh template that is applied where there is existing marsh.**

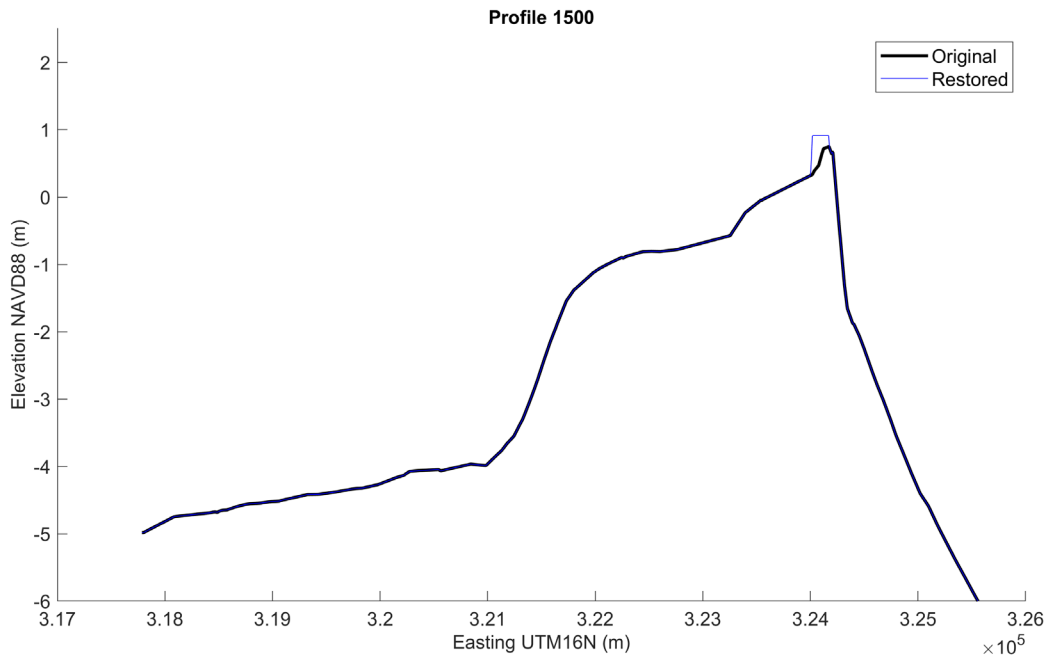
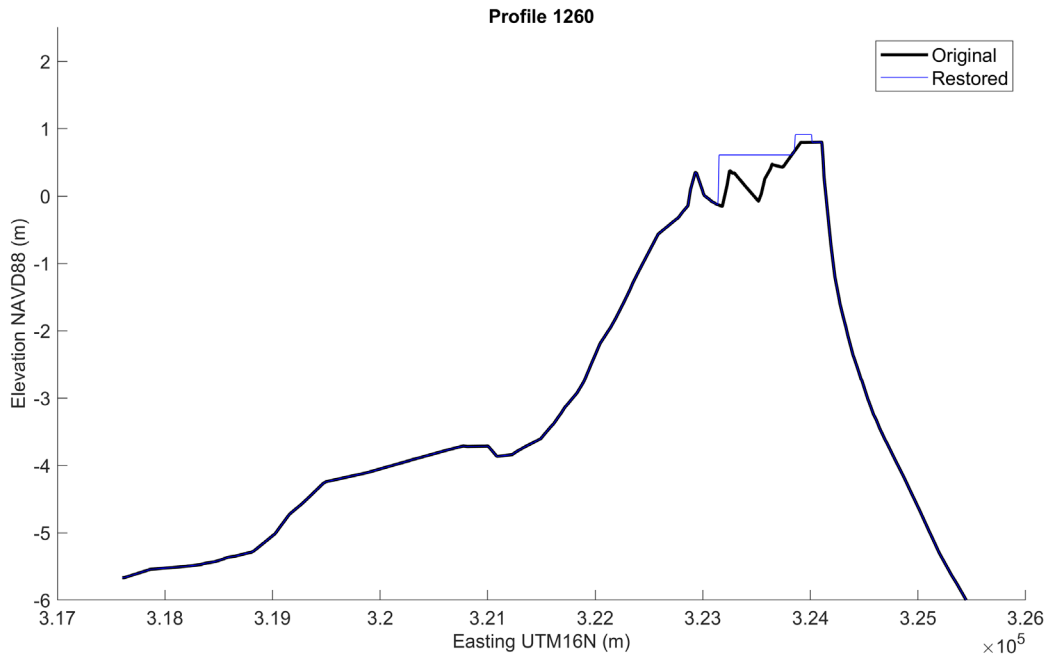


**Figure 27. The marsh restorations applied to the original topo-bathy profile. Top: Beach only template. Bottom: Beach and back marsh template.**

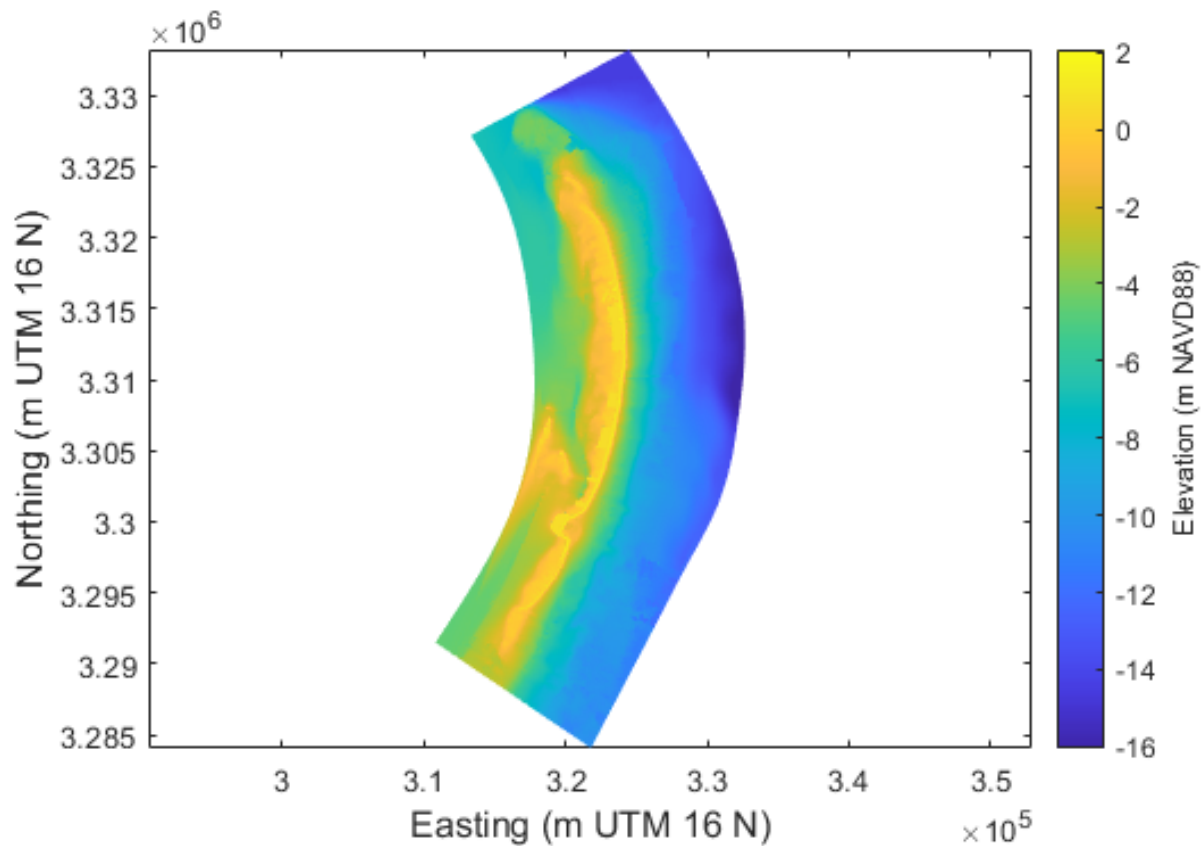


**Figure 28. The restored bathymetry for the marsh end member templates.**

### 3.1.4 Hydrodynamic Scenarios

A set of ‘idealized events’ was used to characterize the storm response of the Chandeleur Islands with and without restoration. These storms, drawn from Mickey et al. (2018) (hereafter referred to as Mickey2018), were generated by binning historical events in the northern Gulf of Mexico based on their calculated extreme TWL (includes the influence of storm surge and wave-driven setup) and duration; additional information can be found in Mickey2018. A selection of three storms were chosen to represent the range of island response: a weak storm, corresponding to bin 1 in Mickey2018; an intermediate storm, corresponding to bin 6 in Mickey2018; and a strong storm, corresponding to bin 11 in Mickey2018 (Table 3). An additional “extreme” storm, corresponding to bin 20 in Mickey2018, was also used for targeted sensitivity testing as described in Section 3.3.3. The time-varying wave boundary conditions for each storm were defined by the significant wave height and dominant wave period with an assumed Joint North Sea Wave Project (JONSWAP) spectrum (Hasselmann et al., 1973); uniform wave and water level boundaries were applied on the offshore and onshore edges of the model domain. Three different wave conditions were considered for each of the three storm bins for the future without action FWOA restoration scenario to test the sensitivity of island elevation to this parameter: shore normal waves, southeast (SE) waves (incident wave angle from 45° south of shore normal), and northeast (NE) waves (incident wave angle 45° north of shore normal). Varying the incident wave angle is predominantly

expected to vary the magnitude and direction of the wave-driven longshore current, with SE waves expected to result in a northward longshore current and NE waves expected to result in a southward longshore current. Due to a combination of the orientation of the Chandeleur Islands, wave sheltering provided by the Mississippi River delta, and the offshore bathymetry, the dominant wave direction for the Chandeleur Islands is from the SE (Dalyander et al., 2017), therefore the two restoration scenarios were tested across storms of varying strength with waves from the SE.

**Table 3. Characteristics of representative storms modeled for the Chandeleur Islands. For each storm class, model runs were conducted for waves coming from directly offshore (shore normal), from the southeast (45° south of short normal), and from the northeast (45° north of shore normal).**

Scenario	Max Wave Height (m)	Max Peak Wave Period (s)	Maximum Tide/Surge (m)	Maximum Water Level (m)	Duration (hours)
Weak	2.30	9.2	0.46	1.18	8
Intermediate	2.85	10.9	0.68	1.57	14
Strong	3.63	13.5	0.80	2.06	33
Extreme	7.78	16.7	1.62	3.71	45

### 3.2. ECOSYSTEM CHARACTERIZATION FOR MODEL ANALYSIS

A set of metrics that can be used to characterize ecosystem value from the numerical model output were derived and applied to contrast the two restoration scenarios and the FWOA scenario.

#### 3.2.1 Calculation of Metrics

Multiple ecosystem health and value indicators, geomorphic categorization schemes, and stability regime classifications have been developed and applied to barrier islands in the Gulf of Mexico and elsewhere (Campbell et al., 2005; Carapuço et al., 2016; Dalyander et al., 2016; Durán Vinent & Moore, 2015; Eliot, 2013; FitzGerald et al., 2018; Goldstein & Moore, 2016; McBride et al., 1995; Penland & Boyd, 1981; Ritchie & Penland, 1988; Rosati & Stone, 2009; Stallins & Corenblit, 2018; Stallins, 2005; Zinnert et al., 2017). A selection of metrics that have been previously used to characterize the state or evolution of barrier islands and associated habitats is found in Table 4.

**Table 4. Indicators for subaerial and shallow water habitats associated with barrier island systems.**

Indicator	Metrics	Link to Resiliency/Habitat Value	Source(s)
Beach Shoreline	<ul style="list-style-type: none"> <li>• Rate of change</li> <li>• Sedimentary characteristics (sand content and erodibility)</li> </ul>	<ul style="list-style-type: none"> <li>• Longshore sediment transport</li> <li>• Important foraging/loafing habitat for birds</li> <li>• Nesting habitat for sea turtles</li> </ul>	(Carruthers et al., 2011; Kombiadou et al., 2020; Walters et al., 2014)

Indicator	Metrics	Link to Resiliency/Habitat Value	Source(s)
Dunes	<ul style="list-style-type: none"> <li>• Spatial extent and sediment volume (i.e., elevation change/year)</li> <li>• Plant diversity &amp; vegetation structure</li> <li>• Aeolian sand transport, surface and vegetation dynamics</li> <li>• Sedimentary characteristics (sand content and erodibility)</li> </ul>	<ul style="list-style-type: none"> <li>• Buffer storm impacts and stabilize islands</li> <li>• Important nesting habitat for birds</li> <li>• Dune vegetation specially adapted to shifting substrates to promote sediment accretion and topographic protection</li> </ul>	(Carruthers et al., 2011; Durán Vinent & Moore, 2015; Feagin et al., 2015; Kombiadou et al., 2020; U.S. Fish and Wildlife Service, 2008; Walters et al., 2014)
Overwash	<ul style="list-style-type: none"> <li>• Areal extent</li> </ul>	<ul style="list-style-type: none"> <li>• Facilitates island migration/transgression</li> <li>• Important source of sediment to maintain marshes</li> <li>• Important foraging habitat for shorebirds</li> </ul>	(Carruthers et al., 2011; Walters et al., 2014)
Back-barrier Tidal Marsh	<ul style="list-style-type: none"> <li>• Area/degree of subsidence through relative elevation data</li> <li>• Sedimentary characteristics (sand content and erodibility)</li> </ul>	<ul style="list-style-type: none"> <li>• Stabilization and maintenance of subaerial exposure</li> <li>• Decrease island migration/transgression rates</li> <li>• Habitat for birds, fish, invertebrates</li> </ul>	(Fearnley et al., 2009b; Kombiadou et al., 2020; Walters et al., 2014)
Seagrass Beds	<ul style="list-style-type: none"> <li>• Areal extent, distribution, species composition</li> </ul>	<ul style="list-style-type: none"> <li>• Stabilize sediments and keep island above sea level</li> <li>• Important habitat for fish, sharks, sea turtles, invertebrates, marine mammals, and waterfowl</li> </ul>	(Deepwater Horizon Natural Resource Damage Assessment Trustees, 2016; Handley et al., 2018; Kenworthy et al., 2017; U.S. Fish and Wildlife Service, 2008)

Barrier island habitat varies on spatial scales of square meters to tens of square meters and is closely tied to geomorphology and vegetation cover, which on a barrier island are intrinsically linked. Elevation relative to water level drives frequency of inundation from tides or storms, which is a controlling factor of vegetation type. Conversely, presence, density, and type of vegetation controls the transport, erosion, and deposition of sediment by both hydrodynamic and aeolian (wind-driven) processes and resultant morphological evolution (Feagin et al., 2015; Roman & Nordstrom, 1988; Zinnert et al., 2019). As a result, elevation relative to tidal levels and recurrent regional storm surge is a dominant factor in differentiating habitat types including intertidal, beach, and dune (Enwright et al., 2017, 2018a, 2019). The elevation of barrier islands is also closely tied to patterns of sediment transport that influence the

islands' resilience, which ultimately dictate the habitat value these dynamic ecosystems can provide in the short- and long-term. Elevation can be predicted with numerical models used to evaluate restoration alternatives, including the XBeach model being used in this study. For this reason, metrics for evaluating state and resiliency of the Chandeleur Islands have been selected based on elevation criteria (Table 5).

**Table 5. Metrics of characterizing the Chandeleur Island response to storms for this study. These metrics have been chosen based on their value in assessing the current habitat state of the barrier islands (Table 4) and their short- and long-term resiliency.**

Metric	Island Resiliency and Habitat Implications
<p><b><i>Subaerial volume</i></b>  <i>(V<sub>aer</sub>; m<sup>3</sup>):</i> Volume of sediment located within or above the intertidal zone</p>	<p>Barrier islands that cannot preserve subaerial sediment volume over time will ultimately become submerged with loss of associated habitat for species that utilize dune, upper and lower beach, and backbarrier regions. In addition, loss of subaerial island exposes habitats in the lee of the island, such as seagrass beds, to increased wave energy.</p>
<p><b><i>Post-storm subaerial volume (V<sub>aer1</sub>; m<sup>3</sup>) within the pre-storm island footprint:</i></b> Volume of sediment located within or above the intertidal zone within the pre-storm footprint of the islands</p>	<p>This metric captures the fraction of the barrier island that has remained in place following a storm event. The difference between this value and post-storm <i>subaerial volume (V<sub>aer</sub>)</i> may be indicative of sand transport landward or seaward and reduced habitat within the original island footprint (sand transported landward does benefit backbarrier habitats and promotes island resiliency to RSLR).</p>
<p><b><i>Net seaward sediment volume deposition</i></b>  <i>(V<sub>sea</sub>; m<sup>3</sup>):</i> Net change in sediment volume seaward of the pre-storm shoreline</p>	<p>The location of sediment deposition following a storm event is important to a barrier island resiliency. At the Chandeleur Islands, sediment transported offshore is potentially lost from the subaerial island system, reducing the overall amount of sediment volume available in the system and decreasing island resiliency. A high positive value of <i>net seaward sediment volume deposition (V<sub>sea</sub>)</i> may indicate the island is susceptible to submergence (losing subaerial footprint).</p>
<p><b><i>Net landward sediment volume deposition (V<sub>land</sub>; m<sup>3</sup>):</i></b> Net change in sediment volume landward of the pre-storm shoreline</p>	<p>Landward sediment transport reflects island migration to shallower portions of the continental shelf platform prolonging submergence. This sediment can be reworked to reform the island landward of its original location. A high positive value of <i>net seaward sediment volume deposition (V<sub>land</sub>)</i> may indicate the island has potential to remain subaerial as it migrates landward.</p>
<p><b><i>Net sediment volume deposition in Hewes Point (V<sub>Hewes</sub>; m<sup>3</sup>):</i></b> Net change in sediment volume in the Hewes Point region</p>	<p>Hewes Point is a sediment sink for the Chandeleur Islands and the depositional zone for sand that is transported north from the island during storm events. This sediment is lost from the active littoral zone of the main island arc, reflecting a decrease in island resiliency.</p>

Island Resiliency and Habitat Implications	
<b>Metric</b> <b><i>Distribution of shallow and subaerial elevation by area (<math>A_{dist}</math>; <math>m^2</math>):</i></b> Histogram of area by elevation, delineated by onshore and offshore of the pre-storm shoreline	Because subaerial island habitats are closely tied to elevation, this metric is a proxy for habitat distribution. In addition, the distribution can be used to evaluate patterns in sediment transport on- and offshore, with associated implications for island resiliency.
<b><i>Potential seagrass area (<math>A_{sg}</math>; <math>m^2</math>):</i></b> Area characterized as potential seagrass area by depth and exposure criteria	This metric captures the nearshore area in the lee of the Chandeleur Islands that is potentially suitable for seagrass colonization.

The *subaerial volume* ( $V_{aer}$ ) is calculated from the pre-storm and post-storm DEMs by integrating the total sediment volume within each cell where the elevation is greater than -0.17 m mean low water (MLW; 0 m NAVD88), corresponding to approximately the intertidal zone (Figure 29, Equation 1). A mask is applied prior to calculation to isolate only those areas that are above this depth criterion ( $z_{sa,post}$ ).

$$V_{aer} = \int_x \int_y z_{sa,post} dx dy \quad [1]$$

The *post-storm subaerial volume within the pre-storm island footprint* ( $V_{aerI}$ ) is calculated similarly, but in this case the mask isolates only those areas where the pre-storm elevation is greater than -0.17 m MLW ( $z_{sa,I}$ ; Equation 2). This metric is only calculated for the post-storm DEM. For the pre-storm DEM,  $V_{aerI}$  is equivalent to the *subaerial sediment volume* ( $V_{aer}$ ).

$$V_{aerI} = \int_x \int_y z_{sa,I} dx dy \quad [2]$$

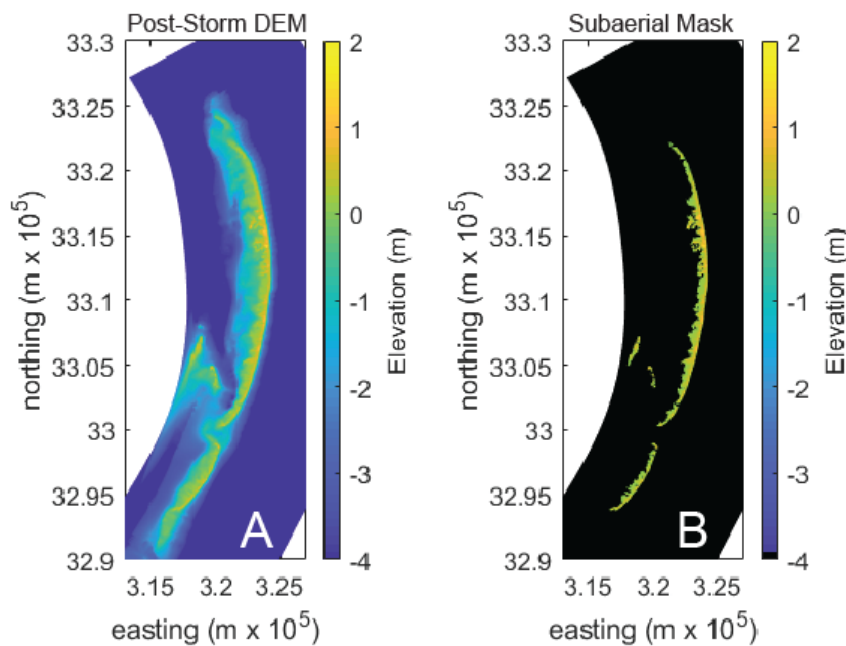


**Figure 29. (A) Post-storm DEM for a low-intensity storm with incident on-shore waves. (B) To calculate the post-storm subaerial volume, areas with elevation less than -0.17 m mean low water**

(MLW) (0 m NAVD88) are masked out (black shading) and the total subaerial volume is integrated over the remaining cells.

The net seaward sediment volume deposition ( $V_{sea}$ ) is calculated by taking the elevation difference between the post-storm and pre-storm DEMs, with positive reflecting a gain in elevation during the storm and negative reflecting a loss in elevation during the storm (Figure 30, Equation 3). Subaqueous regions to the north and south of the island are excluded from calculation. A mask is used to isolate only those areas of the DEM seaward of the pre-storm island shoreline ( $z_{pre,seaward}$  and  $z_{post,seaward}$  for the pre- and post-storm elevation, respectively). The pre-storm island shoreline is identified as an elevation of -0.17 m (0.5 ft) mean low water (MLW; 0 m NAVD88). For profiles that do not have a shoreline defined in this way (e.g., in Katrina Cut), the cross-shore position of maximum elevation is used.

$$V_{sea} = \int_x \int_y (z_{post,seaward} - z_{pre,seaward}) dx dy \quad [3]$$

The net landward sediment volume deposition ( $V_{land}$ ) is similarly calculated for the region landward of the pre-storm shoreline. The net deposition in Hewes Point ( $V_{Hewes}$ ) is calculated by integrating the net volume change for regions within the Hewes Point masking area (Figure 31).

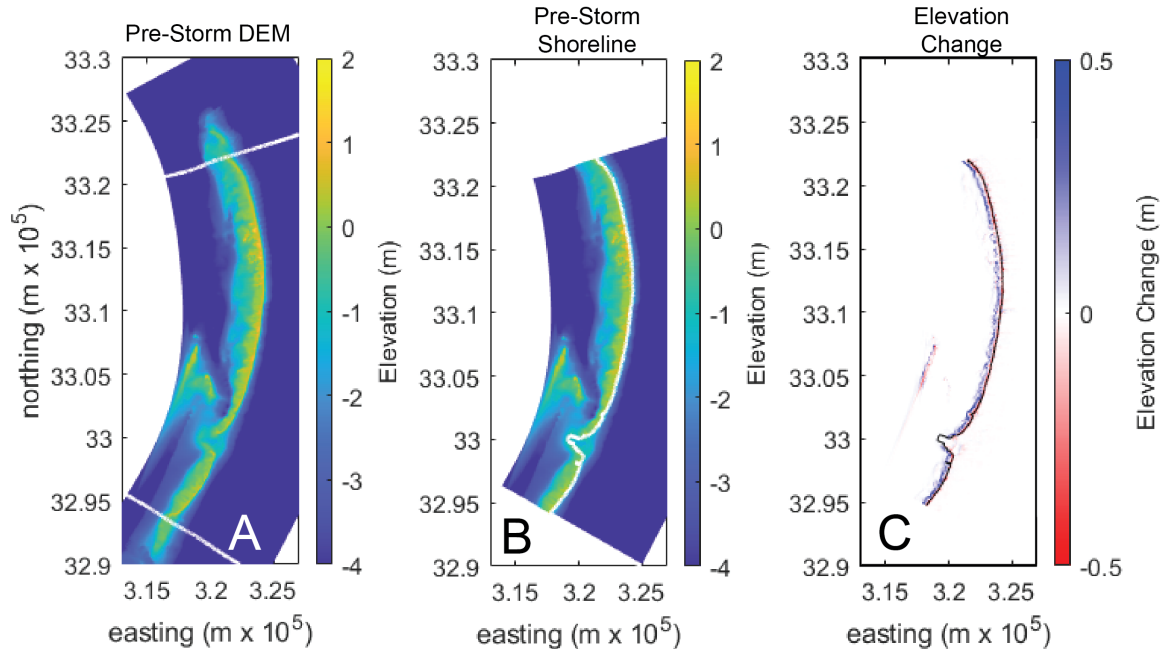


**Figure 30. Calculation methodology for  $V_{sea}$ , the net volume of sediment deposition seaward of the pre-storm shoreline, and  $V_{land}$ , the net volume of sediment deposition landward of the pre-storm shoreline. First, the domain is cropped to remove subaqueous areas to the north and south of the islands (A). A pre-storm shoreline is extracted as the 0 m NAVD88 contour (B); if a profile does not have a shoreline, the location of maximum elevation is used. The net sediment volume change is then calculated for the seaward and landward regions of the pre-storm shoreline for  $V_{sea}$  and  $V_{land}$ , respectively (C).**

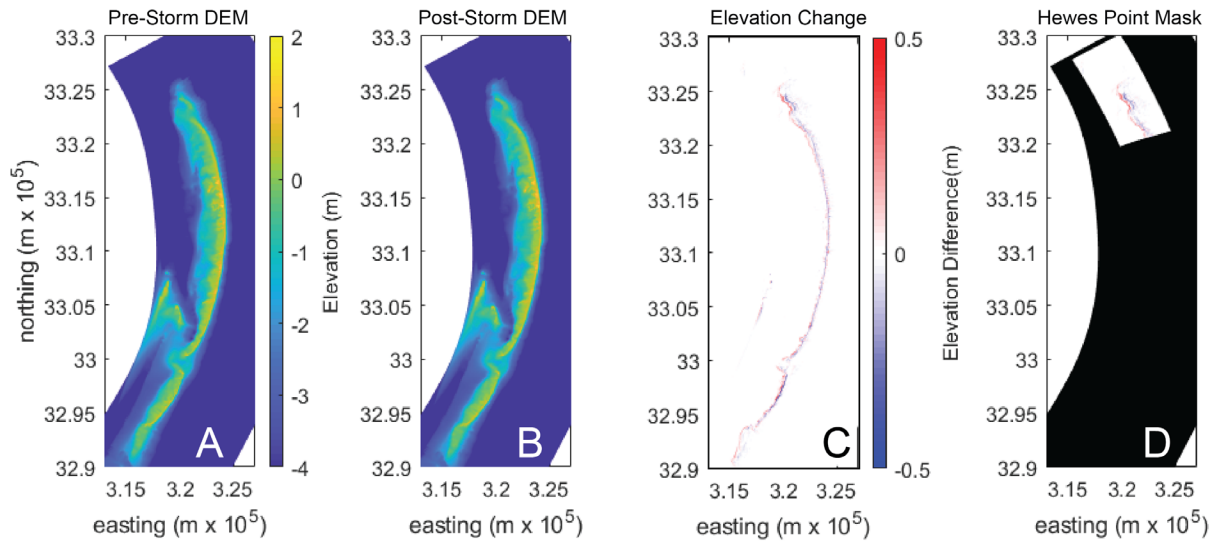


**Figure 31. Calculation methodology for VHewes, the net volume of sediment transported to Hewes Point. The difference between the pre-storm (A) and post-storm (B) elevation is taken (C), then the net sediment volume change is calculated in the region of Hewes Point (D) with the rest of the domain masked out (in black).**

To calculate the *distribution of shallow and subaerial elevation by area* ( $A_{dist}$ ), the DEM is first divided into landward (onshore of the pre-storm shoreline) and seaward (offshore of the pre-storm shoreline) regions. A histogram of pre- and post-storm elevation for the landward and seaward regions is created by identifying model cells that fall within 0.25 m bins, then summing the total area of the DEM within those cells (Figure 32). The difference between these pre- and post-storm histograms is calculated to illustrate the change in elevation and associated habitat resulting from the event.

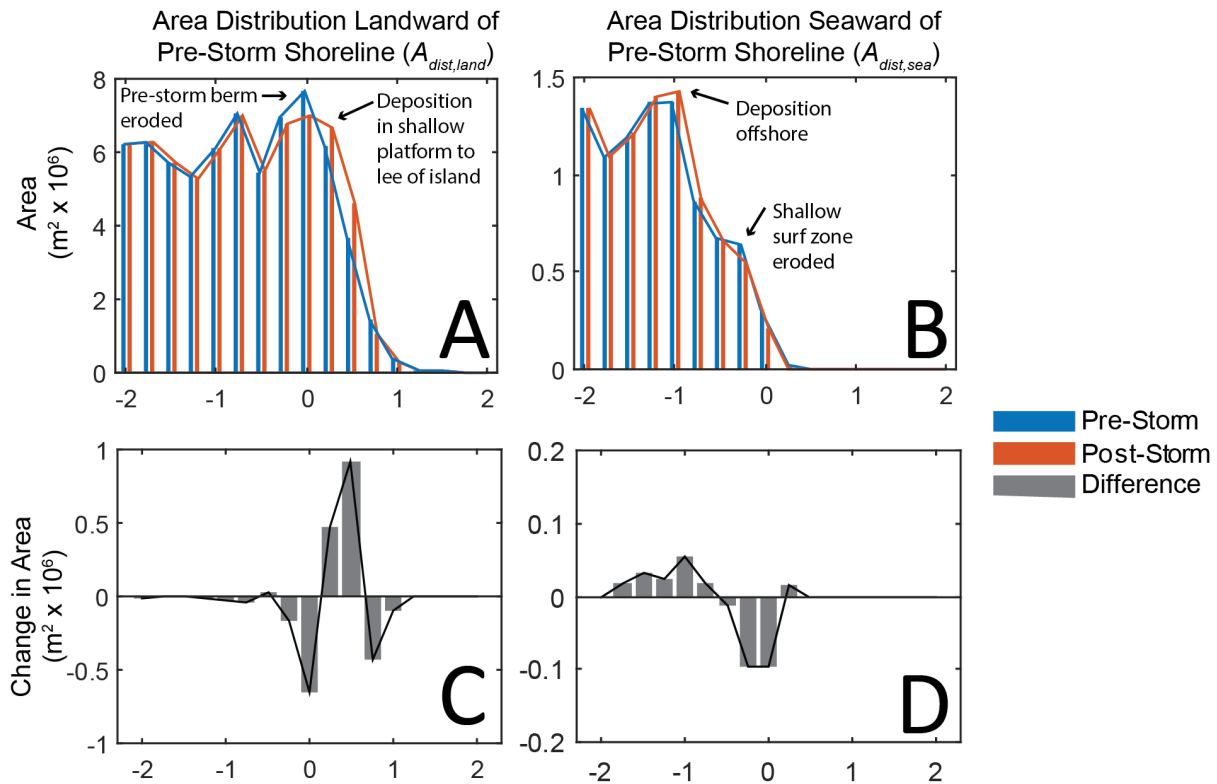


**Figure 32. Example histograms of the distribution of shallow and subaerial elevation by area ( $A_{dist}$ ) (A) landward and (B) seaward of the pre-storm shoreline for a strong storm with SE waves. Increases (or decreases) in the landward area indicate sediment had been gained (or lost) at locations that were to the west of the pre-storm shoreline, whereas increases (or decreases) in the seaward area indicate sediment has been gained (or lost) to the east of the pre-storm shoreline. Elevation is divided into 0.25m increments. The difference between the histograms represents the change in island elevation due to the storms (C) landward and (D) seaward of the pre-storm shoreline.**

To calculate the *potential seagrass area* ( $A_{sg}$ ), a mask is first applied to isolate the areas of the domain inshore of the Chandeleur Islands with elevation falling between -0.17 m and -1.31 m MLW (0 m to -1.15 m NAVD88) (Figure 33). This elevation corresponds to observations of the depth range of *Thalassia testudinum* at the Chandeleur Islands (Darnell et al., 2017). A second filter was then applied to remove any areas that were not protected by a subaerial island, defined as having elevation points higher than 0.04 m MLW (0.21 m NAVD88). This criteria was applied to be consistent with observations that the wave energy attenuation (sheltering) provided by the subaerial island is critical for preserving and protecting seagrass habitat (Darnell et al., 2017; Poirrier & Handley, 2007) and is consistent with observations of seagrass extent made at the Chandeleur Islands (Figure 34).

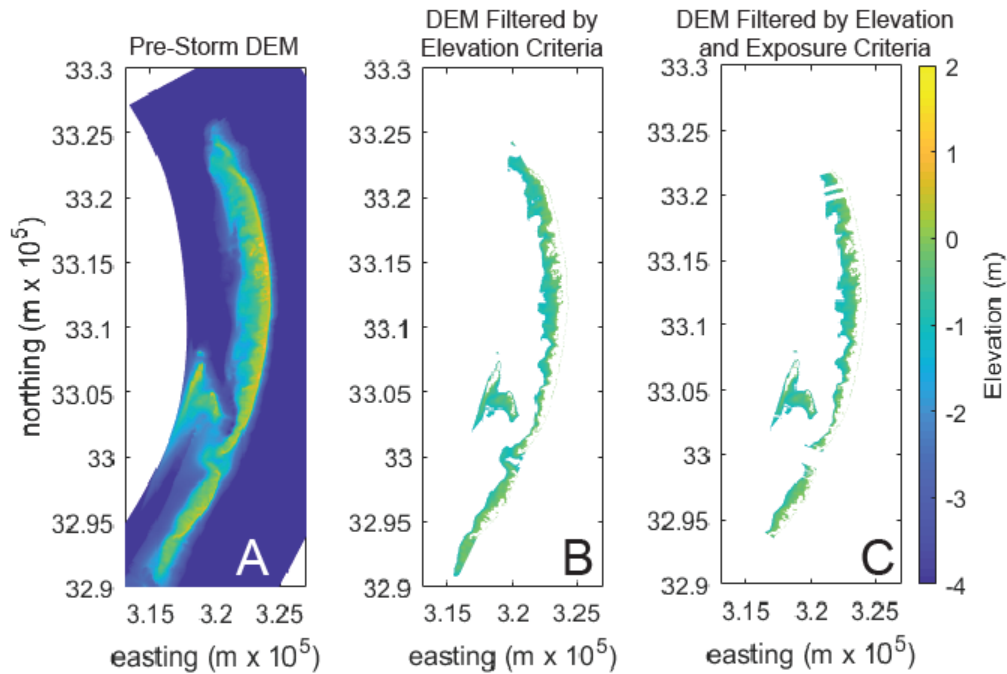


**Figure 33. Calculation methodology for potential seagrass area (Asg). The DEM (A) is first filtered to retain only those elevations that fall between -0.17 m and -1.31 m MLW (0 m to -1.15 m NAVD88). A second filter is then applied to remove those areas that are not protected by a subaerial island, defined as having elevation points higher than 0.04 m MLW (0.21 m NAVD88).**



**Figure 34. Distribution of seagrass at the Chandeleurs during 2010 (Kenworthy et al., 2017). Background imagery is a composite of Bands 1, 2, and 3 from Landsat 7. Imagery date is December 27, 2010.**

### 3.2.2 Interpretation of Metrics

The *distribution of shallow and subaerial elevation by area ( $A_{dist}$ )* provides a snapshot in time of the habitat distribution available for utilization by barrier island species. Elevations higher than the tidal range represent beach, dune, and backbarrier flat habitat; elevations within the tidal range on the Gulf side represent intertidal habitat and on the bayside representing either sandy intertidal areas or areas of potential marsh habitat; and elevations below the tidal range represent shallow subaqueous habitat.

Potential for seagrass habitat is further delineated with the *potential seagrass area* ( $A_{sg}$ ) metric, which accounts for both depth and exposure (e.g., presence or absence of fronting barrier island) as limiting factors for seagrass habitat. Evaluation of these metrics prior to and after restoration templates are applied to capture the short-term value the restoration is providing.

Comparison of metrics pre- and post-storm, in the context of island sediment dynamics and historical evolution (see Section 3.2.1), can be used to evaluate island trajectory, resiliency, and long-term habitat availability. By comparing these metrics for the two restoration cases to the FWOA scenario, the metrics can also inform an understanding of the long-term benefit restoration will have for the island. The first pair of metrics, the *subaerial volume* and *post-storm subaerial volume within the island footprint* ( $V_{aer}$  and  $V_{aer}$ ), evaluate the stability of the island and its resiliency to the storm event. If the storm has minimal impact to the subaerial island, the pre- and post- storm *subaerial volume* will be similar. A storm that has net erosional impact on the island will result in a decrease in *subaerial volume* during the storm event, while an increase in *subaerial volume* represents an accretion event. Impacts can be further understood by considering *post-storm subaerial volume within the island footprint*. If there is minimal change in pre- and post-storm *subaerial volume* but a significant decrease in *post-storm subaerial volume within the island footprint* compared to pre-storm *subaerial volume*, the island has migrated landward while maintaining subaerial sand volume. This can further be understood using the *net seaward sediment volume deposition* and *net landward sediment volume deposition* ( $V_{sea}$  and  $V_{land}$ ) metrics: an island that is migrating landward through overwash and inundation will have a positive *net landward sediment volume deposition* while an island that is losing sediment offshore will have a positive *net seaward sediment volume deposition*. The *net sediment volume deposition at Hewes Point* ( $V_{Hewes}$ ) metric similarly informs understanding of island resiliency by quantifying the sediment volume deposited at Hewes Point, a historical sediment sink for the Chandeleur Islands. The greater the *net sediment volume deposition at Hewes Point*, the more sediment that has been transported to the north and lost from the littoral system, with sediment that is deposited offshore of the island platform lost potentially lost from the system (either ends up in Hewes Point or transported to deep water offshore).

The change in *distribution of shallow and subaerial elevation by area* ( $A_{dist}$ ) is also informative for understanding the interaction of storms and potential restoration alternatives and the implications for island resiliency. When water levels from a storm overtop the berm or dune of the island and sediment is transported onshore, erosion and loss of the elevations corresponding to higher elevation regions is likely to occur with a shift toward increased area at low-lying elevation corresponding to overwash. This reflects short-term destruction of higher elevation habitat; however, overwash deposits preserve sediment within the active coastal system and can be reworked by aeolian (wind-driven) processes to reform higher elevation dune or berm features or at least over the long term they will be made available to the beach once the Gulf shoreline has eroded to that location in the backbarrier. Conversely, a storm that does not overtop the dune or berm may erode the subaerial beach and transport sediment offshore, resulting in an increase in subaqueous area on the Gulf side of the islands. If this sediment deposition is at a shallow enough depth, it may be reworked within the coastal system and redeposited on the island as part of recovery. However, sediment in the shallow surf zone can also be transported alongshore and eventually lost to the system through deposition at Hewes Point, and sediment deposited deeper offshore than the active surf zone is similarly unavailable to support barrier island recovery following a storm.

### 3.3. CHANDELEUR ISLANDS ECOSYSTEM VALUE WITH AND WITHOUT RESTORATION

#### Chandeaur Islands Ecosystem Value with and Without Restoration Key Findings and Implications for Restoration

- Longshore transport to the north during storm events and deposition at Hewes Point is significantly reduced for the presently-degraded (post-Katrina) northern Chandeaur Islands. Sand in this northernmost portion of the islands is instead transported in a landward direction during tropical cyclone events, conserving more sand within the active coastal system.
- In a marsh restoration scenario, the lower elevation profile facilitates continued overwash and landward transfer of sand during storm events. During storms, sand eroded from the beach and surf zone (shallow area offshore of the island) is transported onshore and deposited on the backbarrier platform. This sediment is retained within the active coastal sediment transport system and is thus more likely to increase the long-term resilience of the island.
- In a dune restoration scenario, the higher elevation of the dune inhibits overwash and inundation, preventing it or delaying it from occurring depending on the strength of the storm. This results in seaward sediment transport and deposition offshore of the island, where sand may be lost offshore or transported north to Hewes Point and out of the active coastal sediment transport system.
- The findings described above are captured with a new set of volume and area-based evaluation analysis metrics. These metrics can be readily calculated from the outputs of numerical models used in the engineering and design of barrier island restoration projects and characterize sediment transport and deposition patterns relevant to restored island resiliency.
- Calculation of these metrics for the Chandeaur Islands illustrates several aspects of barrier islands that should be considered when evaluating their restoration or conservation value in tools such as the Southeast Conservation Blueprint, including:
  - Barrier islands can change drastically during even a single storm, meaning that “snapshots in time” may not accurately characterize their condition;
  - Barrier island habitats are relatively narrow in the cross-shore (scale of meters), therefore regional metrics calculated on larger spatial scales may not capture their ecosystem value; and
  - The short- and long-term resiliency of the barrier island landform itself should be considered when evaluating conservation/restoration value, given that a loss of barrier island integrity undermines support for subaerial habitat as well as protection of shallow subaqueous habitat (e.g., seagrass beds) in the lee of the island.

### 3.4. FUTURE WITHOUT ACTION (FWOA)

Weak, intermediate, and strong storm events resulted in overwash and inundation of portions of the northern Chandeaur Islands in the FWOA scenario (Figure 35 and Figure 36). These conditions led to erosion of sediment from the beach, dune, and shallow surf zone; onshore sediment transport; and sediment deposition on the lee side of the island. These processes are captured by the island metrics, with positive *net landward sediment volume deposition* and negative *net seaward sediment volume deposition* for all cases (Table 6). Consistent with that result, the post-storm *subaerial volume* exceeds the *post-storm subaerial volume within the island footprint* and reflects landward migration of the island (loss of subaerial volume in the original island footprint and gain of subaerial volume in the lee of the original

footprint). Wave angle during the storms had little influence on morphology change on an island-wide scale, with enhanced bedform migration and longshore transport for waves coming from the SE or NE compared to the shore normal case (Figure 37). The calculation of *subaerial volume* is sensitive to the choice of threshold elevation defining “subaerial”, particularly for the post-storm case where sediment is deposited in low-lying overwash fans in the lee of the island that are slightly above, within, or below the intertidal zone. For example, if the threshold elevation is raised 0.5 m (to 0.33 m MLW or 0.5 m NAVD88) the pre-storm *subaerial volume* decreases by half from  $5.25 \times 10^6 \text{ m}^3$  to  $2.53 \times 10^6 \text{ m}^3$  and the post-storm *subaerial volume* for a strong storm with shore normal waves decreases by more than half from  $5.82 \times 10^6 \text{ m}^3$  to  $2.59 \times 10^6 \text{ m}^3$ .

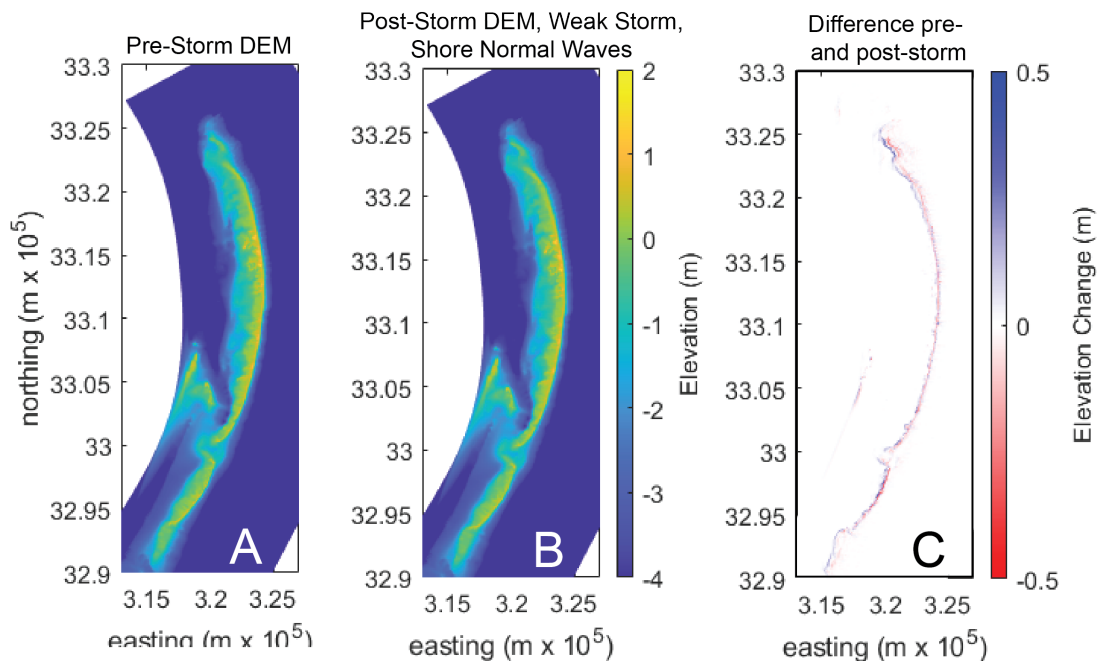


**Figure 35. Pre-storm (A) and post-storm (B) DEM for a weak storm with shore-normal waves (Table 3), along with the elevation change (C) during the storm.**

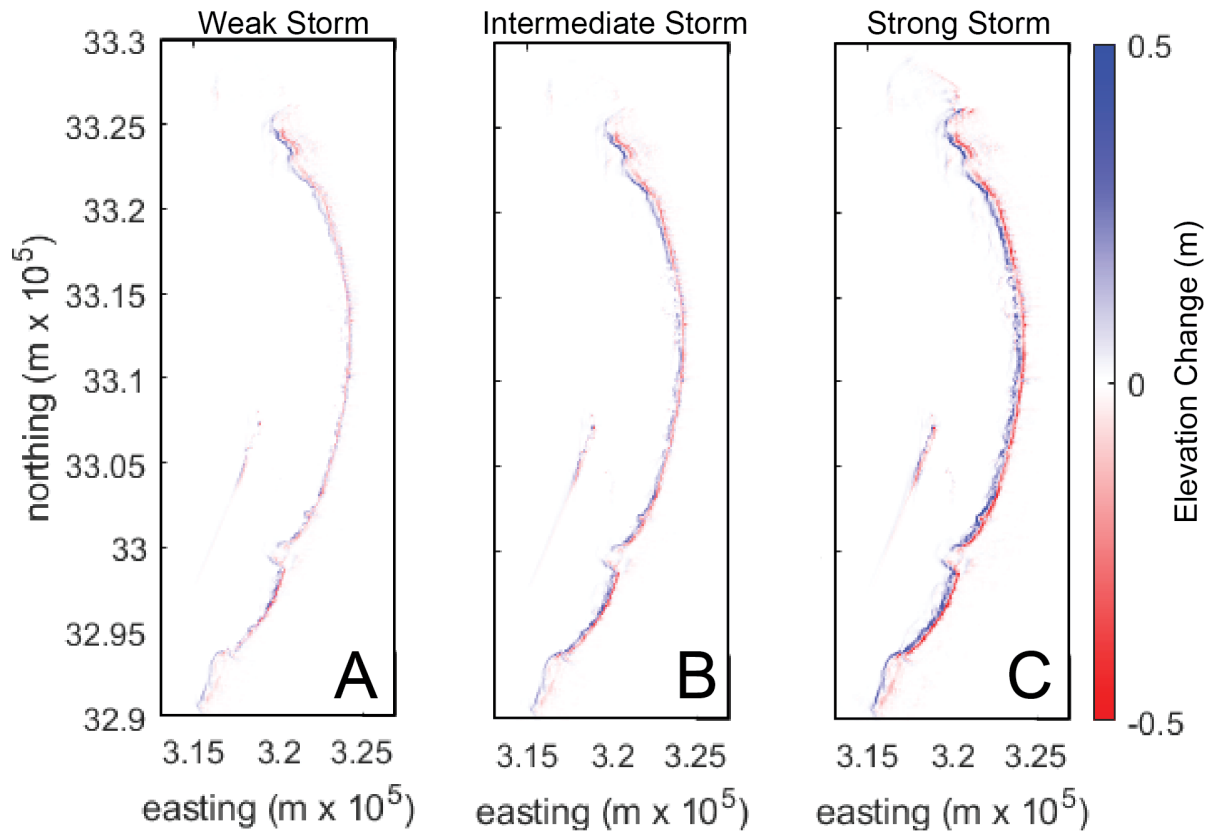


**Figure 36. Elevation change resulting from a weak (A), intermediate (B), and strong (C) storm. Storm characteristics are provided in Table 3.**

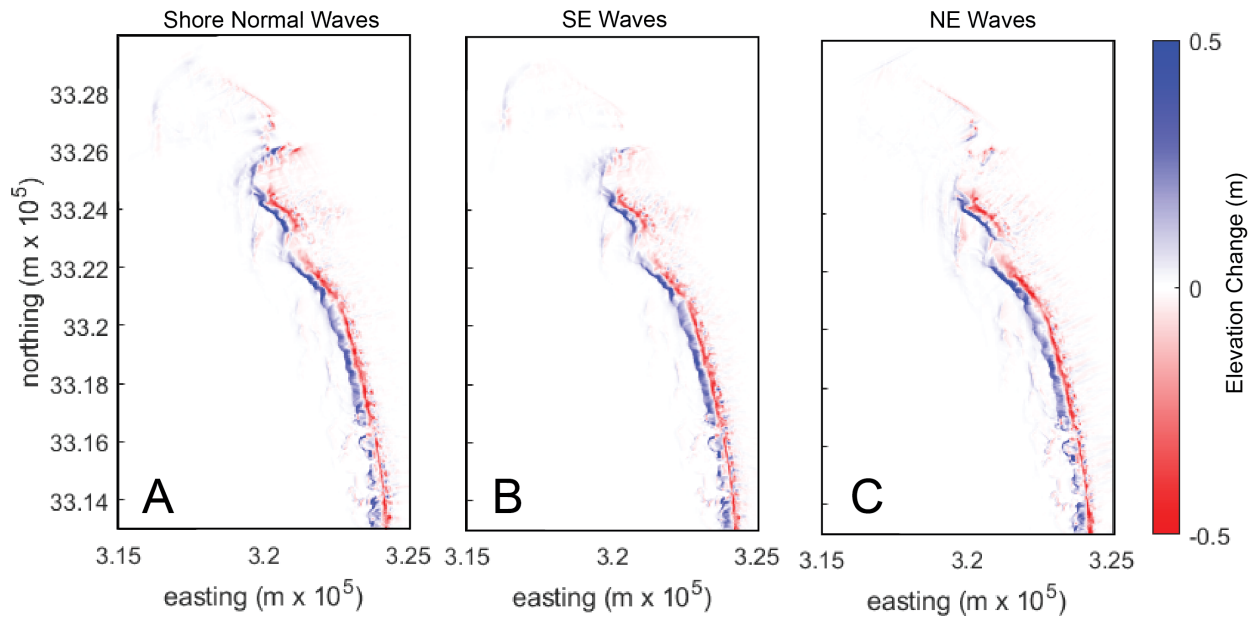


**Figure 37. Elevation change along the northern half of the island chain and at Hewes Point resulting from a strong storm with shore-normal waves (A), waves coming from the SE (B), and waves coming from the NE (C).**

**Table 6. Table summarizing habitat and resiliency metrics for the Chandeleur Islands for varying storm conditions (Table 3) for the FWOA scenario. For comparison, the pre-storm value of  $V_{aer}$  is  $5.25 \times 10^6 \text{ m}^3$  and  $A_{sg}$  is  $28.2 \times 10^6 \text{ m}^2$ . See Table 5 for information on the calculation of each metric.**

Storm	Wave Angle	$V_{aer}$ ( $10^6 \text{ m}^3$ )	$V_{aerI}$ ( $10^6 \text{ m}^3$ )	$V_{land}$ ( $10^6 \text{ m}^3$ )	$V_{sea}$ ( $10^6 \text{ m}^3$ )	$V_{Hewes}$ ( $10^6 \text{ m}^3$ )	$A_{sg}$ ( $10^6 \text{ m}^2$ )
Weak	Shore Normal	5.16	5.08	-0.01	-0.02	0.01	27.6
	SE Waves	5.16	5.08	-0.03	0.01	0.02	27.7
	NE Waves	5.19	5.07	0.04	-0.06	-0.01	27.6
Intermediate	Shore Normal	5.34	5.13	0.21	-0.22	0.01	27.5
	SE Waves	5.41	5.20	0.27	-0.27	0.02	27.7
	NE Waves	5.42	5.19	0.30	-0.31	-0.01	27.5
Strong	Shore Normal	5.67	5.15	0.70	-0.65	0.03	27.3
	SE Waves	5.82	5.31	0.78	-0.71	0.04	27.7
	NE Waves	5.79	5.25	0.77	-0.73	-0.00	27.4

**Metric Definitions**

$V_{aer}$ : subaerial volume

$V_{aer,I}$ : post-storm subaerial volume within the pre-storm island footprint

$V_{sea}$ : net seaward sediment volume deposition

$V_{land}$ : net landward sediment volume deposition

$V_{Hewes}$ : net sediment volume deposition in Hewes Point

$A_{sg}$ : potential sea grass area

The subaerial volume and post-storm subaerial volume within the pre-storm island footprint increased with increasing storm strength (Table 6), which is somewhat counterintuitive given that stronger storms are generally associated with increased erosion from beaches and barrier islands. Although portions of the island overwash during the weak storm, other areas of the island remain in the collision regime (Sallenger Jr., 2000) with associated offshore sediment transport from the beach, berm, and dune to the surf zone (Figure 38). As the storm strength increases, more of the island enters the overwash and inundation regimes, with sediment eroded from the berm and shallow surf zone transported onshore and deposited on the shallow island platform regardless of incident wave angle (Figure 39 and Figure 40). The net result is that post-storm the subaerial volume is greater than pre-storm subaerial volume for the intermediate and strong storm events.

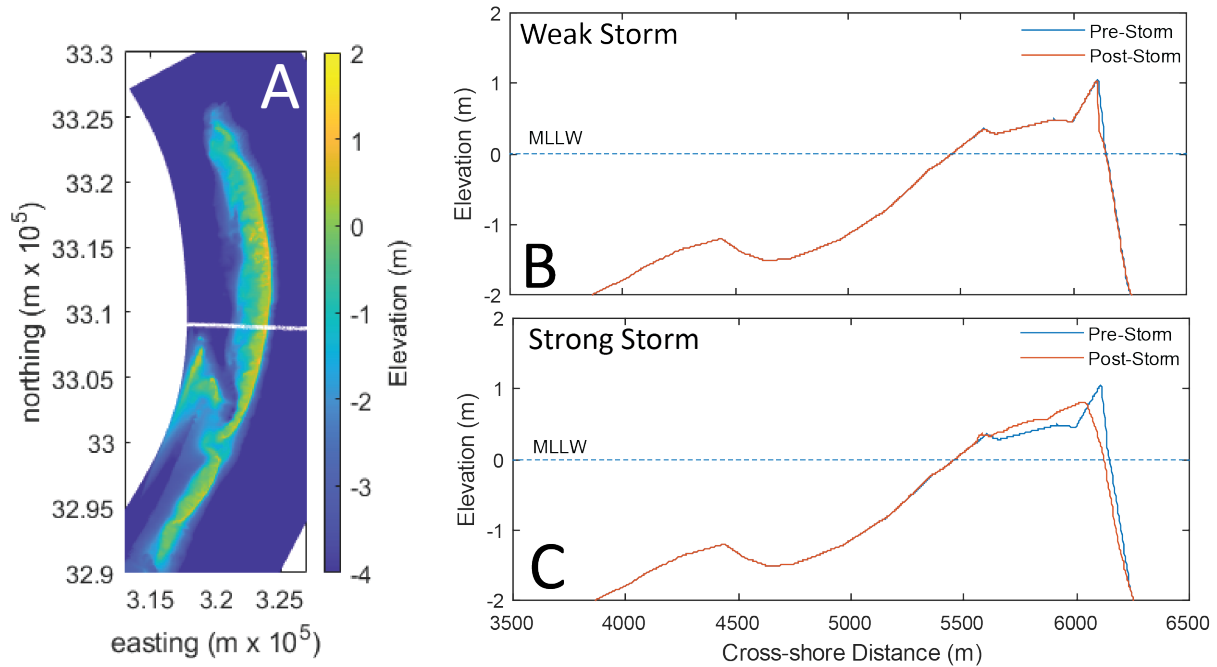


**Figure 38. (A) Pre-storm DEM and the pre- and post-storm cross-shore elevation for the transect shown in white. Results are shown for a weak (B) and strong (C) storm with SE waves.**

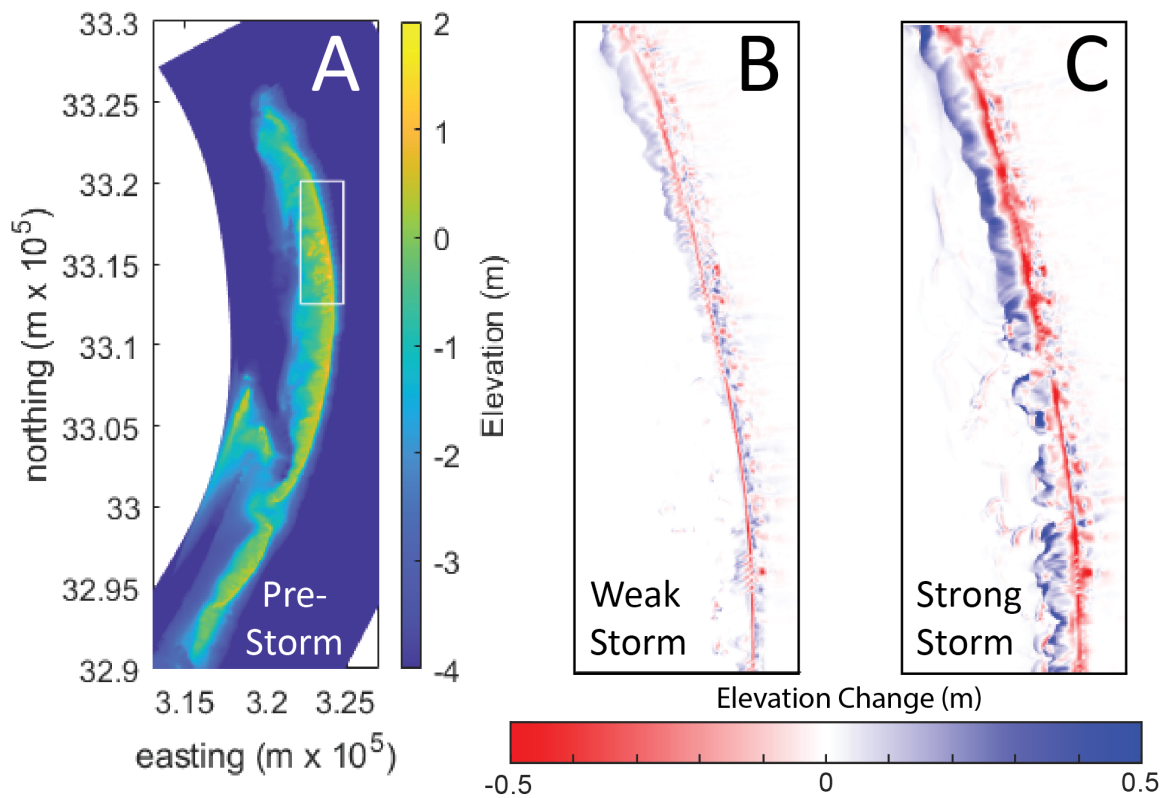


**Figure 39. (A) Pre-storm DEM and the pre- and post-storm elevation change for the region shown in white. Results are shown for a weak (B) and strong (C) storm with shore normal waves.**

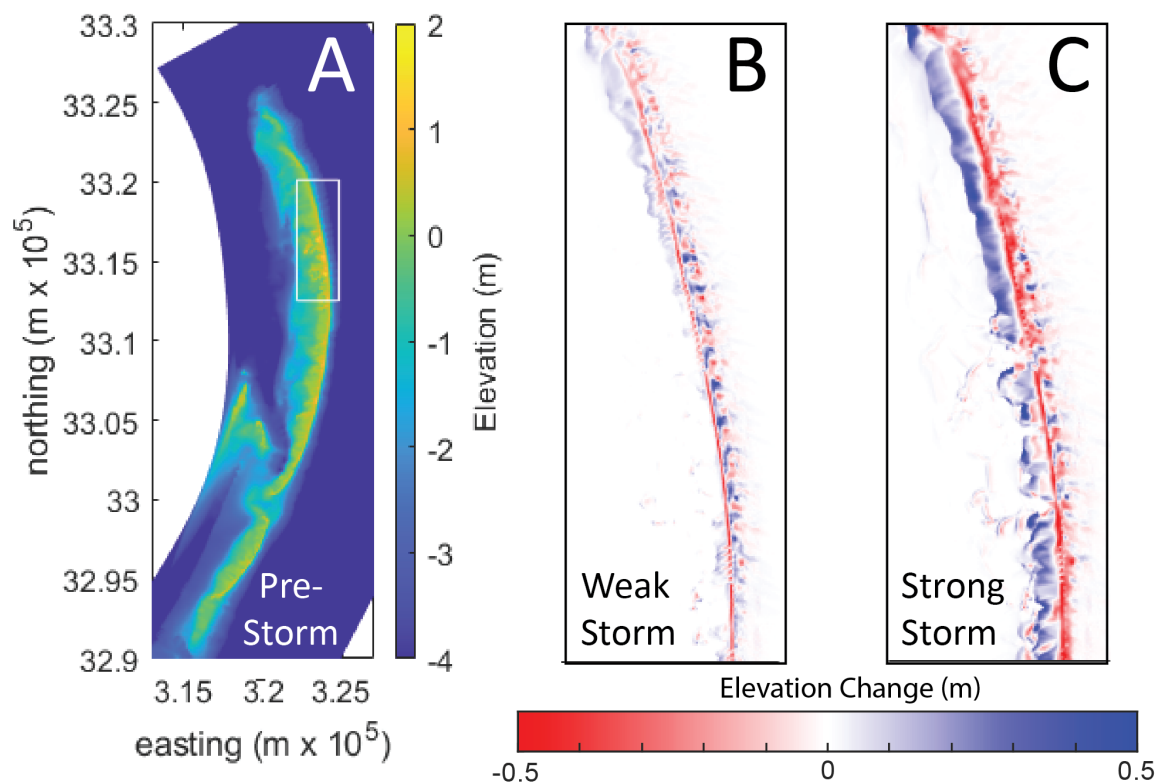


**Figure 40. (A) Pre-storm DEM and the pre- and post-storm elevation change for the region shown in white. Results are shown for a weak (B) and strong (C) storm with SE waves.**

The *net sediment volume deposition in Hewes Point* did not vary considerably across the storm and wave angle scenarios (Table 6). As expected, waves from the SE lead to northward directed longshore currents in the northern Chandeleur Islands (Figure 41) and slightly more net sediment volume deposition in Hewes Point compared to the shore normal and NE waves. However, the overall sediment deposition in the Hewes Point area is small compared to the volume of sediment deposited landward of the pre-storm shoreline during the storms. This pattern of transport with minimal amounts of sand being delivered to Hewes Point is inconsistent with the historical patterns of sediment deposition for the island as discussed earlier regarding the historical (up through Katrina) sediment transport patterns but is indicative of island degradation observed in the north as a result of Katrina and elevation loss leading to increased overwash, inundation, and associated onshore transport at this location. Sand that would have historically been transported to Hewes Point by longshore currents is no longer able to reach that area because landward directed sand transport now dominates. This sand transport regime shift for the post-Katrina island configuration results in more sand being maintained within the active coastal system as the islands migrate landward and is important to consider for island restoration and sediment placement strategy development.

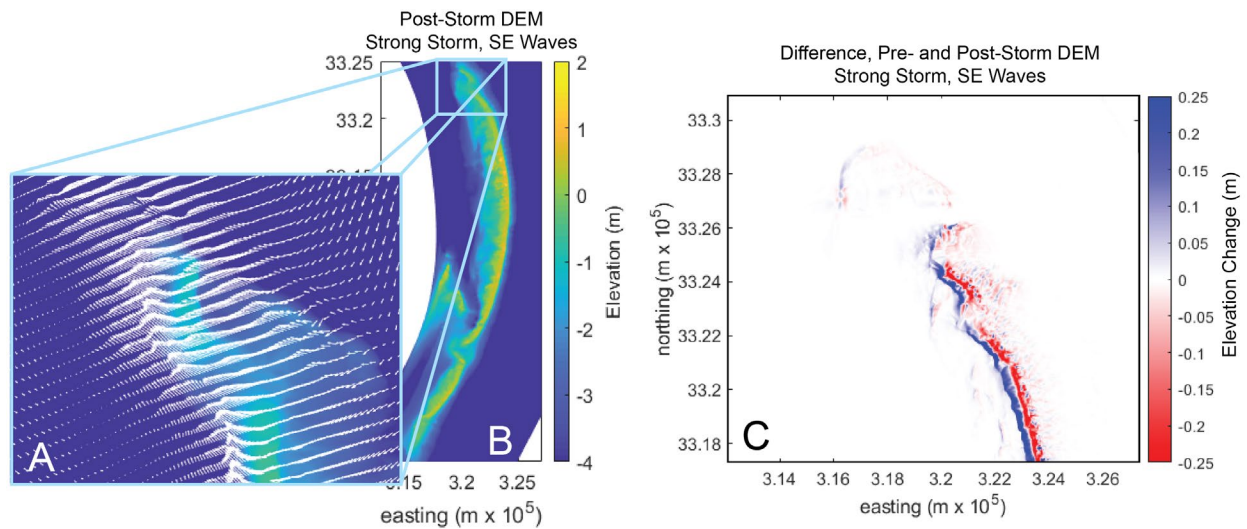


**Figure 41. Pattern of currents (A) for the northernmost portion of the Chandeleur Islands (B) during the peak of a strong storm (Table 3) with waves coming from the SE. Also shown is the elevation difference pre- and post-storm (C). Note that in this modeled scenario minimal sand is delivered to Hewes Point as was historically typical with a pre-Katrina island configuration. In this degraded island condition, dominant sand transport direction along this sector of island is landward instead of alongshore. In this way, more sand is conserved within the coastal system in a landward direction instead of being lost to the deep water sink at Hewes Point.**

The Chandeleur Islands are currently in a degraded state, with the *distribution of shallow and subaerial elevation by area* reflecting subaerial elevations less than 1 m (Figure 42). Subaerial regions are limited to intertidal, beach, and marsh habitats, with shallow subaqueous habitat landward and Gulfward of the island. During modeled storm events, there was a shift with a loss of shallow subaqueous habitat both seaward and landward of the pre-storm shoreline and gains in intertidal and low-lying subaerial habitat landward of the pre-storm shoreline (Figure 43). The loss of shallow subaqueous area is a combination of erosion and deepening of the profile seaward of the pre-storm shoreline and sediment deposition landward of the island. Storm impacts to the *distribution of shallow and subaerial elevation by area* were minimal (Table 6) and resulted from deposition of sediment landward of the island converting some shallow subaqueous areas originally within the depth range for seagrass to intertidal habitat and overwash fans.

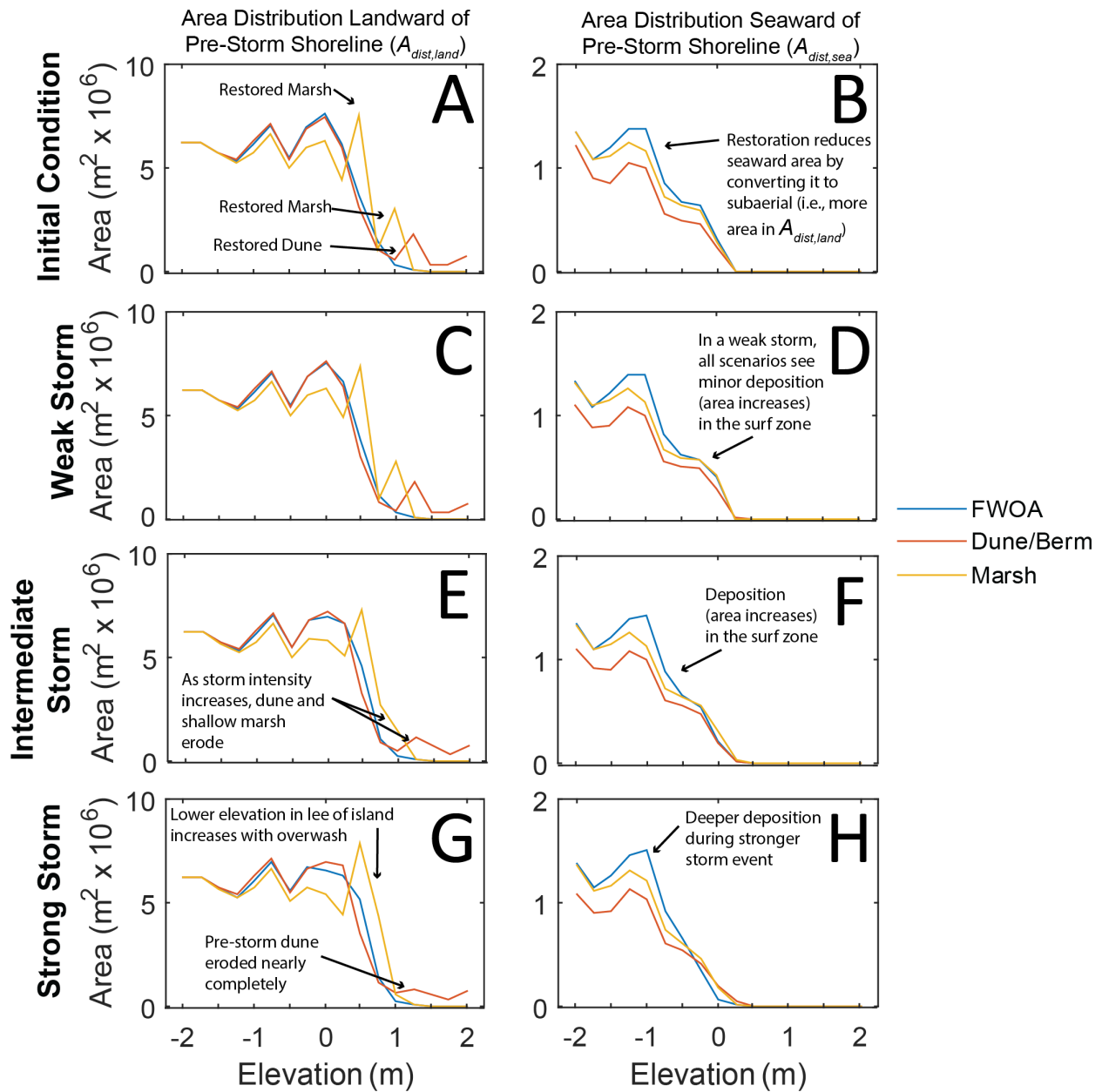


**Figure 42. Distribution of shallow and subaqueous elevation by area ( $A_{dist}$ ) for three scenarios including future without action (FWOA), placement of sediment on the dune and berm, and placement of sediment in the backbarrier marsh. Shown is the distribution of elevation landward (left column) and seaward (right column) of the pre-storm shoreline for each scenario for the (A,B) pre-storm DEM and after a (C,D) weak, (E,F) intermediate, and (G,H) strong storm. This distribution allows the area within different elevation ranges to be clearly seen. For example, restoring the marsh results in an increase in area of between 0-1 m elevation landward of the shoreline, while restoring the dune results in an crease in area of >1 m elevation landward of the shoreline (A). The pre- and post-storm changes for the FWOA are shown in Figure 43.**

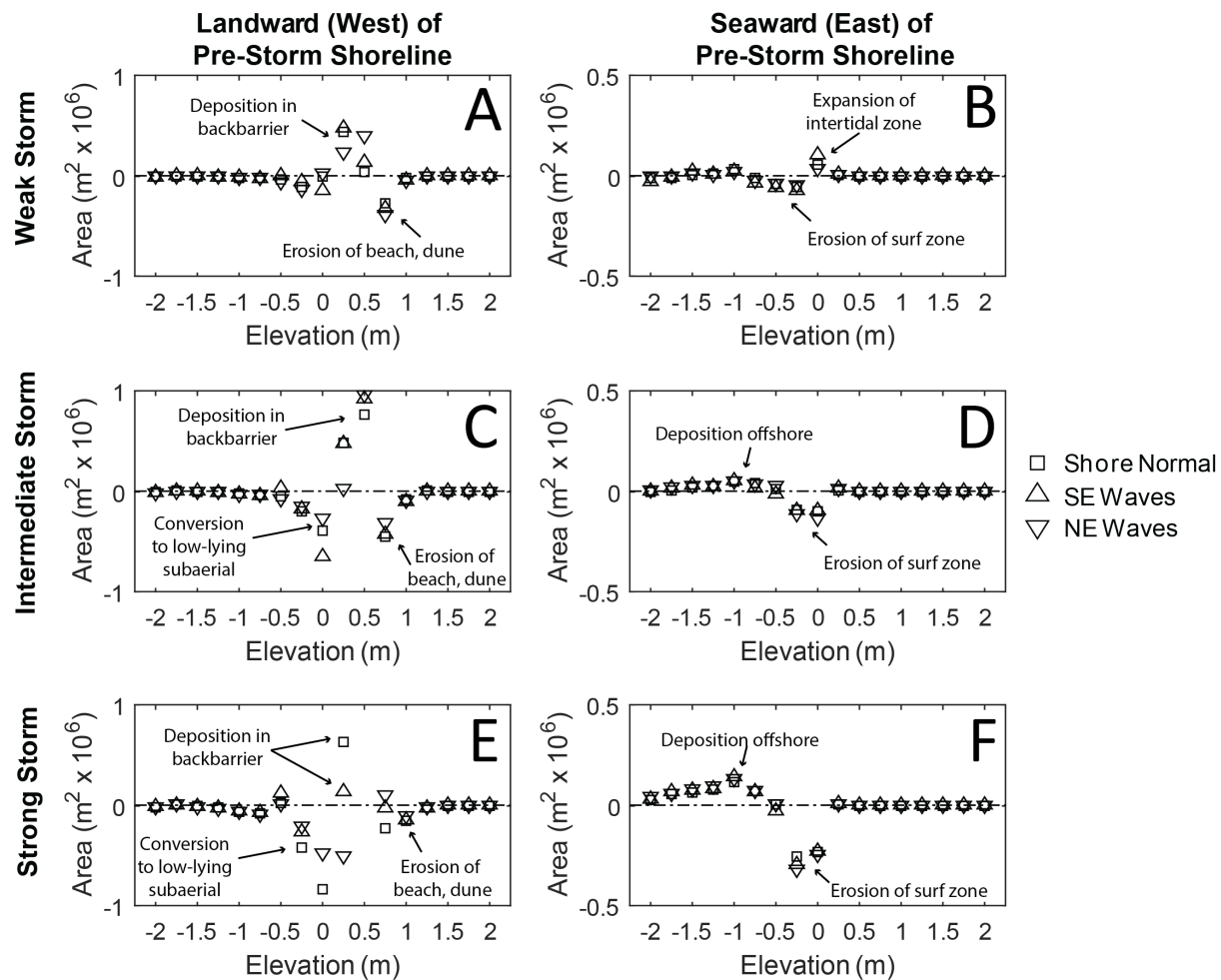


**Figure 43. Change in distribution of shallow and subaqueous elevation by area pre- and post-storm for a weak (A, B), intermediate (C, D), and strong (E, F) storm. The column to the left shows the change in area landward of (west) of the pre-storm shoreline and the column to the right shows area change seaward (east) of the pre-storm shoreline.**

### 3.4.1 Restoration Alternatives

The placement of  $6.5 \times 10^6 m^3$  of sediment increased the pre-storm *subaerial volume* from  $5.25 \times 10^6 m^3$  to  $9.54 \times 10^6 m^3$  and  $9.43 \times 10^6 m^3$  for dune/berm and marsh sediment placement alternatives, respectively. Placement of sediment in a dune and berm feature is reflected in an increase in area of elevation higher than 1 m within the *distribution of shallow and subaqueous elevation by area*, while placement of sediment in the backbarrier marsh increased the area of back-barrier habitat in the 0.5–1 m elevation range (Figure 43). Placement of the dune resulted in no change in *potential seagrass area* from the baseline value of  $28.2 \times 10^6 m^2$  and a slight decrease for the marsh placement (to  $27.2 \times 10^6 m^2$ ) due to sediment placement in some back-barrier areas originally within the depth range for seagrass.

During storm events, there was a shift in regime depending on the restoration alternative and storm magnitude. For the dune/berm sediment placement alternative, most of the restored portion of the island remained in the collision regime even for the strongest storm tested (Figure 44). As a result, there is net offshore sediment transport reflected in positive *net seaward sediment volume deposition* and negative *net*

*landward sediment volume deposition.* There is a decrease in *subaerial volume* both overall and within the pre-storm island footprint (Table 7) for the dune placement, reflecting loss of sediment offshore from the template. As the storm strength increased, more of the island transitioned into the overwash regime with associated sediment deposition landward of the pre-storm shoreline, leading to less sediment deposition seaward of the pre-storm shoreline as the dunes were overtopped or breached. Changes to the *distribution of shallow and subaqueous elevation by area* reflect this regime: erosion of the front face of the dune led to a decrease in area of elevations between 1–1.5 m, while the peak elevation of the dune was unaffected due to lack of overwash and inundation (Figure 42, Figure 45). The loss of the dune resulted in elevation increase of 0–1 m even as sediment was transported offshore due to conversion of the dune/berm areas to lower-lying upper beach. Similar to the unrestored case, there were slight decreases in *potential seagrass area* from the pre-storm values due to deposition of sediment in shallow back-barrier areas during overwash of non-restored portions of the island (Table 7; Table 8).

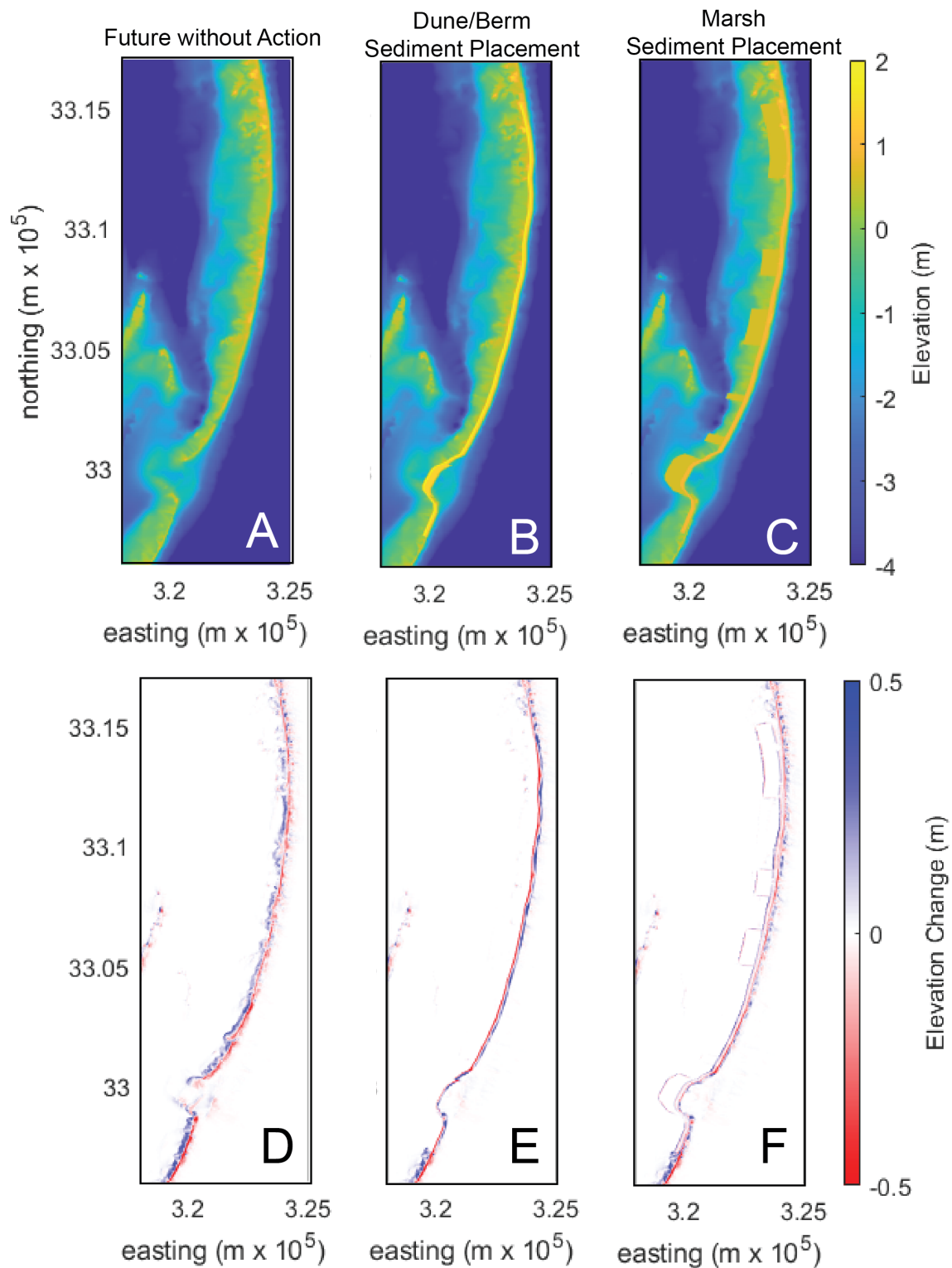


**Figure 44. Pre-storm elevation for the FWOA (A), dune/berm sediment placement (B), and marsh sediment placement (C), along with the change in elevation during a strong storm event with waves from the SE (D-F for FWOA, dune/berm sediment placement, and marsh sediment placement, respectively).**

**Table 7. Summary of habitat and resiliency metrics for the Chandeleur Islands for varying storm conditions (Table 3) for the dune and marsh restoration alternatives. For comparison, the pre-storm value of *subaerial volume* ( $V_{aer}$ ) is  $9.54 \times 10^6 \text{ m}^3$  for the dune/berm case and  $9.43 \times 10^6 \text{ m}^3$  for the marsh case, and the pre-storm value of *potential seagrass area* is  $28.2 \times 10^6 \text{ m}^2$  for the dune/berm case and  $27.2 \times 10^6 \text{ m}^2$ .**

Storm	Wave Angle	$V_{aer}$ ( $10^6 \text{ m}^3$ )	$V_{aerI}$ ( $10^6 \text{ m}^3$ )	$V_{land}$ ( $10^6 \text{ m}^3$ )	$V_{sea}$ ( $10^6 \text{ m}^3$ )	$V_{Hewes}$ ( $10^6 \text{ m}^3$ )	$A_{sg}$ ( $10^6 \text{ m}^2$ )
Dune/Berm Sediment Placement							
Weak	SE Waves	9.22	9.16	-0.31	0.29	0.02	28.0
Intermediate	SE Waves	9.24	9.10	-0.27	0.25	0.02	27.8
Strong	SE Waves	9.20	8.88	-0.25	0.24	0.03	27.5
Marsh Sediment Placement							
Weak	SE Waves	9.24	9.20	-0.17	0.16	0.02	27.7
Intermediate	SE Waves	9.32	9.17	-0.05	0.04	0.02	27.4
Strong	SE Waves	9.64	9.26	0.36	-0.37	0.04	27.0

**Metric Definitions**

$V_{aer}$ : *subaerial volume*

$V_{aerI}$ : *post-storm subaerial volume within the pre-storm island footprint*

$V_{sea}$ : *net seaward sediment volume deposition*

$V_{land}$ : *net landward sediment volume deposition*

$V_{Hewes}$ : *net sediment volume deposition in Hewes Point*

$A_{sg}$ : *potential sea grass area*

There was minimal change in the *net sediment volume deposition in Hewes Point* for the dune/berm restoration scenario, indicating that sediment volume placed in the dune restoration template and eroded during storms does not reach the terminus of the island during a single storm event. Comparison of the post-storm DEM for the FWOA and the dune placement scenario does suggest that sediment eroded from the dune template is deposited in the surf zone and transported northward (alongshore) toward Hewes Point during the storm (Figure 46), which suggests that with multiple storms and during quiescent non-storm conditions the dune restoration alternative island configuration more efficiently supplies sand to Hewes Point, removing it from the littoral system.

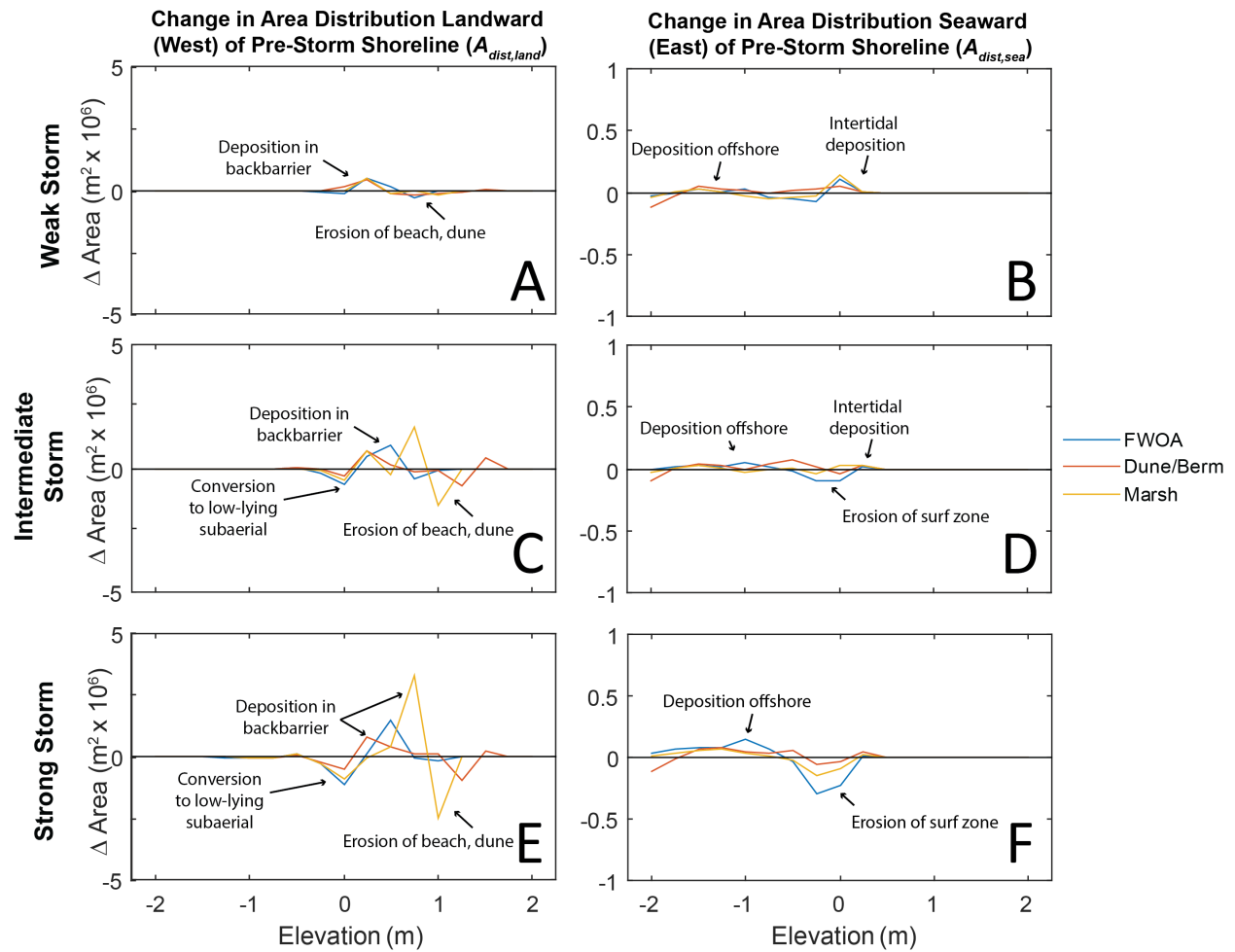


**Figure 45. Change in distribution of shallow and subaqueous elevation by area ( $A_{dist}$ ) for three alternatives including future without action (FWOA), placement of sediment on the dune and berm, and placement of sediment in the backbarrier marsh. Shown is the change in distribution of elevation landward (left column) and seaward (right column) of the pre-storm shoreline for a (A,B) weak, (C,D) intermediate, and (E,F) strong storm.**

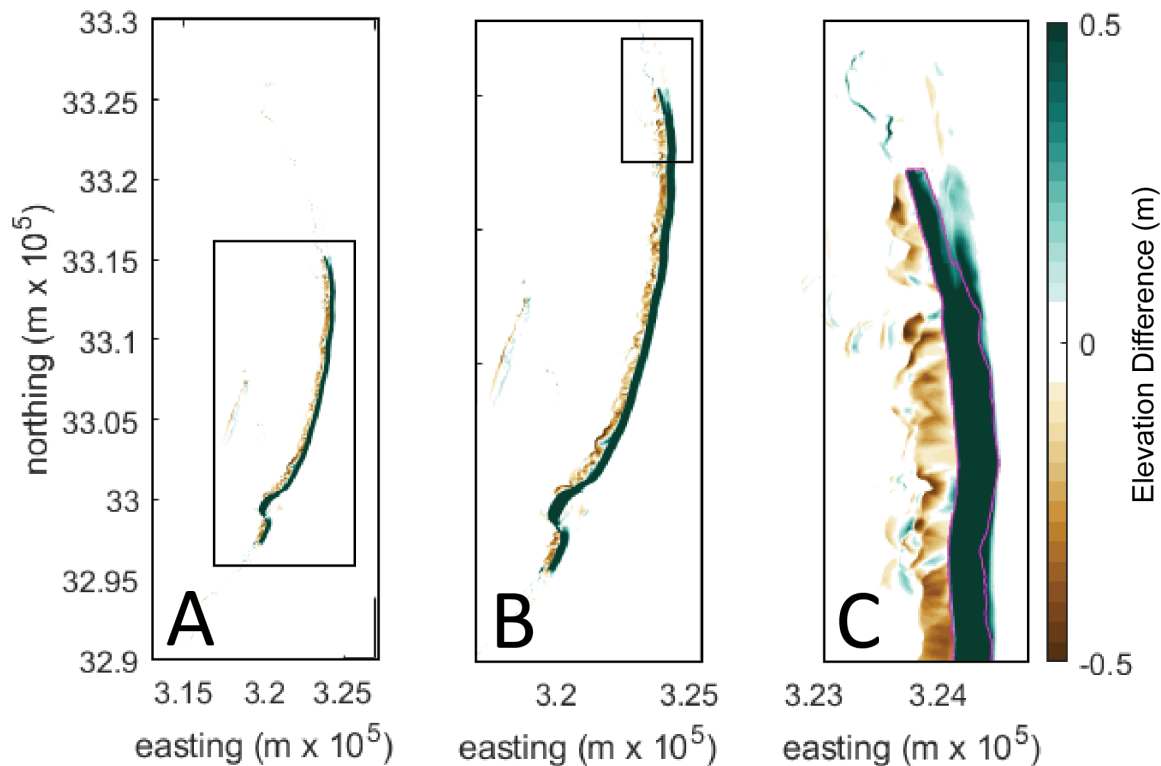


**Figure 46. Difference between the post-storm DEM for the dune/berm restoration and the FWOA scenarios. The pink outline is the location of restoration; elevation changes in this region are directly due to placement of sediment in the dune/berm case. Positive (green) values indicate the dune scenario is higher in elevation, negative (brown) values indicate the FWOA case is higher in elevation. Note in C that storm wave “collision regime” associated with the dune alternative results in offshore transport of sand to the surf zone that is then mobilized in an alongshore direction toward Hewes Point.**

For the marsh sediment placement, the hydrodynamic regime during storms depended on the magnitude of the storm event. For the weak and intermediate storms, portions of the restored island remained in the collision regime and resulted in net offshore transport (Table 7). This resulted in post-storm values of *subaerial volume* and *subaerial volume within the pre-storm island footprint* that were less than the pre-storm values, but still well above the subaerial sediment volumes for the FWOA case (Table 8). In addition, the magnitude of *net seaward sediment volume deposition* was reduced compared to the dune/berm sediment placement case for the weak and intermediate storms. The marsh template was overwashed during the strong storm event, leading to positive *net landward sediment volume deposition* and an increase in *subaerial volume* over the pre-storm subaerial sediment volume for this storm case.

Similar variability was seen in post-storm *distribution of shallow and subaqueous elevation by area*. For all three storms, erosion and overtopping of some portions of the marsh sediment template resulted in loss of area of pre-storm elevations in the ~1 m elevation range (Figure 43). This sediment was transported onshore and deposited landward of the pre-storm shoreline, resulting in increases in area of lower elevation zones in the 0–0.5 m elevation range. Impacts to *potential seagrass area* were minimal and

depended on slight shifts in back-barrier elevation resulting from infilling of low-lying areas and sediment deposition during the storms, with a slight increase in *potential seagrass area* compared to the pre-storm case for the weak and intermediate storms and a slight decrease in *potential seagrass area* for the strong storm case.

**Table 8. Table summarizing habitat and resiliency metrics for the Chandeleur Islands for varying storm conditions (Table 3) for the dune restoration alternative. For comparison, the pre-storm value of *subaerial volume* ( $V_{aer}$ ) is  $9.54 \times 10^6 \text{ m}^3$  for the dune/berm case and  $9.43 \times 10^6 \text{ m}^3$  for the marsh case, and the pre-storm value of *potential seagrass area* ( $A_s$ ) is  $28.2 \times 10^6 \text{ m}^2$  for the dune/berm case and  $27.2 \times 10^6 \text{ m}^2$ .**

Storm	Wave Angle	$V_{aer}$ ( $10^6 \text{ m}^3$ )	$V_{aerI}$ ( $10^6 \text{ m}^3$ )	$V_{land}$ ( $10^6 \text{ m}^3$ )	$V_{sea}$ ( $10^6 \text{ m}^3$ )	$V_{Hewes}$ ( $10^6 \text{ m}^3$ )	$A_s$ ( $10^6 \text{ m}^2$ )
Future without Action (FWOA)							
Weak	SE Waves	5.16	5.08	0.04	-0.04	0.02	27.7
Intermediate	SE Waves	5.41	5.20	0.34	-0.34	0.02	27.7
Strong	SE Waves	5.82	5.31	0.86	-0.84	0.04	27.7
Dune/Berm Sediment Placement							
Weak	SE Waves	9.24	9.20	-0.17	0.16	0.02	27.7
Intermediate	SE Waves	9.24	9.10	-0.27	0.25	0.02	27.8
Strong	SE Waves	9.20	8.88	-0.25	0.24	0.03	27.5
Marsh Sediment Placement							
Weak	SE Waves	9.24	9.20	-0.17	0.16	0.02	27.7
Intermediate	SE Waves	9.32	9.17	-0.05	0.04	0.02	27.4
Strong	SE Waves	9.64	9.26	0.36	-0.37	0.04	27.0
<b>Metric Definitions</b>							
$V_{aer}$ : <i>subaerial volume</i>							
$V_{aer,I}$ : <i>post-storm subaerial volume within the pre-storm island footprint</i>							
$V_{sea}$ : <i>net seaward sediment volume deposition</i>							
$V_{land}$ : <i>net landward sediment volume deposition</i>							
$V_{Hewes}$ : <i>net sediment volume deposition in Hewes Point</i>							
$A_{sg}$ : <i>potential sea grass area</i>							

### 3.4.2 Multiple Storms and an Extreme Storm Case

The storm analysis described in Sections 3.3.1 and 3.3.2 captures the impact of regularly recurring storms on the Chandeleur Islands under the FWOA and restoration cases. To further this analysis, targeted model

runs (Table 9) were conducted to evaluate sediment transport patterns and island evolution with and without restoration under the influence of two strong storms. This simulation captures the impacts of multiple back-to-back storms and does not consider recovery processes such as onshore sediment transport and natural dune-building that would occur between storms that were separated by months or years. In addition, the effects of a more extreme tropical event (e.g., an event of the magnitude of a major Category 3–4 Hurricane) and the impacts of the combination of back-to-back extreme and strong storms were also modeled.

**Table 9. Set of model runs used to evaluate the impacts of multiple and/or extreme storms on the Chandeleurs Islands under the FWOA and restoration cases. All storm combinations were run with waves from the SE. The characteristics of the individual storms comprising these runs may be found in Table 3, with addition details in (Mickey et al., 2018).**

Storm Set	Description
Extreme	<ul style="list-style-type: none"> <li>• Single storm corresponding to bin20 in Mickey 2018</li> </ul>
Strong-Strong	<ul style="list-style-type: none"> <li>• First storm corresponding to bin11 in Mickey2018</li> <li>• Second storm corresponding to bin11 in Mickey2018</li> </ul>
Extreme-Strong	<ul style="list-style-type: none"> <li>• First storm corresponding to bin20 in Mickey2018</li> <li>• Second storm corresponding to bin11 in Mickey2018</li> </ul>

The magnitude of impacts resulting from back-to-back strong storms was larger than for a single strong storm, but sediment transport and morphology change patterns were similar. Overwash and inundation occurred in the FWOA and marsh restoration cases, leading to onshore sediment transport (Table 10). For the dune restoration case, erosion of the placed material occurred, and the height of the dune inhibited overwash leading to net offshore sediment transport.

**Table 10. Volume of post-storm subaerial volume ( $V_{aer}$ ) and the net landward sediment volume deposition ( $V_{land}$ ).  $V_{land}$  is calculated as based on the integrated volume of sediment deposition landward of the pre-storm shoreline; for cases with multiple storms, this is the shoreline prior to the first storm. Positive values indicate net deposition landward of this shoreline. For reference, the pre-storm *subaerial volume* ( $V_{aer}$ ) is for the FWOA, dune restoration end member, and marsh restoration end member are 5.25, 9.54, and 9.43 x 10<sup>6</sup> m<sup>3</sup>, respectively.**

Storm Set	Post-Storm $V_{aer}$ (x10 <sup>6</sup> )			$V_{land}$ (x10 <sup>6</sup> )		
	FWOA	Dune	Marsh	FWOA	Dune	Marsh
Strong-Strong	6.14	9.02	9.85	1.32	-0.32	0.75
Extreme	5.60	9.60	9.19	2.20	0.94	1.72
Extreme-Strong	5.58	9.68	9.14	2.56	1.14	2.00

As with weaker storms, overwash and inundation occurred during an extreme storm for the FWOA (Figure 47) and marsh end member (Figure 48) cases and led to landward sediment transport. The magnitude of *net landward sediment volume deposition* was higher for the extreme storm while the post-storm *subaerial volume* was less than for weaker storms (Table 10). In contrast to the weak, intermediate, and strong storm cases, in which the dune restoration template remained in the collision regime, the extreme storm led to overwash of the dune restoration template and net deposition of sediment landward of the pre-storm shoreline (Figure 49, Table 10). Because the dune inhibited landward sediment transport during the early part of the storm, there is more offshore sediment transport and deposition in the surf

zone for the dune restoration compared to the marsh restoration and FWOA. In addition, sediment deposition for the dune case did not extend as far landward onto the island platform as the other cases did (Figure 47, Figure 48, Figure 49, Figure 50). When a strong storm case was run following an extreme storm case, the loss of the dune during the first storm event resulted in more overwash, inundation, and onshore sediment transport during the second storm (Table 10). However, higher net sand volumes were transported landward in the marsh restoration case, preserving sediment in the shallow backbarrier (Figure 50).

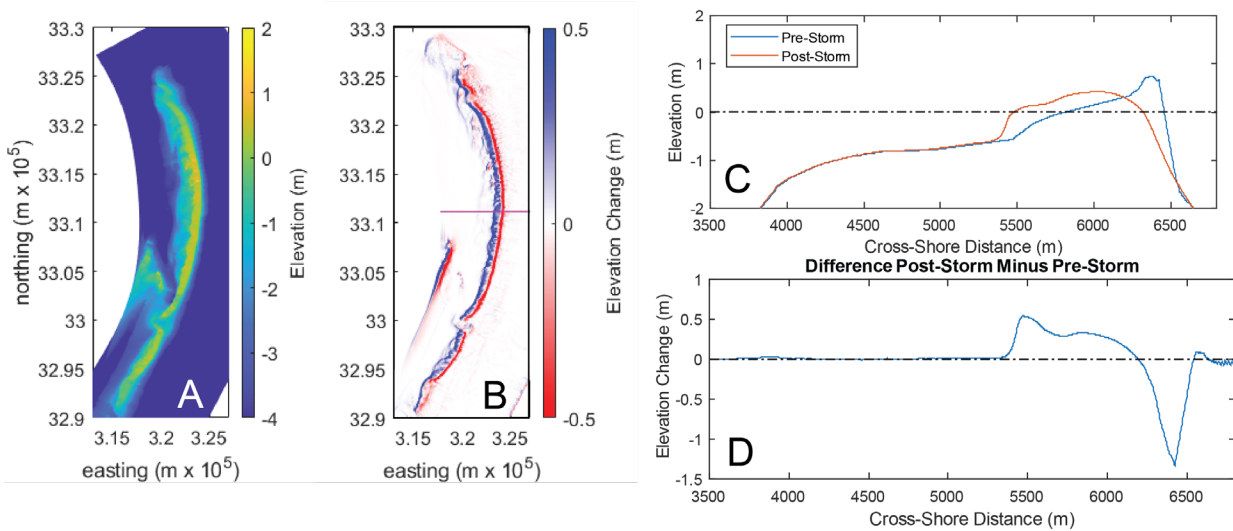


**Figure 47. Post-storm elevation (A) and elevation change (B) for an extreme storm impacting the FWOA case. Also shown are a pre- and post-storm profile (C) and the elevation change during the storm (D) for the profile shown in pink in (B).**

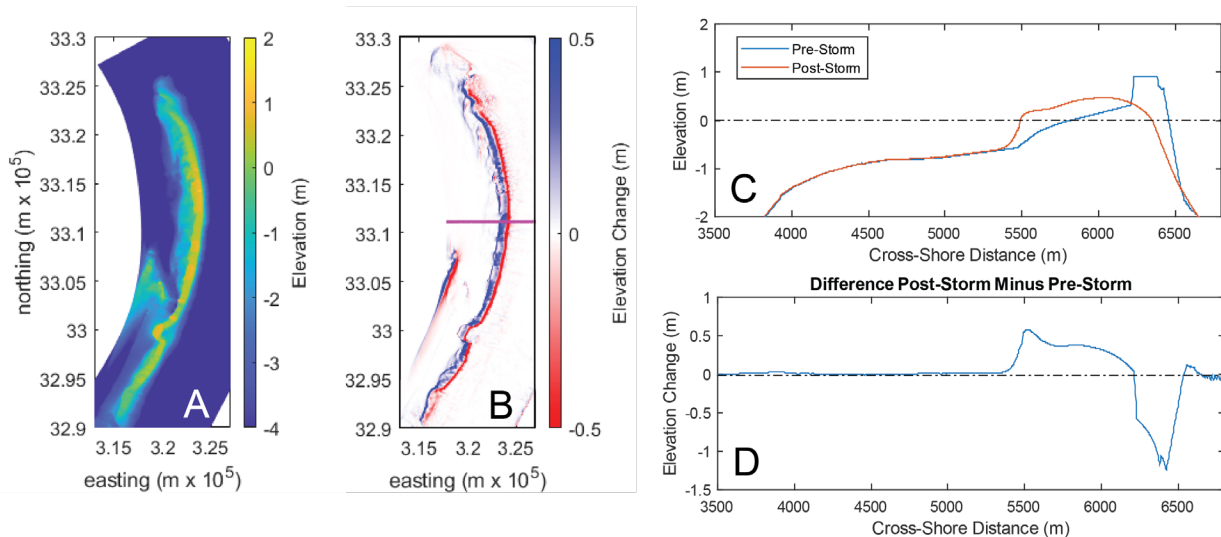


**Figure 48. Post-storm elevation (A) and elevation change (B) for an extreme storm impacting the marsh restoration case. Also shown are a pre- and post-storm profile (C) and the elevation change during the storm (D) for the profile shown in pink in (B).**

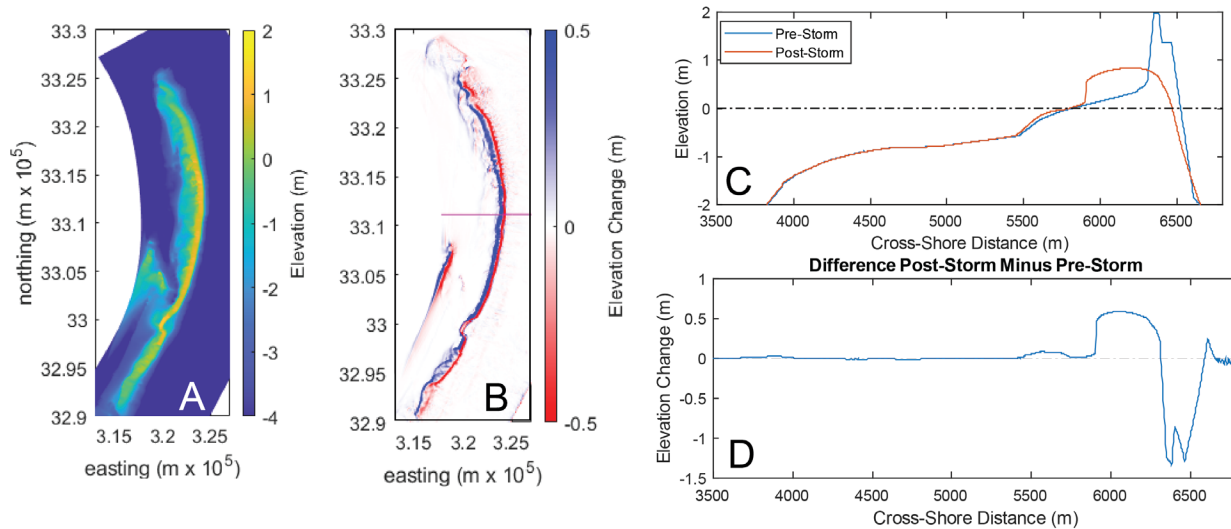


**Figure 49. Post-storm elevation (A) and elevation change (B) for an extreme storm impacting the dune restoration case. Also shown are a pre- and post-storm profile (C) and the elevation change during the storm (D) for the profile shown in pink in (B).**

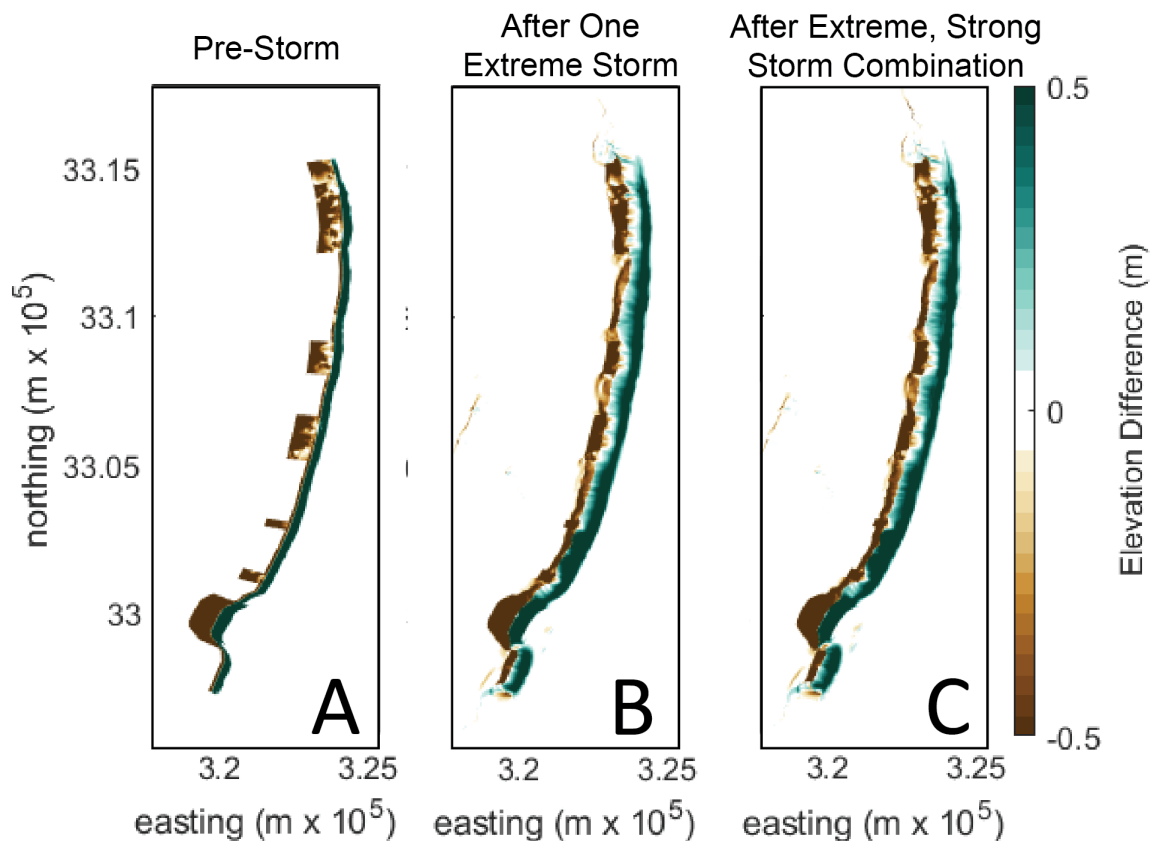


**Figure 50. Difference between the dune and marsh restoration templates before (A) and after an extreme storm (B) and a strong storm after an extreme storm (C). Positive (green) values indicate the dune template is higher in elevation, negative (brown) values indicate the marsh template is higher in elevation.**

## 4.0 Implications for the Chandeleur Islands

The sections below present conclusions and implications drawn from the results of both the analysis of the long-term evolution of the Chandeleur Islands (Section 2.0) and the modeling effort focused on the short-term impacts of storms and potential restoration scenarios (Section 3.0).

### 4.1. SHORT- AND LONG-TERM EVOLUTION OF THE CHANDELEUR ISLANDS WITH AND WITHOUT RESTORATION

A synthesis of available literature on the long-term evolution of the Chandeleur Islands and a modeling study of sediment transport and morphologic evolution of the islands during storms for restoration and future without action cases has found that:

1. As described in Section 2.0, large volumes of sand have accumulated over the long-term in a thick subaqueous spit platform at the northern flank of the island arc (Hewes Point). This downdrift sand reservoir lies outside of the littoral system and provides a unique opportunity as a resource for nourishing the updrift barrier system (i.e., the central arc).
2. North of Redfish Point, much of the remaining sections of island today are built over thick spit platform sands. When the islands originally formed to the north, successive recurved spits extended into the backbarrier to become the foundation for the backbarrier marshes observed over the historical record. As the shoreline and shoreface erode, these relict spit platform sands are liberated in the surf zone and naturally nourish the island north of Redfish Point.
3. The backbarrier marshes that extend into the sound are critical for the long-term resiliency of the islands. They provide a platform for island rollover and a sand source once eroded, and after major storms they also serve as nucleation sites for bar welding and spit development. This process of island stabilization supports a longshore sediment transport system that distributes sediment along the island, providing beach and dune habitat and preserving island integrity to protect the backbarrier and enable establishment of seagrass meadows.
4. Once the Gulf shoreline erodes into the backbarrier marsh shoreline (i.e., it consumes the marsh platform entirely), a threshold is crossed that results in the islands eroding faster, becoming ephemeral and ultimately turning into submerged subaqueous shoals.
5. Modeling results (Section 3.0) show that longshore transport to the north during storm events and deposition at Hewes Point is significantly reduced for the presently-degraded northern Chandeleur Islands. Sand in this northernmost portion of the islands is instead transported in a landward direction during tropical storm events, conserving more sand within the active coastal system.
6. In a marsh restoration scenario, the lower elevation profile facilitates continued overwash and landward transfer of sand. During stronger storms, sand eroded from the surf zone (shallow area offshore of the island) is transported onshore and deposited on the backbarrier platform. This

sediment is retained within the active coastal sediment transport system and is thus more likely to increase the long-term resilience of the island.

7. In a dune restoration scenario, the higher elevation of the dune inhibits overwash and inundation, preventing it or delaying it from occurring until later in the storm event depending on the strength of the storm. This results in more seaward sediment transport and deposition offshore of the island (sand loss from the system) than in the marsh restoration or future without action case.

#### 4.2. DISCUSSION AND CONSIDERATIONS FOR CHANDELEUR ISLANDS RESTORATION

Although further refinement is needed as described in *4.3 Suggested Next Steps in Chandeleur Islands Restoration Evaluation*, analysis of available data and the modeling experiments conducted for this study suggest that restoration at the Chandeleur Islands would benefit from sediment placement in the backbarrier toward the center of the island arc and rather than restoration exclusively through construction of a high dune and berm spanning the length of the barrier island in the alongshore. This approach is likely to maintain sediment transport processes (i.e., overwash and inundation) that retain sand within the coastal system while building up a platform for deposition of material in the back barrier during storms. Restoration that addresses the root cause of island disintegration and attendant ecosystem decline—loss of sand from the system—by placing sand in locations where natural processes can rebuild the islands over time in a way that mimics their natural formation is likely to increase the resiliency of the island in the longer-term. This would include: 1) reintroducing sand lost from the system to updrift backbarrier feeder sites; and 2) using the natural island shoreline retreat (erosion) to liberate placed sand into the littoral system for lateral distribution by waves. This holistic ecosystem restoration approach – which can be refined during Engineering and Design to maximize the benefits to targeted habitat and species – is more likely to provide the barrier island system with the sand supply required to be sustainable for in the longer term. Summarizing potential “best practice” in Chandeleur Islands restoration that can be further explored and refined during engineering and design:

- Nourishment sand recovered from Hewes Point is reintroduced to the barrier sand budget at a centralized location based on longshore sediment transport predictions from Georgiou and Schindler (2009b).
- Sand placement avoids naturally high energy environments where it is likely to be eroded more quickly, unless placement in those locations is necessary for habitat creation where the island has been converted to shoals or stable inlets have formed (e.g., Katrina Cut).
- Sand is placed at a centralized location along the island arc where it will naturally disperse to the flanks. These processes will increase sand in the littoral system and nourish the beach, providing material for aeolian dune building. In the long-term, this is likely to result in increased island resilience and thus storm protection for barrier island habitats and seagrass in the lee of the island.
- The majority of the nourishment sand volume is strategically placed in the backbarrier as vegetated shore perpendicular platforms upon which the island can migrate across. Placement in this locations provides sand reserves that can reintroduce sediment into the littoral system as the

island migrates and erodes into them. Constructing these in a way that builds out the existing backbarrier marsh shoreline in a landward direction is likely to increase island resiliency by extending the time for the islands to cross the transgressive submergence threshold crossing. This restoration design can be incorporated into an overall approach that also provides short-term benefits to the variety of dune, beach, and backbarrier habitats associated with the Chandeleur Islands.

#### 4.3. SUGGESTED NEXT STEPS IN CHANDELEUR ISLANDS RESTORATION EVALUATION

Although storms are a key driver of morphodynamic change in the Chandeleur Islands, the influence of longer-term island processes in post-storm recovery and island evolution (e.g., onshore sediment transport following storm events and berm/dune building via aeolian transport) has not been modeled. Doing so is a key next step to supporting Chandeleur Island management, including the engineering and design of restoration scenarios to maximize the ecosystem services they are providing in the short- and long-term. To evaluate the contribution of these processes to island evolution, the same model grid developed for this study could be coupled with models that predict the long-term evolution of the island under quiescent conditions. For example, the Delft3D model (Deltares, 2014) can predict the influence of quiescent conditions on longshore transport and shoreline change, while the Empirical Dune GRowth (EDGR) model (Dalyander et al., 2020a) can predict the recovery of dune features following storms. Efforts to evaluate the resiliency and long-term evolution the Chandeleurs under varying restoration scenarios can build upon the storm model and evaluation metric system developed here with the addition of these components to evaluate the future evolution and resiliency of the Chandeleur Islands on longer time scales. This model framework could then be used to evaluate the outcomes of detailed restoration designs that build on the conceptual restoration concepts presented here, and the design that has the greatest increase in ecosystem benefit in both the short- and long-term could be chosen for implementation. As part of that engineering and design process, the metrics developed in this study for evaluating subaerial barrier island and seagrass habitat extent could be applied to the outputs of a longer-time scale modeling framework. The potential for sediment placement in backbarrier platforms within the central portion of the island arc to increase island resiliency with longer-term benefit to barrier island and shallow subaqueous habitat—including seagrass—can thus be explicitly evaluated and quantified.

## 5.0 Use of the SECAS Southeast Blueprint in Conservation Planning for Barrier Islands

Several lessons were learned from this study that are relevant to application of the Southeast Blueprint for barrier islands:

1. **Barrier islands are highly dynamic, therefore evaluation of metrics at multiple points in time is more valuable for evaluating conservation/restoration value than calculating metrics at a single point in time.** Significant shifts in the distribution of subaerial and subaqueous habitat were observed during the modeled storms across all restoration scenarios, which could potentially result in large shifts between “low” and “high” conservation value (as defined within the Southeast Blueprint) depending on when data layers were collected relative to a storm. Therefore, it is suggested that metrics of evaluating barrier island conservation/restoration value be taken at

multiple times to provide a more robust assessment. These results could be used to create more accurate metrics to evaluate barrier island conservation/restoration value to then be incorporated into the Southeast Blueprint. For example, metrics taken at multiple times could be analyzed by taking an average value over time, or overall conservation value at multiple times could be calculated and a barrier island designed as “medium” or “high” value based on the maximum conservation value observed. This approach could also address the need to quantify the system trajectory discussed below.

2. **The diversity of habitat types over relatively small spatial scales on barrier islands suggests that evaluating habitat at an island scale is more informative than calculating metrics over a fixed spatial grid.** As is typical—and often necessary—for characterization of habitat value on regional scales, the Southeast Blueprint evaluates habitat on a regular spacing of 30 m (98 ft). At this spatial scale, barrier islands and their associated habitats may be difficult to resolve given the narrowness of features in the cross-shore. It is suggested that targeted calculation of restoration/conservation metrics for barrier islands first be calculated on a finer spatial scale (1–2 m (3.2 ft to 6.5 ft) in the cross-shore and 10s of meters in the long shore) to capture information about the islands’ habitats more accurately. Those islands that include significant restoration/conservation value for one or more of its component habitats can then be identified as “medium” or “high” conservation value within the Southeast Blueprint.
3. **The long-term trajectory and resiliency of barrier islands should be considered in evaluating conservation value and in planning conservation efforts.** For many types of ecosystems, conservation can rely on management of threats to habitats and species without needing to ensure the underlying land remains in place. However, RSLR, changes in the frequency or magnitude of storms, and/or lack of sediment supply are all stressors that can threaten the resiliency of barrier island landforms themselves regardless of additional threats to habitat such as point source pollution or anthropogenic development. For this reason, barrier island conservation value must be approached through the lens of “restore/conserve”, with consideration of if and how the addition of sediment to these systems can increase their resiliency in the longer-term. In practice, this may suggest that the Southeast Blueprint can provide enhanced value for barrier island system management if managers apply the Southeast Blueprint approaches for delineating ecosystem value to predictions of barrier island condition after restoration occurs.

## References

- Allison, M. A., Dellapenna, T. M., Gordon, E. S., Mitra, S., & Petsch, S. T. (2010). Impact of Hurricane Katrina (2005) on shelf organic carbon burial and deltaic evolution. *Geophysical Research Letters*, 37(21), L21605.
- Alymov, V., Cobell, Z., Couvillion, B. R., de Mutsert, K., Dong, Z., Duke-Sylvester, S. M., Fischbach, J. R., Hanegan, K., Lewis, K., Lindquist, D., McCorquodale, J. A., Poff, M., Roberts, H., Schindler, J., Visser, J. M., Wang, Z., & White, E. D. (2017). *2017 Coastal Master Plan: Appendix C: Chapter 4 – Model outcomes and interpretations* (Version Final) (pp. 1–448). Baton Rouge, LA: Coastal Protection and Restoration Authority.
- Bernier, J. C., Miselis, J. L., Buster, N. A., & Flocks, James G. (2019). Application of Sediment End-Member Analysis for Understanding Sediment Fluxes, Northern Chandeleur Islands, Louisiana. In *Proceedings of Coastal Sediments*.
- Bethel, M., & Martinez, L. (2008). Assessment of Seagrass Critical Habitat in Response to Dramatic Shoreline Change Resulting from the 2005 Hurricane Season for the Chandeleur Islands (abstract) (Vol. 40, p. 486). Presented at the Geological Society of America, 2008 Annual Meeting, Abstracts and Programs.
- Boudreau, B., & Jorgensen, B. (2001). The benthic boundary layer: Transport processes and biogeochemistry. *Eos, Transactions American Geophysical Union*, 82(52), 658–658.
- Brown, E. I. (1928). Inlets on sandy coasts. *Proceedings of the American Society of Civil Engineers*, 54(2), 505–554.
- Bureau of Ocean Energy Management. (2021). GoMMAPPS.
- Byrnes, M. R., Berlinghoff, J. L., Griffiee, S. F., & Lee, D. M. (2018). *Louisiana Barrier Island Comprehensive Monitoring Program (BICM): Phase 2 - Updated shoreline compilation and change assessment 1880s-2015* (p. 140). Louisiana Coastal Protection and Restoration Authority.
- Cameron, C., Kiskaddon, E., Parfait, J., Mcinnis, A., Courtois, A., & Carruthers, T. (2020). *Southeast Conservation Blueprint Mechanics* (p. 137). Baton Rouge, LA: The Water Institute of the Gulf. Prepared for and funded by the U.S. Fish and Wildlife Service.
- Campbell, T., Benedet, L., & Finkl, C. W. (2005). Regional strategies for coastal restoration along the Louisiana Chenier Plain. *Journal of Coastal Research*, (44), 268–283.
- Carapuço, M. M., Taborda, R., Silveira, T. M., Psuty, N. P., Andrade, C., & Freitas, M. C. (2016). Coastal geoindicators: Towards the establishment of a common framework for sandy coastal environments. *Earth-Science Reviews*, 154, 183–190.
- Carruthers, T., Beckert, K., Dennison, B., Thomas, J., Saxby, T., Williams, M., Fisher, T., Kumer, J., Schupp, C., Sturgis, B., & Zimmerman, C. (2011). *Assateague Island National Seashore natural resource condition assessment: Maryland, Virginia* (No. 2011/405). Fort Collins, Colorado: National Park Service.
- Carter, G., Criss, G. A., Blossom, G., & Biber, P. (2009, August 21). *Decadal-scale changes in seagrass coverage on the Mississippi barrier islands, northern Gulf of Mexico*.
- Catlin, D. H., Fraser, J. D., Stantial, M., Felio, J. H., Gierdes, K., & Karpanty, S. (2011). *Operations report – Virginia Tech Chandeleur piping plover survey* (Unpublished report prepared for U.S. Fish and Wildlife Service under Permit TE19418A-0). U.S. Fish and Wildlife Service.
- Cecil, J., Sanchez, C., & Hartzler, I. (2009). United States of America. In C. Devenish, D. F. D. Fernández, R. P. Clay, I. Davidson, & I. Y. Zabala (Eds.), *Important Bird Areas Americas - Priority sites for biodiversity conservation* (pp. 369–382). Quito, Ecuador: BirdLife International.
- Chamberlain, E. L., Törnqvist, T. E., Shen, Z., Mauz, B., & Wallinga, J. (2018). Anatomy of Mississippi Delta growth and its implications for coastal restoration. *Science Advances*, 4(4), 9.
- Chen, S.-N., Sanford, L. P., Koch, E. W., Shi, F., & North, E. W. (2007). A nearshore model to investigate the effects of seagrass bed geometry on wave attenuation and suspended sediment transport. *Estuaries and Coasts*, 30(2), 296–310.

- Cipriani, L. E., & Stone, G. W. (2001). Net longshore sediment transport and textural changes in beach sediments along the southwest Alabama and Mississippi Barrier Islands, U.S.A. *Journal of Coastal Research*, 17(2), 443–458.
- Coleman, J. M. (1988). Dynamic changes and processes in the Mississippi River delta, 100, 999–1015.
- CPRA. (2017). *Louisiana's comprehensive master plan for a sustainable coast: committed to our coast* (p. 392). Coastal Protection and Restoration Authority.
- Dalyander, P. S., Meyers, M., Mattsson, B., Steyer, G., Godsey, E., McDonald, J., Byrnes, M., & Ford, M. (2016). Use of structured decision-making to explicitly incorporate environmental process understanding in management of coastal restoration projects: Case study on barrier islands of the northern Gulf of Mexico. *Journal of Environmental Management*, 183, 497–509.
- Dalyander, P. S., Mickey, R. C., Long, J. W., & Flocks, J. G. (2017). *Effects of proposed sediment borrow pits on nearshore wave climate and longshore sediment transport rate Along Breton Island, Louisiana* (Open-File Report No. 2015–1055) (p. 51).
- Dalyander, P. S., Mickey, R. C., Passeri, D. L., & Plant, N. G. (2020a). Development and application of an empirical dune growth model for evaluating barrier island recovery from storms. *Journal of Marine Science and Engineering*, 8(12), 977.
- Dalyander, P. S., Miner, M., Dausman, A., Cameron, C., Dudeck, N., & Georgiou, I. (2020b). *Numerical Modeling of the Louisiana, Mississippi, and Alabama Coastal System (LMACS): Model Inventory and Recommendations* (p. 14). Baton Rouge, LA: The Water Institute of the Gulf, Produced for and funded by the National Oceanic and Atmospheric Administration.
- Darnell, K. M., Carruthers, T. J. B., Biber, P., Georgiou, I. Y., Michot, T. C., & Boustany, R. G. (2017). Spatial and temporal patterns in *Thalassia testudinum* leaf tissue nutrients at the Chandeleur Islands, Louisiana, USA. *Estuaries and Coasts*, 40(5), 1288–1300.
- Deepwater Horizon Natural Resource Damage Assessment Trustees. (2016). *Deepwater Horizon oil spill final programmatic damage assessment and restoration plan and final programmatic environmental impact statement. Chapter 8: Trustee responses to public comments on the draft PDARP/ PIES*. Deepwater Horizon Natural Resource Damage Assessment Trustees.
- Deltares. (2014). *Delft3D-FLOW: Simulation of multidimensional hydrodynamic flows and transport phenomena, including sediments* (User Manual No. Version 3.15.32158). Delft, The Netherlands: Deltares.
- Durán Vinent, O., & Moore, L. J. (2015). Barrier island bistability induced by biophysical interactions. *Nature Climate Change*, 5(2), 158–162.
- Eleuterius, C. K. (1977). Location of the Mississippi Sound oyster reefs as related to salinity of bottom waters during 1973-1975. *Gulf Research Reports*, 6(1), 17–23.
- Eliot, M. (2013). *Application of geomorphic frameworks to sea-level rise impact assessment* (Geoscience Australia No. 193- 01-Rev 0). Innaloo, Western Australia: Damara WA Pty Ltd.
- Ellinwood, M. C. (2008). *Response of barrier island fish assemblages to impacts from multiple hurricanes: assessing resilience of Chandeleur Island fish assemblages to Hurricanes Ivan (2004) and Katrina (2005)* (Master of Earth and Environmental Science). University of New Orleans, New Orleans, LA. Retrieved from <http://scholarworks.uno.edu/td/870/>
- Enwright, N., Borchert, S., Day, R., Feher, L., Osland, M., Wang, L., & Wang, H. (2017). *Barrier Island Habitat Map and Vegetation Survey - Dauphin Island, Alabama, 2015* (Open-File Report No. 2017–1083) (p. 28). U. S. Geological Survey.
- Enwright, N. M., SooHoo, W. M., Dugas, J. L., Conzelmann, C. P., Laurenzano, C., Lee, D. M., Mouton, K., & Stelly, S. J. (2020). *Louisiana Barrier Island Comprehensive Monitoring Program: Mapping habitats in beach, dune, and intertidal environments along the Louisiana Gulf of Mexico shoreline, 2008 and 2015–16* (USGS Numbered Series No. 2020–1030). *Louisiana Barrier Island Comprehensive Monitoring Program: Mapping habitats in beach, dune, and intertidal environments along the Louisiana Gulf of Mexico shoreline, 2008 and 2015–16* (Vol. 2020–1030, p. 72). Reston, VA: U.S. Geological Survey.

- Enwright, N. M., Wang, L., Wang, H., Osland, M. J., Feher, L. C., Borchert, S. M., & Day, R. H. (2019). Modeling barrier island habitats using landscape position information. *Remote Sensing*, *11*(8), 976.
- Enwright, N., SooHoo, W. M., Dugas, J. L., Conzelmann, C. P., Laurenzano, C., Lee, D., Mouton, K., & Stelly, S. J. (2018a). *Louisiana Barrier Island Comprehensive Monitoring Program: Mapping habitats in beach, dune, and intertidal environments along the Louisiana Gulf of Mexico shoreline, 2008 and 2015–16* (Open-File Report No. 2020–1030) (p. 57). U. S. Geological Survey.
- Enwright, N., SooHoo, W. M., Dugas, J. L., Conzelmann, C. P., Laurenzano, C., Lee, D., Mouton, K., & Stelly, S. J. (2018b). *Louisiana Barrier Island Comprehensive Monitoring Program: Mapping Habitats in Beach, Dune, and Intertidal Environments Along the Louisiana Gulf of Mexico Shoreline, 2008 and 2015–16* Open-File Report (Open-File Report No. 2020–1030) (p. 57). U. S. Geological Survey.
- Escoffier, F. F. (1940). *The stability of tidal inlets*. United States Engineer Office Mobile United States.
- Evans, O. F. (1942). The origin of spits, bars, and related structures. *The Journal of Geology*, *50*(7), 846–865.
- Feagin, R. A., Figlus, J., Zinnert, J. C., Sigren, J., Martínez, M. L., Silva, R., Smith, W. K., Cox, D., Young, D. R., & Carter, G. (2015). Going with the flow or against the grain? The promise of vegetation for protecting beaches, dunes, and barrier islands from erosion. *Frontiers in Ecology and the Environment*, *13*(4), 203–210.
- Fearnley, S., Brien, L., Martinez, L., Miner, M. D., Kulp, M. A., & Penland, S. (2009a). *Chenier Plain, south-central Louisiana and Chandeleur Islands: Habitat mapping and change analysis 1996 to 2005. Part I - Methods for habitat mapping and change analysis 1996 to 2005* (p. 11). New Orleans, LA: University of New Orleans Pontchartrain Institute for Environmental Sciences.
- Fearnley, S. M., Miner, M. D., Kulp, M. A., Bohling, C., & Penland, S. (2009b). Hurricane impact and recovery shoreline change analysis of the Chandeleur Islands, Louisiana, USA: 1855 to 2005. *Geo-Marine Letters*, *29*(6), 455–466.
- Fertl, D., Schiro, A. J., Regan, G. T., Beck, C. A., Adimey, N., Price-May, L., Amos, A., Worthy, G. A. J., & Crossland, R. (2005). Manatee Occurrence in the Northern Gulf of Mexico, West of Florida. *Gulf and Caribbean Research*, *17*.
- Fisk, H. N. (1944). *Geological investigations of the alluvial valley of the lower Mississippi River: US Army Corps of Engineers*. Mississippi River Commission, U.S. Army Corps of Engineers.
- FitzGerald, D. M., J. Hein, C., Hughes, Z. J., Kulp, M. A., Georgiou, I. Y., & Miner, M. D. (2018). Runaway barrier island transgression concept: Global case studies. In L. J. Moore & A. B. Murray (Eds.), *Barrier Dynamics and Response to Changing Climate* (pp. 3–56). Cham: Springer International Publishing.
- FitzGerald, D. M., & Miner, M. D. (2021). Tidal Inlets and Lagoons Along Siliciclastic Barrier Coasts☆. In *Reference Module in Earth Systems and Environmental Sciences*. Elsevier.
- Flocks, J., Kindinger, J., Miselis, J., & Locker, S. (2015). Stratigraphy and morphology of the barrier platform of Breton Island, Louisiana: Deltaic, marine and human influences. In *Proceedings of the Coastal Sediments 2015* (p. 14). San Diego, CA.
- Fodrie, F., Heck, K., Andrus, C., & Powers, S. (2020). Determinants of the nursery role of seagrass meadows in the sub-tropical Gulf of Mexico: inshore-offshore connectivity for snapper and grouper. *Marine Ecology Progress Series*, *647*, 135–147.
- Fodrie, F. J., & Heck, K. L. (2011). Response of coastal fishes to the Gulf of Mexico oil disaster. *PLoS ONE*, *6*(7), e21609.
- Frazier, D. E. (1967). Recent deltaic deposits of the Mississippi River: Their development and chronology. *Transactions of the Gulf Coast Association of Geological Societies*, *17*, 287–315.
- Georgiou, I. Y., McCorquodale, J. A., Schindler, J., Retana, A. G., FitzGerald, D. M., Hughes, Z., & Howes, N. (2009). Impact of multiple freshwater diversions on the salinity distribution in the Pontchartrain estuary under tidal forcing. *Journal of Coastal Research*, 59–70.

- Georgiou, I. Y., & Schindler, J. K. (2009a). *Numerical simulation of waves and sediment transport along a transgressive barrier island* (Scientific Investigations Report No. 2009–5252) (p. 31). U.S. Geological Survey.
- Georgiou, I. Y., & Schindler, J. K. (2009b). Wave forecasting and longshore sediment transport gradients along a transgressive barrier island: Chandeleur Islands, Louisiana. *Geo-Marine Letters*, 29(6), 467–476.
- Goldstein, E. B., & Moore, L. J. (2016). Stability and bistability in a one-dimensional model of coastal foredune height. *Journal of Geophysical Research: Earth Surface*, 121(5), 964–977.
- Grzegorzewski, A. S., Cialone, M., Lansen, A. J., van Ledden, M., Smith, J., & Wamsley, T. (2009). The influence of barrier islands on hurricane-generated storm surge and waves in Louisiana and Mississippi. In *Coastal Engineering 2008* (pp. 1037–1049). Hamburg, Germany: World Scientific Publishing Company.
- Grzegorzewski, A. S., & Georgiou, I. Y. (2011). Sediment transport trends along an island terminus: A model study during storms at the northern Chandeleur Islands. In *The Proceedings of the Coastal Sediments 2011* (pp. 2198–2211). Miami, Florida, USA: World Scientific Publishing Company.
- Gulf of Mexico Alliance. (2021). Gulf of Mexico Seagrass Community of Practice - created to support the management, research, restoration, and conservation of seagrasses in the GOM.
- Handley, L., Altsman, D., & DeMay, R. (2007). *Seagrass Status and Trends in the Northern Gulf of Mexico: 1940–2002* (U.S. Geological Survey Scientific Investigations Report No. 2006–5287) (p. 267).
- Handley, L. R., Lockwood, C. M., Spear, K., Finkbeiner, M., & Kenworthy, J. (2018). *Gulf-wide Seagrass Monitoring and Needs Assessment Workshop Report for the Gulf of Mexico Alliance* (No. Contract No. 121701-00) (p. 89). Ocean Springs, MS: Gulf of Mexico Alliance.
- Hart, W. E., & Murray, S. P. (1978). Energy balance and wind effects in a shallow sound. *Journal of Geophysical Research: Oceans*, 83(C8), 4097–4106.
- Hasselmann, K. F., Barnett, T. P., Bouws, E., Carlson, H., Cartwright, D. E., Enke, K., Ewing, J. A., Gienapp, H., Hasselmann, D. E., Kruseman, P., Meerburg, A., Muller, P., Olbers, D. J., Richter, K., Sell, W., & Walden, H. (1973). Measurements of wind-wave growth and swell decay during the Joint North Sea Wave Project (JONSWAP). *Ergaenzungsheft Zur Deutschen Hydrographischen Zeitschrift, Reihe A*.
- Heck, K. L., Carruthers, T. J. B., Duarte, C. M., Hughes, A. R., Kendrick, G., Orth, R. J., & Williams, S. W. (2008). Trophic transfers from seagrass meadows subsidize diverse marine and terrestrial consumers. *Ecosystems*, 11(7), 1198–1210.
- Houser, C., Wernette, P., Rentschlar, E., Jones, H., Hammond, B., & Trimble, S. (2015). Post-storm beach and dune recovery: Implications for barrier island resilience. *Geomorphology*, 234, 54–63.
- Hoyt, J. H., & Henry Jr., V. J. (1967). Influence of island migration on barrier-island sedimentation. *Geological Society of America Bulletin*, 78(1), 77–86.
- Jacob H. Kahn. (1986). Geomorphic recovery of the Chandeleur Islands, Louisiana, after a major hurricane. *Journal of Coastal Research*, 2(3), 337–344.
- Jaffe, B. E., List, J. H., & Sallenger, A. H. (1997). Massive sediment bypassing on the lower shoreface offshore of a wide tidal inlet — Cat Island Pass, Louisiana. *Marine Geology*, 136(3–4), 131–149.
- Johnson, J. S., Cairns, D. M., & Houser, C. (2013). Coastal marsh vegetation assemblages of Galveston Bay: Insights for the East Texas Chenier Plain. *Wetlands*, 33(5), 861–870.
- Kahn, J. H., & Roberts, H. H. (1982). Variations in storm response along a microtidal transgressive barrier-island arc. *Sedimentary Geology*, 33(2), 129–146.
- Kenworthy, W., Cosentino-Manning, N., Handley, L., Wild, M., & Rouhani, S. (2017). Seagrass response following exposure to Deepwater Horizon oil in the Chandeleur Islands, Louisiana (USA). *Marine Ecology Progress Series*, 576, 145–161.
- Kindinger, J. L., Buster, N. A., Flocks, J. G., Bernier, J. C., & Kulp, M. A. (2013). *Louisiana Barrier Island Comprehensive Monitoring (BICM) Program Summary Report: Data and Analyses 2006 through 2010* (Open-File Report No. 2013–1083) (p. 86). U. S. Geological Survey.

- Koch, E. W., Sanford, L. P., Chen, S.-N., Shafer, D. J., & Smith, J. M. (2006). *Waves in seagrass systems: Review and technical recommendations* (Final Report No. ERDC TR-06-15) (p. 92). Fort Belvoir, VA: Defense Technical Information Center.
- Kolb, C. R., & van Lopik, J. R. (1958). *Geology of the Mississippi River Deltaic Plain, Southeastern Louisiana Waterways Experiment Station* (Technical Report No. 3-483) (p. 120). Vicksburg, Mississippi: U. S. Army Corps of Engineers.
- Kombiadou, K., Matias, A., Costas, S., Rita Carrasco, A., Plomaritis, T. A., & Ferreira, Ó. (2020). Barrier island resilience assessment: Applying the ecological principles to geomorphological data. *CATENA*, *194*, 104755.
- Lavoie, D. (2009). *Sand Resources, Regional Geology, and Coastal Processes of the Chandeleur Islands Coastal System: an Evaluation of the Breton National Wildlife Refuge* (Scientific Investigations Report No. 2009-5252) (p. 211). Reston, VA: U.S. Geological Survey.
- List, J. H., Jaffe, B. E., Jr., A. H. S., & Hansen, M. E. (1997). Bathymetric comparisons adjacent to the Louisiana barrier aslands: Processes of large-scale change. *Journal of Coastal Research*, *13*(3), 670-678.
- Long, J., Dalyander, P. S., Poff, M., Spears, B., Borne, B., Thompson, D., Mickey, R., Dartez, S., & Grandy, G. (2020). Event and decadal-scale modeling of barrier island restoration designs for decision support. *Shore & Beach*, *88*(1), 49-57.
- Louisiana Department of Wildlife and Fisheries. (2021). Rare Species and Natural Communities by Parish.
- Martinez, L., O’Brein, M., Tethel, S., Penland, S., & Kulp, M. (2009). *Louisiana Barrier Island Comprehensive Monitoring Program (BICM) Volume 2: Shoreline Changes and Barrier Island Land Loss 1800’s-2005*. University of New Orleans, Pontchartrain Institute for Environmental Sciences, New Orleans.
- McBride, R. A., & Byrnes, M. R. (1995). A megascale systems approach for shoreline change analysis and coastal management along the northern Gulf of Mexico. *Gulf Coast Association of Geological Societies Transactions*, *45*, 405-414.
- McBride, R. A., Byrnes, M. R., & Hiland, M. W. (1995). Geomorphic response-type model for barrier coastlines: A regional perspective. *Marine Geology*, *126*(1-4), 143-159.
- McBride, R. A., Penland, S., Hiland, M. W., Williams, S. J., Westphal, K. A., Jaffe, B. E., & Sallenger Jr., A. H. (1992). Analysis of barrier shoreline change in Louisiana from 1853 to 1989. In S. J. Williams, S. Penland, & A. H. Sallenger Jr (Eds.), *Louisiana from 1853 to 1989: Atlas of shoreline changes in Louisiana from 1885 to 1989* (pp. 36-97). U.S. Geological Survey.
- McKenzie, J. F. (2013). *Occurrence and genetic diversity of lemon sharks (Negaprion brevirostris) at a nursery ground at the Chandeleur Islands, Louisiana*. University of New Orleans, Louisiana.
- Meysman, F., Middelburg, J., & Heip, C. (2006). Bioturbation: a fresh look at Darwin’s last idea. *Trends in Ecology & Evolution*, *21*(12), 688-695.
- Michot, T. C., & Chadwick, P. C. (1994). Winter biomass and nutrient values of three seagrass species as potential foods for redheads (*Aythya americana* Eyton) in Chandeleur Sound, Louisiana. *Wetlands*, *14*(4), 276-283.
- Mickey, R. C., Long, J. W., Dalyander, P. S., Plant, N. G., & Thompson, D. M. (2018). A framework for modeling scenario-based barrier island storm impacts. *Coastal Engineering*, *138*, 98-112.
- Mickey, R. C., Long, J. W., Plant, N. G., Thompson, D. M., & Dalyander, P. S. (2017). *A methodology for modeling barrier island storm-impact scenarios* (USGS Numbered Series No. 2017-1009). *A methodology for modeling barrier island storm-impact scenarios* (Vol. 2017-1009). Reston, VA: U.S. Geological Survey.
- Middelburg, J. J. (2019). *Marine Carbon Biogeochemistry: A Primer for Earth System Scientists*. Cham: Springer International Publishing.
- Miner, M. D., Georgiou, I. Y., Twichell, D., Flocks, J., & Lavoie, D. (2009a). Geomorphic-Based Barrier Island Transgression Management, Chandeleur Islands, Louisiana (Vol. 41, p. 583). Presented at the Geological Society of America, Abstracts with Programs.

- Miner, M. D., Kulp, M. A., & FitzGerald, D. M. (2007). Tidal versus shoreface ravinement and tidal inlet fill preservation potential for transgressive tidal inlets, Mississippi River Delta Plain, U.S.A. *Journal of Coastal Research, Special Issue(50)*, 805–809.
- Miner, M. D., Kulp, M. A., FitzGerald, D. M., Flocks, J. G., & Weathers, H. D. (2009b). Delta lobe degradation and hurricane impacts governing large-scale coastal behavior, South-central Louisiana, USA. *Geo-Marine Letters*, 29(6), 441–453.
- Miner, M. D., Kulp, M. A., FitzGerald, D. M., & Georgiou, I. Y. (2009c). Hurricane-associated ebb-tidal delta sediment dynamics. *Geology*, 37(9), 851–854.
- Miner, M. D., Kulp, M. A., Weathers, H. D., & Flocks, J. (2009d). *Chapter D. Historical (1869–2007) Sea Floor Evolution and Sediment Dynamics Along the Chandeleur Islands in Sand Resources, Regional Geology, and Coastal Processes of the Chandeleur Islands Coastal System: an Evaluation of the Breton National Wildlife Refuge* (No. 2009–5252) (pp. 47–74). Reston, VA: U.S. Department of the Interior and U.S. Geological Survey.
- Miner, M. D., Kulp, M., Penland, S., Weathers, H. D., Motti, J. P., McCarty, P., Brown, M., Martinez, L., Torres, J., Flocks, J. G., DeWitt, N. T., Ferina, N., Reynolds, B. J., Twitchell, D., Baldwin, W., Danforth, B., Worely, C., & Bergeron, E. (2009e). *Bathymetry and historical seafloor change 1869-2007 Part 1: South-central Louisiana and northern Chandeleur Islands, bathymetry methods and uncertainty analysis* (No. Volume 3, Part 1) (p. 45). U.S. Geological Survey, Pontchartrain Institute for Environmental Sciences.
- Miner, M. D., Weathers, H. D., Kulp, M. A., & Refferty, R. (2012). *Louisiana Barrier Island Comprehensive Monitoring Program (BICM), Volume 3: Bathymetry and Historical Seafloor Change 1869-2007, Part 4: Historical Seafloor Change Analysis* (p. 44). University of New Orleans - Pontchartrain Institute for Environmental Sciences, Submitted to Louisiana Department of Natural Resources and Coastal Protection and Restoration Authority of Louisiana.
- Miselis, J. L., Buster, N. A., & Kindinger, J. L. (2014). Refining the link between the Holocene development of the Mississippi River Delta and the geologic evolution of Cat Island, MS: implications for delta-associated barrier islands. *Marine Geology*, 355, 274–290.
- Miselis, J. L., Long, J. W., Dalyander, P. S., Flocks, J. G., Buster, N. A., & Mickey, R. C. (2015a). Integrating geophysical and oceanographic data to assess interannual variability in longshore sediment transport. *The Proceedings of the Coastal Sediments 2015*.
- Miselis, J. L., Long, J. W., Dalyander, P. S., Flocks, J. G., Buster, N. A., & Mickey, R. C. (2015b). Integrating Geophysical and Oceanographic Data to Assess Interannual Variability in Longshore Sediment Transport. *The Proceedings of the Coastal Sediments 2015*.
- Moore, L. J., Patsch, K., List, J. H., & Williams, S. J. (2014). The potential for sea-level-rise-induced barrier island loss: Insights from the Chandeleur Islands, Louisiana, USA. *Marine Geology*, 355, 244–259.
- Morton, R. A. (2008). Historical Changes in the Mississippi-Alabama Barrier-Island Chain and the Roles of Extreme Storms, Sea Level, and Human Activities. *Journal of Coastal Research*, 246, 1587–1600.
- Mullin, K. D. (1988). *Comparative seasonal abundance and ecology of bottlenose dolphins (Tursiops truncatus) in three habitats of the north-central Gulf of Mexico* (Dissertation). Mississippi State University, Mississippi.
- Nelson, T. L. (2017). *Hydrodynamic controls on the morphodynamic evolution of subaqueous landforms* (Master of Science in Earth and Environmental Science). University of New Orleans, New Orleans, LA. Retrieved from <https://scholarworks.uno.edu/td/2425>
- Ogren, L. (1989). *Survey and reconnaissance of sea turtles in the northern Gulf of Mexico* (No. 566) (p. 9). Panama City, FL: United States National Marine Fisheries Service, Panama City Laboratory.
- Otvos, E. G. (1981). Barrier Island formation through nearshore aggradation — Stratigraphic and field evidence. *Marine Geology*, 43(3–4), 195–243.

- Otvos, E. G., & Carter, G. A. (2013). Regressive and transgressive barrier islands on the North-Central Gulf Coast — Contrasts in evolution, sediment delivery, and island vulnerability. *Geomorphology*, 198, 1–19.
- Park, K., Powers, S. P., Bosarge, G. S., & Jung, H.-S. (2014). Plugging the leak: Barrier island restoration following Hurricane Katrina enhances larval retention and improves salinity regime for oysters in Mobile Bay, Alabama. *Marine Environmental Research*, 94, 48–55.
- Penland, S., & Boyd, R. (1981). Shoreline changes on the Louisiana barrier coast. *Oceans*, 91, 209–219.
- Penland, S., & Boyd, R. (1985). *Transgressive Depositional Environments of the Mississippi River Delta Plain: A Guide to the Barrier Islands, Beaches, and Shoals in Louisiana*. Baton Rouge, LA: Department of Natural Resources, Louisiana Geological Survey.
- Penland, S., Boyd, R., & Suter, J. R. (1988). Transgressive depositional systems of the Mississippi delta plain: A model for barrier shoreline and shelf sand development. *Journal of Sedimentary Petrology*, 58(6), 932–949.
- Peterson, M. S., & Waggy, G. L. (2004). *A Field Guide to Aquatic Habitats and Common Fauna of the Northern Gulf of Mexico: Chandeleur Islands, Louisiana to Perdido Key, Florida*. University of Southern Mississippi, Mississippi-Alabama Sea Grant Consortium.
- Pham, L. T., Biber, P. D., & Carter, G. A. (2014). Seagrasses in the Mississippi and Chandeleur Sounds and problems associated with decadal-scale change detection. *Gulf of Mexico Science*, 32(1), 24–43.
- Plant, N. G., Flocks, J., Stockdon, H. F., Long, J. W., Guy, K., Thompson, D. M., Cormier, J. M., Smith, C. G., Miselis, J. L., & Dalyander, P. S. (2014). Predictions of barrier island berm evolution in a time-varying storm climatology: Barrier-island berm evolution. *Journal of Geophysical Research: Earth Surface*, 119(2), 300–316.
- Poirrier, M. A., & Handley, L. R. (2007). Chandeleur Islands. In *Seagrass status and trends in the northern Gulf of Mexico* (Vol. 2002, pp. 62–71).
- Remsen, J. V., Wallace, B. P., Seymour, M. A., O'Malley, D. A., & Johnson, E. I. (2019). The regional, national, and international importance of Louisiana's coastal avifauna. *The Wilson J. of Ornithology*, 13, 221:242.
- Reyes, E., Georgiou, I. Y., Reed, D. J., & McCorquodale, J. A. (2005). Using models to evaluate the effects of barrier islands on estuarine hydrodynamics and habitats: a numerical experiment. *Journal of Coastal Research*, (44), 176–185.
- Ritchie, W., & Penland, S. (1988). Rapid dune changes associated with overwash processes on the deltaic coast of South Louisiana. *Marine Geology*, 81(1–4), 97–122.
- Roberts, H. H. (1997). Dynamic changes of the Holocene Mississippi River delta plain: The delta cycle. *Journal of Coastal Research*, 13(3), 605–627.
- Roelvink, D., Reniers, A., van Dongeren, A., van Thiel de Vries, J., McCall, R., & Lescinski, J. (2009). Modelling storm impacts on beaches, dunes and barrier islands. *Coastal Engineering*, 56(11–12), 1133–1152.
- Rogers, B. E., Kulp, M. A., & Miner, M. D. (2009). Late Holocene chronology, origin, and evolution of the St. Bernard Shoals, Northern Gulf of Mexico, USA. *Geo-Marine Letters*, 29(6), 379–394.
- Roman, C. T., & Nordstrom, K. F. (1988). The effect of erosion rate on vegetation patterns of an east coast barrier island. *Estuarine, Coastal and Shelf Science*, 26(3), 233–242.
- Rosati, J. D., & Stone, G. W. (2009). Geomorphologic evolution of barrier islands along the northern U.S. Gulf of Mexico and implications for engineering design in barrier restoration. *Journal of Coastal Research*, 25(1), 8–22.
- Russell, R. J. (1936). Physiography of the Lower Mississippi Delta. In *Lower Mississippi Delta: Reports on the Geology of Plaquemines and St. Bernard Parishes: New Orleans, Louisiana*. Louisiana Department of Conservation.
- Sallenger Jr., A. H. (2000). Storm impact scale for barrier islands. *Journal of Coastal Research*, 16(3), 890–895.

- Sallenger Jr., A. H., Jr., Wright, C. W., Howd, P., Doran, K., & Guy, K. (2009). *Extreme Coastal Changes on the Chandeleur Islands, Louisiana, During and After Hurricane Katrina* (Scientific Investigations Report No. 2009–5252). U.S. Geological Survey.
- Schindler, J. (2010, December). *Estuarine dynamics as a function of barrier island transgression and wetland loss: Understanding the transport and exchange process* (Master of Science in Earth and Environmental Science: Coastal Sciences). University of New Orleans, New Orleans, LA.
- Schupp, C. A., Winn, N. T., Pearl, T. L., Kumer, J. P., Carruthers, T. J. B., & Zimmerman, C. S. (2013). Restoration of overwash processes creates piping plover (*Charadrius melodus*) habitat on a barrier island (Assateague Island, Maryland). *Estuarine, Coastal and Shelf Science*, *116*, 11–20.
- Selman, W., Hess, T. J., & Linscombe, J. (2016). Long-Term Population and Colony Dynamics of Brown Pelicans (*Pelecanus occidentalis*) in Rapidly Changing Coastal Louisiana, USA. *Waterbirds*, *39*(1), 45–57.
- Sherwood, C. R., Long, J. W., Dickhudt, P. J., Dalyander, P. S., Thompson, D. M., & Plant, N. G. (2014). Inundation of a barrier island (Chandeleur Islands, Louisiana, USA) during a hurricane: Observed water-level gradients and modeled seaward sand transport. *Journal of Geophysical Research: Earth Surface*, *119*(7), 1498–1515.
- Soulsby, R. (1997). *Dynamics of Marine Sands: A Manual for Practical Applications*. Thomas Telford.
- Southeast Conservation Adaptation Strategy. (2021, February 21). Online guide to using the Southeast Blueprint.
- Stalk, C. A., DeWitt, N. T., Bernier, J. C., Kindinger, J. G., Flocks, J. G., Miselis, J. L., Locker, S. D., Kelso, K. W., & Tuten, T. M. (2017). *Coastal single-beam bathymetry data collected in 2015 from the Chandeleur Islands, Louisiana* (USGS Numbered Series No. 1039). *Coastal single-beam bathymetry data collected in 2015 from the Chandeleur Islands, Louisiana* (Vol. 1039). Reston, VA: U.S. Geological Survey.
- Stallins, A. J., & Corenblit, D. (2018). Interdependence of geomorphic and ecologic resilience properties in a geographic context. *Geomorphology*, *305*, 76–93.
- Stallins, J. A. (2005). Stability domains in barrier island dune systems. *Ecological Complexity*, *2*(4), 410–430.
- Stockdon, H. F., Fauver, L. A., Sallenger Jr, A. H., Wright, C. W., Farris, G. S., Smith, G. J., Crane, M. P., Demas, C. R., Robbins, L. L., & Lavoie, D. L. (2005). Impacts of Hurricane Rita on the beaches of western Louisiana. *Science and the Storms—the USGS Response to the Hurricanes Of*, 119–24.
- Stockdon, H. F., Holman, R. A., Howd, P. A., & Sallenger, A. H. (2006). Empirical parameterization of setup, swash, and runup. *Coastal Engineering*, *53*(7), 573–588.
- Stone, G. W. (2006). Tropical cyclone and winter storm impacts on the short-term evolution of barriers along the northeastern Gulf of Mexico. *Gulf Coast Association of Geological Societies Transactions*, *56*, 793–795.
- Stone, G. W., Liu, B., Pepper, D. A., & Wang, P. (2004). The importance of extratropical and tropical cyclones on the short-term evolution of barrier islands along the northern Gulf of Mexico, USA. *Marine Geology*, *210*(1–4), 63–78.
- Stone, G. W., & Stapor Jr, F. W. (1996). A nearshore sediment transport model for the northeast Gulf of Mexico coast, U.S.A. *Journal of Coastal Research*, *12*(3), 786–793.
- Stutz, M. L., & Pilkey, O. H. (2001). A review of global barrier island distribution. In *Journal of Coastal Research* (pp. 15–22). New Zealand.
- Suir, G. M., & Sasser, C. E. (2019). Redistribution and impacts of nearshore berm sediments on the Chandeleur barrier islands, Louisiana. *Ocean & Coastal Management*, *168*, 103–116.
- Suter, J., Penland, S., Williams, S. J., & Kindinger, J. (1988). Stratigraphic Evolution of the Chandeleur Islands, Louisiana (Vol. 72, pp. 1124–1125). Presented at the Gulf Coast Association of Geological Societies Transactions.
- Teague, W. J., Jarosz, E., Keen, T. R., Wang, D. W., & Hulbert, M. S. (2006). Bottom scour observed under Hurricane Ivan. *Geophysical Research Letters*, *33*(7), 3.

- Tornqvist, T. E., Kidder, T. R., Autin, W. J., van der Borg, K., de Jong, A. F. M., Klerks, C. J. W., Snijders, E. M. A., Storms, J. E. A., van Dam, R. L., & Wiemann, M. C. (1996). A revised chronology for Mississippi River subdeltas. *Science*, 273, 1693–1696.
- Twichell, D. C., Pendleton, E. A., Baldwin, W. E., Flocks, J. G., Miner, M. D., & Kulp, M. A. (2011). Geologic controls on sediment distribution and transport pathways around the Chandeleur Islands, LA., USA. In *The Proceedings of the Coastal Sediments 2011* (Vol. 3, pp. 2184–2197). Miami, Florida, USA: World Scientific Publishing Company.
- Twichell, D., Pendleton, E., Baldwin, W., & Flocks, J. (2009a). *Geologic Mapping of Distribution and Volume of Potential Resources* (Scientific Investigations Report No. 2009–5252) (p. 29). U.S. Geological Survey.
- Twichell, D., Pendleton, E., Baldwin, W., & Flocks, J. (2009b). Subsurface control on seafloor erosional processes offshore of the Chandeleur Islands, Louisiana. *Geo-Marine Letters*, 29(6), 349–358.
- U.S. Army Corps of Engineers. (1958). *Geological Investigation of the Mississippi River-Gulf Outlet Channel* (Miscellaneous Paper No. 3–259) (p. 22). Vicksburg, Mississippi: U.S. Army Engineer Waterways Experiment Station.
- U.S. Fish and Wildlife Service. (2008). *Delta and Breton National Wildlife Refuges: Comprehensive Conservation Plan* (Comprehensive Conservation Plan) (p. 140). Atlanta, GA: U.S. Department of the Interior, U.S. Fish and Wildlife Service, Southeast Region.
- U.S. Fish and Wildlife Service. (2013). *Habitat Management Plan for Delta and Breton National Wildlife Refuges* (p. 104). Atlanta, GA: U.S. Department of the Interior, Fish and Wildlife Service, Southeast Region.
- Walters, D., Moore, L. J., Duran Vinent, O., Fagherazzi, S., & Mariotti, G. (2014). Interactions between barrier islands and backbarrier marshes affect island system response to sea level rise: Insights from a coupled model: Barrier Islands and Backbarrier Marshes. *Journal of Geophysical Research: Earth Surface*, 119(9), 2013–2031.
- Zdravkovic, M. G. (2013). *Conservation Plan for the Wilson's Plover* (*Charadrius Wilsona*) (p. 170). Manomet Center for Conservation Sciences.
- Zinnert, J. C., Stallins, J. A., Brantley, S. T., & Young, D. R. (2017). Crossing scales: The complexity of barrier-island processes for predicting future change. *BioScience*, 67(1), 39–52.
- Zinnert, J. C., Via, S. M., Nettleton, B. P., Tuley, P. A., Moore, L. J., & Stallins, J. A. (2019). Connectivity in coastal systems: Barrier island vegetation influences upland migration in a changing climate. *Global Change Biology*, 25(7), 2419–2430.